Experimental Diabetes Research

Importance of Aggregated Islet Amyloid Polypeptide for the Progressive Beta-Cell Failure in Type 2 Diabetes and in Transplanted Human Islets

Guest Editors: Gunilla T. Westermark, Per Westermark, and Steven A. Kahn

Importance of Aggregated Islet Amyloid Polypeptide for the Progressive Beta-Cell Failure in Type 2 Diabetes and in Transplanted Human Islets

Experimental Diabetes Research

Importance of Aggregated Islet Amyloid Polypeptide for the Progressive Beta-Cell Failure in Type 2 Diabetes and in Transplanted Human Islets

Guest Editors: Gunilla T. Westermark, Per Westermark, and Steven A. Kahn

Contents

Hindawi Publishing Corporation
Experimental Diabetes Research
Volume 2008, Article ID 528354, 2 pages
doi:10.1155/2008/528354

Editorial

Importance of Aggregated Islet Amyloid Polypeptide for the Progressive Beta-Cell Failure in Type 2 Diabetes and in Transplanted Human Islets

Gunilla T. Westermark[1, 2] and Per Westermark[3]

[1] *Division of Cell Biology, Diabetes Research Centre, Department of Clinical and Experimental Medicine, Linköping University, 58185 Linköping, Sweden*
[2] *Department of Medical Cell Biology, Uppsala University, 75123 Uppsala, Sweden*
[3] *Department of Genetics and Pathology, Uppsala University, 75185 Uppsala, Sweden*

Correspondence should be addressed to Gunilla T. Westermark, gunilla.westermark@mcb.uu.se

Received 31 December 2008; Accepted 31 December 2008

The almost constantly appearing amyloid deposits in islets of Langerhans of individuals with type 2 diabetes was for long time regarded as more or less innocent bystanders. Even after that the amyloid was shown to be an aggregated form of a novel polypeptide hormone, islet amyloid polypeptide (IAPP or amylin), the deposits themselves attracted little interest. This can appear peculiar today and is in sharp contrast to another localized form of amyloid deposition occurring in the brain particularly in association with Alzheimer's disease. The protein forming the brain amyloid, Aβ-peptide, was discovered just two years (1984) before IAPP (1986), and aggregation of Aβ became immediately a central issue in the studies of the pathogenesis of Alzheimer's disease. So, why did almost the whole research field on senile and presenile dementia so rapidly focus on amyloid while most diabetologists, with a few exceptions, disregarded islet amyloid? A possible reason is that while Alzheimer researchers fumbled after a possible pathogenic mechanism for the brain pathology, the research field of type 2 diabetes was already established and in a high degree directed towards the development of insulin resistance. Many researchers regarded the obvious failure of beta-cells only as a secondary event due to some elusive mechanism of "glucose toxicity." In addition, experimentalists in diabetes research most often used mice or rats as models, and in these species, islet amyloid cannot develop due to the amino acid sequence of their IAPP molecules.

After the discovery of IAPP, there was a strong interest in the possible physiological role of the molecule and in the effect it may have on the development of type 2 diabetes. It was found early that the peptide induces insulin insensitivity in peripheral tissues. However, this effect was reached only after nonphysiological levels of IAPP. More established effects of the peptide include regulation of satiety, gastric emptying and para- or autocrine signalling of insulin, and glucagon secretion. All these effects seem to modulate the action of insulin, leading to a more even blood glucose level. Since IAPP is a beta-cell product and these cells are lost in type 1 diabetes, IAPP in a modified form has been introduced as supplement to insulin treatment.

Today, however, we can note an increasing interest in the importance of the development of IAPP-derived islet amyloid on the beta-cell function. Earlier it was believed that islet amyloid could not be of any significance since even in cases with pronounced deposits, there are always well-granulated beta-cells left. There are two essentially new findings that are of particularly great interest. First, islet amyloid may initially assemble intracellularly with severe consequences for the affected cell. Second, there is growing evidence that small, oligomeric, prefibrillar aggregates of IAPP are directly toxic to beta-cells. Interestingly, there is also increasing evidence that this reflects a generic mechanism common to many protein aggregates in which beta-sheet formation are essential. Such aggregates of often completely nonrelated peptides seem to have similar or identical effects

on cells. It is still very incompletely understood which these effects are. Eventually, the interactions may lead to cell death, and aggregated IAPP is a strong candidate as an important cause of beta-cell loss in type 2 diabetes. Cell death and accumulation of diffuse amyloid deposits within the islet of Langerhans are sufficient to destroy the islet architecture which is important for maintaining optimal signaling.

The finding that isolated normal human islets, transplanted into nude mice, very rapidly develop IAPP-derived amyloid deposits intra- and extracellularly, lead to the suspicion that such an event could be an important cause of the loss of function of islets transplanted into type 1 diabetic individuals. This hypothesis was recently strongly supported by the analysis of a liver of a deceased person, who had received intraportal islet transplants on three occasions. Almost 50% of identified islets were found to contain amyloid deposits. Obviously, this may mean that a beta-cell lesion, typical of type 2 diabetes, may develop in originally normal islets transplanted into a type 1 diabetic individual. Methods to inhibit amyloid formation may be important to develop in order to prolong the survival of transplanted islets.

The present issue of Experimental Diabetes Research deals with different aspects of islet amyloid and IAPP. We hope that the papers will lead to further interest in this field which sometimes has been neglected in diabetes research.

Gunilla T. Westermark
Per Westermark

Hindawi Publishing Corporation
Experimental Diabetes Research
Volume 2008, Article ID 421287, 9 pages
doi:10.1155/2008/421287

Review Article

Recent Insights in Islet Amyloid Polypeptide-Induced Membrane Disruption and Its Role in β-Cell Death in Type 2 Diabetes Mellitus

Lucie Khemtémourian,[1] J. Antoinette Killian,[1] Jo W. M. Höppener,[2] and Maarten F. M. Engel[1,2]

[1] *Department of Metabolic and Endocrine Diseases, Division of Biomedical Genetics, University Medical Center Utrecht, P.O. Box 85090, 3508 AB Utrecht, The Netherlands*
[2] *Research group Chemical Biology and Organic Chemistry, Bijvoet Institute and Institute of Biomembranes, Utrecht University, Padualaan 8, 3584 CH Utrecht, The Netherlands*

Correspondence should be addressed to Maarten F. M. Engel, m.engel@leeds.ac.uk

Received 9 October 2007; Accepted 18 February 2008

Recommended by Per Westermark

The presence of fibrillar protein deposits (amyloid) of human islet amyloid polypeptide (hIAPP) in the pancreatic islets of Langerhans is thought to be related to death of the insulin-producing islet β-cells in type 2 diabetes mellitus (DM2). The mechanism of hIAPP-induced β-cell death is not understood. However, there is growing evidence that hIAPP-induced disruption of β-cell membranes is the cause of hIAPP cytotoxicity. Amyloid cytotoxicity by membrane damage has not only been suggested for hIAPP, but also for peptides and proteins related to other misfolding diseases, like Alzheimer_s disease, Parkinson's disease, and prion diseases. Here we review the interaction of hIAPP with membranes, and discuss recent progress in the field, with a focus on hIAPP structure and on the proposed mechanisms of hIAPP-induced membrane damage in relation to β-cell death in DM2.

1. INTRODUCTION

Long before discovery of the primary structure of the main component of amyloid in the islets of Langerhans, detailed ultra structural investigations had revealed that islet amyloid was often in contact with β-cell membranes [1]. In fact, it was found that amyloid fibrils were oriented perpendicular to the membrane of islet β-cells, with some fibril bundles sticking into membrane invaginations [1]. In 1987, the main component of islet amyloid was identified as a 37-amino acid residue peptide called islet amyloid polypeptide (IAPP) or amylin [2, 3]. Since then, the presence of IAPP amyloid at the β-cell membrane, and the concomitant morphological changes of these membranes, has been reported frequently [4–9]. These reports have contributed to the current hypothesis that the interaction between IAPP and cellular membranes could be a cause of IAPP cytotoxicity and β-cell death in DM2. Before reviewing IAPP-membrane interactions, we will briefly discuss the present knowledge on IAPP fibril formation.

2. IAPP FIBRIL FORMATION

2.1. From monomer to fibril

The amino acid sequence of IAPP varies slightly from organism to organism [10]. For instance, six residues are different between human IAPP (hIAPP) and mouse IAPP (mIAPP) (see Figure 1). Importantly, the latter does not aggregate into amyloid fibrils, and amyloid is generally not observed in the pancreas of wild-type mice. Nevertheless, transgenic mouse models that express human IAPP develop fibrillar deposits and exhibit signs of diabetes [11].

The in vitro aggregation and fibril formation of hIAPP have been studied extensively in the last years [12–22]. In most of these studies, hIAPP aggregation is initiated by dilution of, usually synthetic, monomeric hIAPP into a physiological buffer. This results in the "spontaneous" aggregation of hIAPP monomers into amyloid fibrils, as can be observed, for example, by electron microscopy. The in vitro aggregation of hIAPP is typically completed in a few hours, depending amongst others on peptide concentration

Figure 1: Comparison of the amino acid sequences of human IAPP (hIAPP) and mouse IAPP (mIAPP). Mouse IAPP differs from the human peptide by six residues (in red). The N-terminal region is thought to be responsible for membrane interaction (residues in blue). The amino acid region suggested to be important for fibril formation is represented in the underlined.

and presence of lipids [18]. This is significantly faster than the aggregation of most other amyloidogenic peptides. Fibril formation of IAPP, as well as of some other amyloidogenic peptides, generally occurs via a nucleation dependent aggregation process [18, 23]. This means that the formation of a nucleus, usually a slow step, is required for initiation of the growth of stable fibrils. The nucleus is an ordered oligomeric hIAPP species that can serve as a template for fibrillar hIAPP. The kinetics of hIAPP fibril growth can be monitored in time by the commonly used method of specific binding of the fluorescent molecule Thioflavin T (ThT) to amyloid fibrils [24]. A kinetic trace of hIAPP fibril growth shows a lag phase and a sigmoidal transition that are typical for fibril growth of amyloidogenic proteins and peptides (see Figure 2) [23]. After dilution of initially monomeric hIAPP in buffer, the thermodynamically unfavourable process of nucleation occurs, although the initial horizontal baseline of the ThT curve indicates that no fibrils are formed in the beginning (lag phase). The sigmoidal increase in the ThT curve indicates propagation of fibril growth with consumption of monomer. Next to the monomeric and fibrillar states of hIAPP, several intermediate (oligomeric) states have been observed, as will be discussed later. Elongation of fibrils proceeds via addition of monomers or oligomers to both fibril ends.

2.2. Three-dimensional molecular structure of hIAPP

The three-dimensional structure of amyloid fibrils, and lately also the structure of monomers and oligomers, has been the subject of research into the molecular background of amyloid diseases. However, only little structural information is available for the IAPP monomer, oligomer, and fibril. In 1992, the first, limited information of the three-dimensional structure of soluble hIAPP was obtained [25]. It was shown that hIAPP exhibits a random coil structure with small components of α-helical and β-sheet conformations. Recent studies confirmed that soluble hIAPP has mainly unordered backbone structure [26–28]. In contrast, hIAPP dissolved in the organic solvent trifluoroethanol (TFE, a membrane mimicking solvent) predominantly adopts an α-helical conformation [25]. Our observations have indicated that hIAPP dissolved in TFE initially adopts α-helical structure, before transforming into β-sheet structure (unpublished results). These observations suggest that hIAPP could also adopt α-helical structure in a membrane environment.

hIAPP oligomers or aggregates ranging from dimers up to 6000 molecules have been reported by several research groups [7, 29–31]. These oligomers appear to represent intermediates on the path to fibril formation. There are recent indications that hIAPP oligomers, in presence of membranes, exhibit α-helical structure [28]. This is surprising since it would seem thermodynamically unfavourable for a monomer with random coil structure to first adopt α-helical structure before changing into β-sheet rich fibrillar structure. Aggregation intermediates have been observed for many types of amyloid proteins, such as α-synuclein and Aβ [32, 33]. Glabe and coworkers have produced a conformation-dependent antibody that is specific for soluble oligomers and does not recognize natively folded proteins, monomer, or fibrils [34]. They showed that this antibody recognizes soluble oligomers from a wide variety of amyloid-forming peptides and proteins such as hIAPP, Prion 106–126, human insulin, Aβ peptide, and polyglutamine, which suggests that these oligomers might have a common structure.

The three-dimensional structure of hIAPP fibrils has been studied by various high-resolution techniques, like electron microscopy, X-ray diffraction, electron diffraction, and electron paramagnetic resonance [26, 35–38]. These studies clearly reveal that hIAPP fibrils contain a significant amount of well-ordered cross-β structure, typical of amyloid fibrils. During fibril formation, hIAPP undergoes a conformational change from random coil to a mixture of β-sheet and α-helical structure [26]. These results are consistent with the work of Kayed [15], who also measured a random coil to β-sheet transition for hIAPP fibril formation. hIAPP fibrils are polymorphic, ranging from thin protofilaments with a diameter of about 5 nm to thicker fibrils with diameter of up to 15 nm that appear to be rope-like bundles of protofilaments. The predominant type of fibril contains three protofilaments in a left-handed coil with a pitch of 25–50 nm.

2.3. Which amino acid residues are important for hIAPP fibril formation?

Structural studies have shown that amino acid residues 20–29 of hIAPP are crucial for amyloid formation [12]. A proline scan of this decamer (hIAPP20–29) has demonstrated that substitution of a single proline at either position 22, 24 or at positions 26–28 leads to a drastic reduction of amyloid formation [39]. Note that three of the six differences between hIAPP and the nonamyloidogenic mIAPP involve a proline, a residue that is predicted to disrupt ordered structure, like the β-sheet structure in amyloid fibrils.

Currently, research groups are developing molecules in an attempt to reduce hIAPP-induced β-cell death by inhibiting hIAPP fibril formation. Some of these "inhibitors" are based on synthetically modified hIAPP peptides or hIAPP fragments that are not able to form fibrils themselves, but are suggested to bind to, and to stop the elongation of growing hIAPP fibrils [40–42]. A recent study indicated that a single amino acid substitution in hIAPP, where Ile on position 26 is

replaced by Pro (I26P), yields a potent fibrillization inhibitor [43].

Although residues 20–29 play an important role in hIAPP fibril formation, these may not be the only residues involved. It has been hypothesized that aromatic-aromatic interactions are also important in hIAPP fibril formation [44]. Human IAPP contains three aromatic residues at positions 15, 23, and 37 (see Figure 1). The aromatic-aromatic and aromatic-hydrophobic interactions in amyloid formation were studied using a hIAPP triple mutant [45]. The triple mutant F15L/F23L/Y37L, lacking aromatic residues, still forms amyloid fibrils in vitro, indicating that the aromatic residues are not essential in hIAPP fibril formation. However, the substitution decreases the rate of fibril formation and alters the tendency of fibrils to aggregate. Some studies demonstrate that the amino acid region from residues 11 to 20 is also important for hIAPP fibril formation [46, 47]. A recent study shows that the hIAPP fragment consisting of residues 14–20 can form amyloid fibrils [38].

hIAPP contains a single histidine at position 18 (see Figure 1), which is the only residue in this peptide that has a charge that depends on pH in a physiological pH range. Consequently, fibril formation of hIAPP could depend on the pH. A recent study showed that hIAPP fibril formation is faster at a lower pH (4.0) than at a higher pH (8.8) [48]. This could be important in a physiological context since in the β-cell granules of the pancreas, where hIAPP is stored, the pH is 5.5, but when hIAPP is released into the extracellular compartment, it experiences a pH of 7.4 [49].

Another characteristic of hIAPP is the intramolecular disulfide bond between cysteines residues 2 and 7 (see Figure 1). The disulfide does not contribute to the amyloid fiber core structure; however it somehow must play a central role in the assembly mechanism, since loss of the disulfide significantly reduces fibril formation [20].

3. hIAPP AGGREGATION AND FIBRIL FORMATION IN THE PRESENCE OF MEMBRANES

3.1. Membrane phospholipids catalyse hIAPP fibril formation

It has been observed that phospholipid membranes promote the aggregation of hIAPP [28, 50, 51]. In the presence of phospholipids, the kinetic profile of hIAPP fibril growth is characterized by a reduction in the lag time resulting in earlier fibril formation [50]. Cellular membranes could accelerate hIAPP fibril formation by enhancing nucleation. The lipid composition may play an important role in this process, since it has been demonstrated that hIAPP aggregation is accelerated in the presence of membranes that contain negatively charged lipids such as 1,2-dioleoyl-*sn*-glycero-3-phospho-L-serine (DOPS) or 1,2-Dioleoyl-sn-Glycero-3-[Phospho-rac-(1-glycerol)](DOPG) [27, 50, 51]. In the presence of such membranes, hIAPP fibril formation occurs within a few minutes as opposed to a few hours in the absence of membranes [27, 50]. A membrane-induced change in the conformation in hIAPP could possibly result in formation and/or stabilization of a nucleus, which could in turn result in acceleration of hIAPP fibril formation. Hence, elucidation of the conformation of hIAPP in interaction with the membrane is an important issue. Knowledge of this conformation would give valuable insights into the mechanism of membrane damage and would aid in developing new drugs and/or finding new targets for the treatment of DM2.

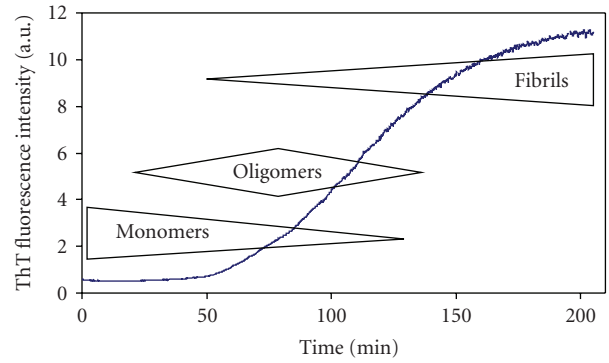

Figure 2: Typical shape of the kinetics of hIAPP fibril formation, characterized by a lag phase and a sigmoidal transition. The approximate aggregation state of IAPP is indicated at the various time points. Fibril formation was induced by adding, at time 0, a monomeric stock solution of hIAPP in DMSO to buffer containing Thioflavin T.

3.2. Insight in the conformation of membrane-interacting hIAPP

Recently, studies have been performed to determine the conformation of hIAPP that interacts with model membranes, that is, large unilamellar vesicles (LUVs) [27, 28, 52]. In these studies, the LUVs are composed of a combination of a neutral phospholipid, for instance, 1,2-dioleoyl-*sn*-glycero-3-phosphocholine (DOPC), and a negatively charged phospholipid, for instance, 1,2-dioleoyl-*sn*-glycero-3-phospho-L-serine (DOPS). In the presence of LUVs, hIAPP initially displays α-helical structure [27], corresponding with the structure of hIAPP in the membrane-mimicking solvent TFE [25]. However, after 40 minutes incubation with LUVs, the conformation of hIAPP changes to predominantly β-sheet conformation, characteristic of fibril formation [27]. Recently, the structure of hIAPP in membrane bilayers was studied using microscopy techniques [53]. It was found that hIAPP forms pores that are composed of five subunits, in which each subunit is suggested to represent an hIAPP monomer. This hIAPP morphology was connected to channel-like behavior in planar bilayers, indicating that these oligomeric hIAPP pores could incorporate in membranes and change their barrier properties. Unfortunately, high-resolution structural information of hIAPP in a membrane environment is still lacking, mainly because of the instability of the membrane-interacting hIAPP aggregates. Preliminary results of our group indicate that hIAPP fibrils grown in the presence of phospholipids have the same characteristic structure as fibrils formed in the absence of lipids.

3.3. Which residues are important in the interaction with membrane?

It is likely that the presence of membranes causes additional residues in IAPP to be involved in fibril formation, as compared to the situation without membranes. Several residues that are important for hIAPP-membrane interactions can be identified. It can be anticipated that the positively charged residues, which are all located at the N-terminal part of hIAPP at positions 1, 11, and 18 (see Figure 1), will be important in the interaction of hIAPP with negatively charged phospholipid membranes. Indeed, there are indications that hIAPP molecules cluster at the membrane surface, prior to fibrillogenesis, with their N-termini oriented towards the membrane [50]. More recently, it was shown that an N-terminal hIAPP fragment (hIAPP1–19) has a significantly higher ability to insert in phospholipid monolayers than a fragment from the central, amyloidogenic region of hIAPP (hIAPP20–29) [54]. These findings suggest that the N-terminal part of hIAPP, whilst not significantly involved in hIAPP fibril growth, is important in light of hIAPP-membrane interactions.

4. MECHANISM OF CYTOTOXICITY

In 1993, work on the amyloidogenic Alzheimer's related peptide Abeta had indicated that an amyloidogenic protein can form ion-selective membrane channels, providing a first hypothesis for the mechanism of amyloid (neuro)toxicity [55, 56]. The observations that IAPP fibrils are located at the cellular membrane in the Islets of Langerhans and that this is accompanied by alterations in membrane morphology [1, 4–9] made researchers hypothesize that the membrane might be the target of cytotoxic IAPP and that this could cause death of the insulin producing β-cells, similar to Abeta neurotoxicity in Alzheimer's disease. The first experimental evidence that indeed hIAPP can cause membrane disruption came from work by the Kagan group [57]. It was found from experiments with planar lipid bilayers that synthetic hIAPP forms ion-permeable channels "pores" in the membrane, whereas the nonamyloidogenic mouse IAPP does not form channels. Mature hIAPP fibrils were found to be less cytotoxic; moreover, they did not cause significant membrane disruption in comparison to oligomeric hIAPP [58, 59]. Still, the exact mechanism of hIAPP-induced membrane disruption is far from understood, and various mechanisms have been hypothesized during the last 10 years [7, 29, 31, 34, 50, 51, 54, 57, 60–63]. It is, for example, unclear what the exact nature of the hIAPP species that interacts with or even disrupts membranes is. The main hypothesis, based on in vitro evidence, suggests a major role for a specific prefibrillar hIAPP aggregate, commonly known as hIAPP oligomer, as the membrane-disrupting species [7, 29, 31, 34, 57, 59, 60, 64]. The various suggested mechanisms for hIAPP-induced membrane disruption will be discussed below.

4.1. hIAPP oligomers cause membrane damage and are cytotoxic

Recently, it has been suggested that prefibrillar aggregates (or oligomers), formed early during aggregation and not mature amyloid fibrils are the cytotoxic species in protein misfolding diseases [65]. Considering amyloid cytotoxicity in DM2, the prevailing view is that IAPP-induced membrane damage, and concomitant β-cell death, is caused by cytotoxic hIAPP oligomers [7, 28, 29, 31, 53, 57, 60, 64]. There are indications that these oligomers form ion channels [53, 57], as has been suggested for other amyloidogenic proteins [55, 66]. Other studies indicate that hIAPP oligomer-induced membrane damage is not specific for ions [31] but results in membrane leakage of molecules with a size of up to 600 Da (Calcein), indicating a general membrane disruption mechanism by hIAPP oligomers [28, 51, 59, 63, 67].

Small hIAPP aggregates have been shown to be cytotoxic in cell cultures, and these aggregates were also able to destabilize model membranes [7]. Similarly, oligomeric hIAPP was found to form membrane pores, allowing molecules with the size of a calcium ion to pass. These pores disappeared, and membrane damage decreased, when hIAPP fibrils grew and oligomers were consumed [29, 60]. Electron microscopy analysis showed that hIAPP formed spherical shapes with a diameter of 3 to 20 nm, consistent with the presence of hIAPP oligomers [31, 60]. In a test tube, oligomeric hIAPP can be prepared under specific experimental conditions. Addition of such preparations to human neuroblastoma cells that were loaded with fluorescent dye resulted in the cellular leakage of this dye [59]. This indicates that hIAPP oligomers, when applied to the outside of cells, are cytotoxic via a general membrane destabilizing effect and not via a specific ion pore. The monomeric and fibrillar form of hIAPP clearly did not have this effect. Later it was also shown that when applied from the inside of cells, using cells that overexpress hIAPP, the hIAPP oligomers are also able to perform their cytotoxic action [64]. Recently, it has been suggested that ER and mitochondrial membranes might be the target of cytotoxic hIAPP, resulting in ER stress and β-cell apoptosis [68]. Moreover, intracellular hIAPP oligomers were indirectly demonstrated in the pancreatic β-cells of hIAPP-transgenic mice using an oligomer-specific antibody [69]. The latter study also showed that oligomer-specific antibodies could not prevent hIAPP-induced β-cell death, indicating that toxic events might occur inside the cell.

The exact mechanism of membrane disruption by hIAPP oligomers is not known. Some groups show that preassembled hIAPP oligomers disrupt membranes [31, 60], whereas others suggest that hIAPP monomers first interact with the membrane and only then form oligomeric hIAPP with membrane disrupting capacity [28]. These two models of membrane damage by hIAPP oligomers have been schematically depicted in Figure 3.

In conclusion, many observations indicate that hIAPP oligomers are a likely candidate for inducing cell death. In contrast, hIAPP fibrils are found not to damage membranes and could in fact be the result of a physiological mechanism

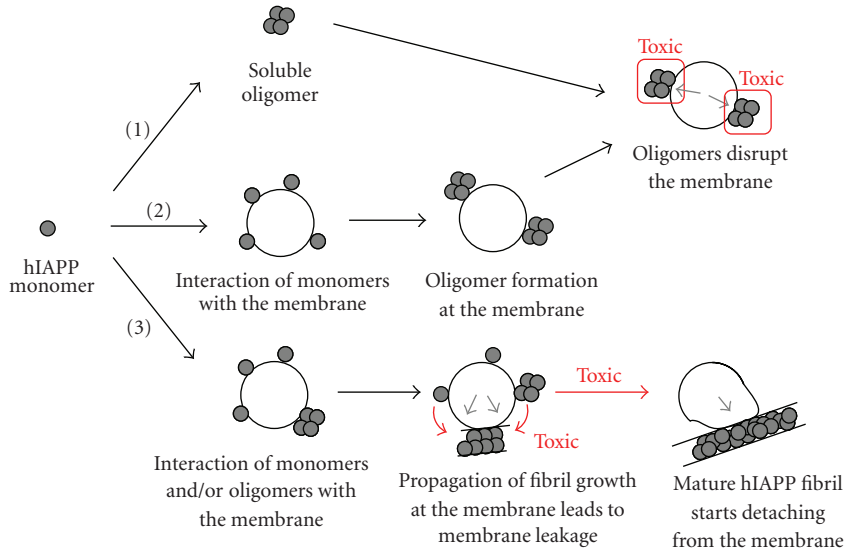

Figure 3: Simplified schematic representation of the different models of hIAPP-membrane interaction in relation to membrane damage and hIAPP cytotoxicity. The red rectangles show the toxic species and the red arrows show the toxic processes according to different hypotheses. The black circle represents a phospholipid membrane (vesicle), the grey circles represent hIAPP monomers, and clusters of 4 or more circles represent hIAPP oligomers and hIAPP fibrils, respectively. Membrane damage is schematically indicated by the grey arrows. Model (1) includes two steps: (i) formation of soluble hIAPP oligomers, (ii) interaction of the toxic oligomers with the membrane leading to membrane damage. Model (2) includes three steps: (i) binding of monomeric, random coil hIAPP to the membrane and folding to α-helix, (ii) oligomer formation of membrane-bound hIAPP, and (iii) interaction of the toxic hIAPP oligomer with the membrane leading to membrane damage. Model (3) includes 3 steps: (i) interaction of monomeric and possibly oligomeric hIAPP to the membrane, (ii) growth of hIAPP fibrils at the membrane (red arrows) leading to a forced change in membrane morphology and concomitant membrane disruption, and (iii) detachment of mature fibrils from distorted membrane.

in which toxic oligomer species are disposed of in a nontoxic, fibrillar form.

4.2. *Membrane damage by fibril growth at the membrane*

In addition to the hypothesis that oligomers are the toxic species, recent reports suggest also other mechanisms for hIAPP cytotoxicity. One such hypothesis is that membrane damage is not caused by a specific hIAPP species, such as an oligomer, but by the process of fibril growth at the cellular membrane. There are several recent indications that growth of hIAPP fibrils at the membrane can cause membrane damage. In this model, the initial steps of the interaction of hIAPP with membranes are adsorption, followed by insertion of hIAPP into the membrane, either as monomer or as oligomer (see Figure 3). The interaction of monomeric hIAPP with membranes is likely as monomeric hIAPP has a strong tendency to insert in phospholipid monolayers [52, 54]. In the next step, interactions of membrane-located hIAPP species with each other, or with hIAPP species in solution, lead to growth of fibrils at the membrane (model 3 in Figure 3). The mechanism of membrane damage could entail growth of a rigid hIAPP fibril on a flexible phospholipid bilayer, which would result in a forced change in membrane curvature. This change in membrane curvature leads to deformation of the shape of the membrane. Interestingly, disruption, blebbing and vesicle budding of cell membranes in the presence of synthetic [5, 7, 9] and cell-derived hIAPP [6, 8, 70] have been noticed in many studies. Our recent results indicate that the kinetics of membrane damage is very similar to the kinetics of fibril formation (see Figure 2). Both processes, fibril formation and membrane damage, were characterized by the presence of a lag phase and a strong enhancing effect on the kinetics upon the addition of seeds [71]. In case of the Alzheimer's disease-related Abeta peptide, it has been suggested recently that not a particular species but ongoing amyloid fibrillogenesis is responsible for membrane damage [72]. Together, these notions suggest that a cytotoxic mechanism based on fibril growth at the membrane could represent a common mechanism for amyloid-induced cell death. Finally, another factor that could contribute to membrane damage by fibril growth is uptake of membrane lipids in amyloid, a phenomenon that has been observed, both in vitro [51, 73, 74] and in vivo [75].

5. INITIATION OF HARMFUL IAPP-MEMBRANE INTERACTIONS IN DM2

Since the combination of hIAPP and membranes in non-diabetic people does not normally result in β-cell death; certain DM2-related conditions should exist that initiate hIAPP-induced membrane damage. An increase in the level of hIAPP, which is coproduced and cosecreted with insulin, in a state of insulin resistance, could initiate hIAPP fibril formation. More specific, an altered ratio of insulin to hIAPP, as observed in diabetic patients [16], could lead to a decrease of the inhibitory effect of insulin on hIAPP amyloid

fibril formation. This inhibitory effect of insulin on hIAPP fibril formation has been observed in vitro [76–78]. On the other hand, a changing lipid composition of the β-cells, in particular an increase in negatively charged lipids as inferred from studies with mouse and rat models for DM2 [79], could also trigger an increase in hIAPP-membrane interactions. In vitro studies show that negatively charged lipids increase the rate of hIAPP fibril formation [27, 50] and also enhance hIAPP-induced membrane damage [28, 51]. The membrane itself could promote hIAPP growth by increasing the local concentration of (membrane bound) hIAPP and/or by promoting a specific orientation or conformation of the peptide that makes hIAPP molecules more susceptible to aggregation into oligomers or fibrils. Recent research shows that not only phospholipid bilayers, but also a polyanion like heparin [80] or a dichloromethane/water interface [22] can induce nucleation and aggregation of hIAPP. These results indicate that charge and a hydrophobic/hydrophilic interface (both present in biological membranes) are important factors that promote hIAPP fibril formation.

6. FUTURE PERSPECTIVES AND CHALLENGES

During the last years, the understanding of hIAPP-membrane interactions has significantly increased. We have now important indications that oligomeric hIAPP, in contrast to fibrillar hIAPP, is the main species involved in membrane damage and is a likely candidate to cause β-cell death in DM2. However, in a cellular environment, such toxic oligomers have not (yet) been directly demonstrated. More insight is required into the question whether hIAPP oligomers are inherently cytotoxic and persist as toxic oligomer after their cytotoxic action, or whether they are transient participants in the process of fibril growth at the membrane. A major challenge is to elucidate the mechanism by which hIAPP induces membrane damage and cytotoxicity. This knowledge would be essential to develop new strategies to battle hIAPP-induced β-cell death in DM2. Determination of the three-dimensional structure of membrane disrupting hIAPP would be an important contribution in elucidation of the cytotoxic mechanism. Moreover, the importance of hIAPP-membrane interactions, discussed here, indicates that inhibition or alteration of hIAPP-membrane interactions might be an alternative strategy to reduce amyloid cytotoxicity and to prevent β-cell death in DM2, in addition to the "traditional strategy" to reduce amyloid by the development of molecules that inhibit amyloid fibril formation.

ACKNOWLEDGMENTS

This research was financially supported by the Dutch Diabetes Research Foundation (Grant no. 2002.00.019). Lucie Khemtémourian was supported by the European Commission (Marie Curie Postdoctoral fellowship).

REFERENCES

[1] P. Westermark, "Fine structure of islets of Langerhans in insular amyloidosis," *Virchows Archiv A*, vol. 359, no. 1, pp. 1–18, 1973.

[2] P. Westermark, C. Wernstedt, E. Wilander, D. W. Hayden, T. D. O'Brien, and K. H. Johnson, "Amyloid fibrils in human insulinoma and islets of Langerhans of the diabetic cat are derived from a neuropeptide-like protein also present in normal islet cells," *Proceedings of the National Academy of Sciences of the United States of America*, vol. 84, no. 11, pp. 3881–3885, 1987.

[3] G. J. S. Cooper, A. C. Willis, A. Clark, R. C. Turner, R. B. Sim, and K. B. M. Reid, "Purification and characterization of a peptide from amyloid-rich pancreases of type 2 diabetic patients," *Proceedings of the National Academy of Sciences of the United States of America*, vol. 84, no. 23, pp. 8628–8632, 1987.

[4] A. Clark, C. E. Lewis, A. C. Willis, et al., "Islet amyloid formed from diabetes-associated peptide may be pathogenic in type-2 diabetes," *The Lancet*, vol. 330, no. 8553, pp. 231–234, 1987.

[5] A. Lorenzo, B. Razzaboni, G. C. Weir, and B. A. Yankner, "Pancreatic islet cell toxicity of amylin associated with type-2 diabetes mellitus," *Nature*, vol. 368, no. 6473, pp. 756–760, 1994.

[6] T. D. O'Brien, P. C. Butler, D. K. Kreutter, L. A. Kane, and N. L. Eberhardt, "Human islet amyloid polypeptide expression in COS-1 cells. A model of intracellular amyloidogenesis," *American Journal of Pathology*, vol. 147, no. 3, pp. 609–616, 1995.

[7] J. Janson, R. H. Ashley, D. Harrison, S. McIntyre, and P. C. Butler, "The mechanism of islet amyloid polypeptide toxicity is membrane disruption by intermediate-sized toxic amyloid particles," *Diabetes*, vol. 48, no. 3, pp. 491–498, 1999.

[8] H. J. Hiddinga and N. L. Eberhardt, "Intracellular amyloidogenesis by human islet amyloid polypeptide induces apoptosis in COS-1 cells," *American Journal of Pathology*, vol. 154, no. 4, pp. 1077–1088, 1999.

[9] E. L. Saafi, B. Konarkowska, S. Zhang, J. Kistler, and G. J. S. Cooper, "Ultrastructural evidence that apoptosis is the mechanism by which human amylin evokes death in RINm5F pancreatic islet β-cells," *Cell Biology International*, vol. 25, no. 4, pp. 339–350, 2001.

[10] C. Betsholtz, L. Christmansson, U. Engström, et al., "Sequence divergence in a specific region of islet amyloid polypeptide (IAPP) explains differences in islet amyloid formation between species," *FEBS Letters*, vol. 251, no. 1-2, pp. 261–264, 1989.

[11] J. W. M. Höppener, C. Oosterwijk, M. G. Nieuwenhuis, et al., "Extensive islet amyloid formation is induced by development of type II diabetes mellitus and contributes to its progression: pathogenesis of diabetes in a mouse model," *Diabetologia*, vol. 42, no. 4, pp. 427–434, 1999.

[12] P. Westermark, U. Engström, K. H. Johnson, G. T. Westermark, and C. Betsholtz, "Islet amyloid polypeptide: pinpointing amino acid residues linked to amyloid fibril formation," *Proceedings of the National Academy of Sciences of the United States of America*, vol. 87, no. 13, pp. 5036–5040, 1990.

[13] S. B. P. Chargé, E. J. P. de Koning, and A. Clark, "Effect of pH and insulin on fibrillogenesis of islet amyloid polypeptide in vitro," *Biochemistry*, vol. 34, no. 44, pp. 14588–14593, 1995.

[14] A. Kapurniotu, J. Bernhagen, N. Greenfield, et al., "Contribution of advanced glycosylation to the amyloidogenicity of islet amyloid polypeptide," *European Journal of Biochemistry*, vol. 251, no. 1-2, pp. 208–216, 1998.

[15] R. Kayed, J. Bernhagen, N. Greenfield, et al., "Conformational transitions of islet amyloid polypeptide (IAPP) in amyloid formation in vitro," *Journal of Molecular Biology*, vol. 287, no. 4, pp. 781–796, 1999.

[16] E. T. A. S. Jaikaran, C. E. Higham, L. C. Serpell, et al., "Identification of a novel human islet amyloid polypeptide β-sheet domain and factors influencing fibrillogenesis," *Journal of Molecular Biology*, vol. 308, no. 3, pp. 515–525, 2001.

[17] S. B. Padrick and A. D. Miranker, "Islet amyloid polypeptide: identification of long-range contacts and local order on the fibrillogenesis pathway," *Journal of Molecular Biology*, vol. 308, no. 4, pp. 783–794, 2001.

[18] S. B. Padrick and A. D. Miranker, "Islet amyloid: phase partitioning and secondary nucleation are central to the mechanism of fibrillogenesis," *Biochemistry*, vol. 41, no. 14, pp. 4694–4703, 2002.

[19] J. L. Larson, E. Ko, and A. D. Miranker, "Direct measurement of islet amyloid polypeptide fibrillogenesis by mass spectrometry," *Protein Science*, vol. 9, no. 2, pp. 427–431, 2000.

[20] B. W. Koo and A. D. Miranker, "Contribution of the intrinsic disulfide to the assembly mechanism of islet amyloid," *Protein Science*, vol. 14, no. 1, pp. 231–239, 2005.

[21] J. A. Williamson and A. D. Miranker, "Direct detection of transient α-helical states in islet amyloid polypeptide," *Protein Science*, vol. 16, no. 1, pp. 110–117, 2007.

[22] A. M. Ruschak and A. D. Miranker, "Fiber-dependent amyloid formation as catalysis of an existing reaction pathway," *Proceedings of the National Academy of Sciences of the United States of America*, vol. 104, no. 30, pp. 12341–12346, 2007.

[23] J. D. Harper and P. T. Lansbury Jr., "Models of amyloid seeding in Alzheimer's disease and scrapie: mechanistic truths and physiological consequences of the time-dependent solubility of amyloid proteins," *Annual Review of Biochemistry*, vol. 66, pp. 385–407, 1997.

[24] H. Naiki, K. Higuchi, M. Hosokawa, and T. Takeda, "Fluorometric determination of amyloid fibrils in vitro using the fluorescent dye, thioflavine T," *Analytical Biochemistry*, vol. 177, no. 2, pp. 244–249, 1989.

[25] L. R. McLean and A. Balasubramaniam, "Promotion of β-structure by interaction of diabetes associated polypeptide (amylin) with phosphatidylcholine," *Biochimica et Biophysica Acta*, vol. 1122, no. 3, pp. 317–320, 1992.

[26] C. Goldsbury, K. Goldie, J. Pellaud, et al., "Amyloid fibril formation from full-length and fragments of amylin," *Journal of Structural Biology*, vol. 130, no. 2-3, pp. 352–362, 2000.

[27] S. A. Jayasinghe and R. Langen, "Lipid membranes modulate the structure of islet amyloid polypeptide," *Biochemistry*, vol. 44, no. 36, pp. 12113–12119, 2005.

[28] J. D. Knight, J. A. Hebda, and A. D. Miranker, "Conserved and cooperative assembly of membrane-bound α-helical states of islet amyloid polypeptide," *Biochemistry*, vol. 45, no. 31, pp. 9496–9508, 2006.

[29] M. Anguiano, R. J. Nowak, and P. T. Lansbury Jr., "Protofibrillar islet amyloid polypeptide permeabilizes synthetic vesicles by a pore-like mechanism that may be relevant to type II diabetes," *Biochemistry*, vol. 41, no. 38, pp. 11338–11343, 2002.

[30] J. D. Green, C. Goldsbury, J. Kistler, G. J. S. Cooper, and U. Aebi, "Human amylin oligomer growth and fibril elongation define two distinct phases in amyloid formation," *Journal of Biological Chemistry*, vol. 279, no. 13, pp. 12206–12212, 2004.

[31] R. Kayed, Y. Sokolov, B. Edmonds, et al., "Permeabilization of lipid bilayers is a common conformation-dependent activity of soluble amyloid oligomers in protein misfolding diseases," *Journal of Biological Chemistry*, vol. 279, no. 45, pp. 46363–46366, 2004.

[32] J.-C. Rochet, K. A. Conway, and P. T. Lansbury Jr., "Inhibition of fibrillization and accumulation of prefibrillar oligomers in mixtures of human and mouse α-synuclein," *Biochemistry*, vol. 39, no. 35, pp. 10619–10626, 2000.

[33] C. G. Glabe and R. Kayed, "Common structure and toxic function of amyloid oligomers implies a common mechanism of pathogenesis," *Neurology*, vol. 66, no. 2, supplement 1, pp. S74–S78, 2006.

[34] R. Kayed, E. Head, J. L. Thompson, et al., "Common structure of soluble amyloid oligomers implies common mechanism of pathogenesis," *Science*, vol. 300, no. 5618, pp. 486–489, 2003.

[35] C. Goldsbury, G. J. S. Cooper, K. N. Goldie, et al., "Polymorphic fibrillar assembly of human amylin," *Journal of Structural Biology*, vol. 119, no. 1, pp. 17–27, 1997.

[36] O. Sumner Makin and L. C. Serpell, "Structural characterisation of islet amyloid polypeptide fibrils," *Journal of Molecular Biology*, vol. 335, no. 5, pp. 1279–1288, 2004.

[37] S. A. Jayasinghe and R. Langen, "Identifying structural features of fibrillar islet amyloid polypeptide using site-directed spin labeling," *Journal of Biological Chemistry*, vol. 279, no. 46, pp. 48420–48425, 2004.

[38] M. R. Sawaya, S. Sambashivan, R. Nelson, et al., "Atomic structures of amyloid cross-β spines reveal varied steric zippers," *Nature*, vol. 447, no. 7143, pp. 453–457, 2007.

[39] D. F. Moriarty and D. P. Raleigh, "Effects of sequential proline substitutions on amyloid formation by human amylin$_{20-29}$," *Biochemistry*, vol. 38, no. 6, pp. 1811–1818, 1999.

[40] D. T. S. Rijkers, J. W. M. Höppener, G. Posthuma, C. J. M. Lips, and R. M. J. Liskamp, "Inhibition of amyloid fibril formation of human amylin by N-alkylated amino acid and α-hydroxy acid residue containing peptides," *Chemistry: A European Journal*, vol. 8, no. 18, pp. 4285–4291, 2002.

[41] Y. Porat, Y. Mazor, S. Efrat, and E. Gazit, "Inhibition of islet amyloid polypeptide fibril formation: a potential role for heteroaromatic interactions," *Biochemistry*, vol. 43, no. 45, pp. 14454–14462, 2004.

[42] L.-M. Yan, M. Tatarek-Nossol, A. Velkova, A. Kazantzis, and A. Kapurniotu, "Design of a mimic of nonamyloidogenic and bioactive human islet amyloid polypeptide (IAPP) as nanomolar affinity inhibitor of IAPP cytotoxic fibrillogenesis," *Proceedings of the National Academy of Sciences of the United States of America*, vol. 103, no. 7, pp. 2046–2051, 2006.

[43] A. Abedini, F. Meng, and D. P. Raleigh, "A single-point mutation converts the highly amyloidogenic human islet amyloid polypeptide into a potent fibrillization inhibitor," *Journal of the American Chemical Society*, vol. 129, no. 37, pp. 11300–11301, 2007.

[44] R. Azriel and E. Gazit, "Analysis of the minimal amyloid-forming fragment of the islet amyloid polypeptide—an experimental support for the key role of the phenylalanine residue in amyloid formation," *Journal of Biological Chemistry*, vol. 276, no. 36, pp. 34156–34161, 2001.

[45] P. Marek, A. Abedini, B. Song, et al., "Aromatic interactions are not required for amyloid fibril formation by islet amyloid polypeptide but do influence the rate of fibril formation and fibril morphology," *Biochemistry*, vol. 46, no. 11, pp. 3255–3261, 2007.

[46] Y. Mazor, S. Gilead, I. Benhar, and E. Gazit, "Identification and characterization of a novel molecular-recognition and

self-assembly domain within the islet amyloid polypeptide," *Journal of Molecular Biology*, vol. 322, no. 5, pp. 1013–1024, 2002.

[47] L. A. Scrocchi, K. Ha, Y. Chen, L. Wu, F. Wang, and P. E. Fraser, "Identification of minimal peptide sequences in the (8–20) domain of human islet amyloid polypeptide involved in fibrillogenesis," *Journal of Structural Biology*, vol. 141, no. 3, pp. 218–227, 2003.

[48] A. Abedini and D. P. Raleigh, "The role of His-18 in amyloid formation by human islet amyloid polypeptide," *Biochemistry*, vol. 44, no. 49, pp. 16284–16291, 2005.

[49] A. Clark and M. R. Nilsson, "Islet amyloid: a complication of islet dysfunction or an aetiological factor in type 2 diabetes?" *Diabetologia*, vol. 47, no. 2, pp. 157–169, 2004.

[50] J. D. Knight and A. D. Miranker, "Phospholipid catalysis of diabetic amyloid assembly," *Journal of Molecular Biology*, vol. 341, no. 5, pp. 1175–1187, 2004.

[51] E. Sparr, M. F. M. Engel, D. V. Sakharov, et al., "Islet amyloid polypeptide-induced membrane leakage involves uptake of lipids by forming amyloid fibers," *FEBS Letters*, vol. 577, no. 1-2, pp. 117–120, 2004.

[52] D. H. J. Lopes, A. Meister, A. Gohlke, A. Hauser, A. Blume, and R. Winter, "Mechanism of islet amyloid polypeptide fibrillation at lipid interfaces studied by infrared reflection absorption spectroscopy," *Biophysical Journal*, vol. 93, no. 9, pp. 3132–3141, 2007.

[53] A. Quist, I. Doudevski, H. Lin, et al., "Amyloid ion channels: a common structural link for protein-misfolding disease," *Proceedings of the National Academy of Sciences of the United States of America*, vol. 102, no. 30, pp. 10427–10432, 2005.

[54] M. F. M. Engel, H. Yigittop, R. C. Elgersma, et al., "Islet amyloid polypeptide inserts into phospholipid monolayers as monomer," *Journal of Molecular Biology*, vol. 356, no. 3, pp. 783–789, 2006.

[55] N. Arispe, H. B. Pollard, and E. Rojas, "Giant multilevel cation channels formed by Alzheimer disease amyloid β-protein [AβP-(1–40)] in bilayer membranes," *Proceedings of the National Academy of Sciences of the United States of America*, vol. 90, no. 22, pp. 10573–10577, 1993.

[56] N. Arispe, H. B. Pollard, and E. Rojas, "The ability of amyloid β-protein [AβP (1–40)] to form Ca^{2+} channels provides a mechanism for neuronal death in Alzheimer's disease," *Annals of the New York Academy of Sciences*, vol. 747, pp. 256–266, 1994.

[57] T. A. Mirzabekov, M.-C. Lin, and B. L. Kagan, "Pore formation by the cytotoxic islet amyloid peptide amylin," *Journal of Biological Chemistry*, vol. 271, no. 4, pp. 1988–1992, 1996.

[58] B. Konarkowska, J. F. Aitken, J. Kistler, S. Zhang, and G. J. S. Cooper, "The aggregation potential of human amylin determines its cytotoxicity towards islet β-cells," *FEBS Journal*, vol. 273, no. 15, pp. 3614–3624, 2006.

[59] A. Demuro, E. Mina, R. Kayed, S. C. Milton, I. Parker, and C. G. Glabe, "Calcium dysregulation and membrane disruption as a ubiquitous neurotoxic mechanism of soluble amyloid oligomers," *Journal of Biological Chemistry*, vol. 280, no. 17, pp. 17294–17300, 2005.

[60] Y. Porat, S. Kolusheva, R. Jelinek, and E. Gazit, "The human islet amyloid polypeptide forms transient membrane-active prefibrillar assemblies," *Biochemistry*, vol. 42, no. 37, pp. 10971–10977, 2003.

[61] K. Balali-Mood, R. H. Ashley, T. Hauß, and J. P. Bradshaw, "Neutron diffraction reveals sequence-specific membrane insertion of pre-fibrillar islet amyloid polypeptide and inhibition by rifampicin," *FEBS Letters*, vol. 579, no. 5, pp. 1143–1148, 2005.

[62] T. A. Harroun, J. P. Bradshaw, and R. H. Ashley, "Inhibitors can arrest the membrane activity of human islet amyloid polypeptide independently of amyloid formation," *FEBS Letters*, vol. 507, no. 2, pp. 200–204, 2001.

[63] J. D. Green, L. Kreplak, C. Goldsbury, et al., "Atomic force microscopy reveals defects within mica supported lipid bilayers induced by the amyloidogenic human amylin peptide," *Journal of Molecular Biology*, vol. 342, no. 3, pp. 877–887, 2004.

[64] J. J. Meier, R. Kayed, C.-Y. Lin, et al., "Inhibition of human IAPP fibril formation does not prevent β-cell death: evidence for distinct actions of oligomers and fibrils of human IAPP," *American Journal of Physiology*, vol. 291, no. 6, pp. E1317–E1324, 2006.

[65] M. Bucciantini, E. Giannoni, F. Chiti, et al., "Inherent toxicity of aggregates implies a common mechanism for protein misfolding diseases," *Nature*, vol. 416, no. 6880, pp. 507–511, 2002.

[66] J. I. Kourie, A. L. Culverson, P. V. Farrelly, C. L. Henry, and K. N. Laohachai, "Heterogeneous amyloid-formed ion channels as a common cytotoxic mechanism: implications for therapeutic strategies against amyloidosis," *Cell Biochemistry and Biophysics*, vol. 36, no. 2-3, pp. 191–207, 2002.

[67] J. R. Brender, U. H. N. Dürr, D. Heyl, M. B. Budarapu, and A. Ramamoorthy, "Membrane fragmentation by an amyloidogenic fragment of human islet amyloid polypeptide detected by solid-state NMR spectroscopy of membrane nanotubes," *Biochimica et Biophysica Acta*, vol. 1768, no. 9, pp. 2026–2029, 2007.

[68] C.-J. Huang, C.-Y. Lin, L. Haataja, et al., "High expression rates of human islet amyloid polypeptide induce endoplasmic reticulum stress-mediated β-cell apoptosis, a characteristic of humans with type 2 but not type 1 diabetes," *Diabetes*, vol. 56, no. 8, pp. 2016–2027, 2007.

[69] C.-Y. Lin, T. Gurlo, R. Kayed, et al., "Toxic human islet amyloid polypeptide (h-IAPP) oligomers are intracellular, and vaccination to induce anti-toxic oligomer antibodies does not prevent h-IAPP-induced β-cell apoptosis in h-IAPP transgenic mice," *Diabetes*, vol. 56, no. 5, pp. 1324–1332, 2007.

[70] S. Andrikopoulos, C. B. Verchere, J. C. Teague, et al., "Two novel immortal pancreatic β-cell lines expressing and secreting human islet amyloid polypeptide do not spontaneously develop islet amyloid," *Diabetes*, vol. 48, no. 10, pp. 1962–1970, 1999.

[71] M. F. M. Engel, L. Khémtemourian, C. Kleijer, et al., "Membrane damage by human islet amyloid polypeptide through fibril growth at the membrane," *Proceedings of the National Academy of Sciences of the United States of America*, vol. 105, no. 16, pp. 6033–6038, 2008.

[72] M. Wogulis, S. Wright, D. Cunningham, T. Chilcote, K. Powell, and R. E. Rydel, "Nucleation-dependent polymerization is an essential component of amyloid-mediated neuronal cell death," *Journal of Neuroscience*, vol. 25, no. 5, pp. 1071–1080, 2005.

[73] H. Zhao, A. Jutila, T. Nurminen, S. A. Wickström, J. Keski-Oja, and P. K. J. Kinnunen, "Binding of endostatin to phosphatidylserine-containing membranes and formation of amyloid-like fibers," *Biochemistry*, vol. 44, no. 8, pp. 2857–2863, 2005.

[74] H. Zhao, E. K. J. Tuominen, and P. K. J. Kinnunen, "Formation of amyloid fibers triggered by phosphatidylserine-containing

membranes," *Biochemistry*, vol. 43, no. 32, pp. 10302–10307, 2004.

[75] G. P. Gellermann, T. R. Appel, A. Tannert, et al., "Raft lipids as common components of human extracellular amyloid fibrils," *Proceedings of the National Academy of Sciences of the United States of America*, vol. 102, no. 18, pp. 6297–6302, 2005.

[76] S. Gilead, H. Wolfenson, and E. Gazit, "Molecular mapping of the recognition interface between the islet amyloid polypeptide and insulin," *Angewandte Chemie International Edition*, vol. 45, no. 39, pp. 6476–6480, 2006.

[77] P. Westermark, Z.-C. Li, G. T. Westermark, A. Leckström, and D. F. Steiner, "Effects of β cell granule components on human islet amyloid polypeptide fibril formation," *FEBS Letters*, vol. 379, no. 3, pp. 203–206, 1996.

[78] E. T. A. S. Jaikaran, M. R. Nilsson, and A. Clark, "Pancreatic β-cell granule peptides form heteromolecular complexes which inhibit islet amyloid polypeptide fibril formation," *Biochemical Journal*, vol. 377, part 3, pp. 709–716, 2004.

[79] I. Rustenbeck, A. Matthies, and S. Lenzen, "Lipid composition of glucose-stimulated pancreatic islets and insulin-secreting tumor cells," *Lipids*, vol. 29, no. 10, pp. 685–692, 1994.

[80] T. Konno, S. Oiki, and T. Morii, "Synergistic action of polyanionic and non-polar cofactors in fibrillation of human islet amyloid polypeptide," *FEBS Letters*, vol. 581, no. 8, pp. 1635–1638, 2007.

Hindawi Publishing Corporation
Experimental Diabetes Research
Volume 2008, Article ID 697035, 8 pages
doi:10.1155/2008/697035

Research Article

Human Islet Amyloid Polypeptide Transgenic Mice: In Vivo and Ex Vivo Models for the Role of hIAPP in Type 2 Diabetes Mellitus

J. W. M. Höppener,[1,2] H. M. Jacobs,[1,3] N. Wierup,[4] G. Sotthewes,[1] M. Sprong,[1,3] P. de Vos,[5] R. Berger,[1,2] F. Sundler,[4] and B. Ahrén[6]

[1] *Division of Biomedical Genetics, Department of Metabolic and Endocrine Diseases, University Medical Center Utrecht, P.O. Box 85090, 3508 AB Utrecht, The Netherlands*
[2] *Netherlands Metabolomics Centre, location Utrecht, P.O. Box 85090, 3508 AB Utrecht, The Netherlands*
[3] *Division Laboratories and Pharmacy, Department of Endocrinology, University Medical Center Utrecht, P.O. Box 85090, 3508 AB Utrecht, The Netherlands*
[4] *Department of Experimental Medical Sciences, Lund University, BMC, C 12, S-221 84 Lund, Sweden*
[5] *Division of Medical Biology, Department of Pathology and Laboratory Medicine, University of Groningen, Hanzeplein 1, 9700 RB, Groningen, The Netherlands*
[6] *Department of Clinical Sciences, Lund University, BMC, C 12, S-221 84 Lund, Sweden*

Correspondence should be addressed to J. W. M. Höppener, j.w.m.hoeppener@umcutrecht.nl

Received 9 October 2007; Revised 30 January 2008; Accepted 14 February 2008

Recommended by Hiroshi Okamoto

Human islet amyloid polypeptide (hIAPP), a pancreatic islet protein of 37 amino acids, is the main component of islet amyloid, seen at autopsy in patients with type 2 diabetes mellitus (DM2). To investigate the roles of hIAPP and islet amyloid in DM2, we generated transgenic mice expressing hIAPP in their islet beta cells. In this study, we found that after a long-term, high-fat diet challenge islet amyloid was observed in only 4 of 19 hIAPP transgenic mice. hIAPP transgenic females exhibited severe glucose intolerance, which was associated with a downregulation of GLUT-2 mRNA expression. In isolated islets from hIAPP males cultured for 3 weeks on high-glucose medium, the percentage of amyloid containing islets increased from 5.5% to 70%. This ex vivo system will allow a more rapid, convenient, and specific study of factors influencing islet amyloidosis as well as of therapeutic strategies to interfere with this pathological process.

1. INTRODUCTION

Islet amyloid polypeptide (IAPP), also referred to as amylin, is a 37 amino acid protein produced in the pancreatic islet beta cells. Human IAPP (hIAPP) is implicated in the pathophysiology of type 2 diabetes mellitus (DM2) since it forms proteinaceous tissue deposits in the pancreatic islets ("islet amyloid") [1–3]. Islet amyloid has been demonstrated in more than 80% of patients with DM2 [4, 5]. Islet amyloid formation is implicated in development of beta cell failure which, in addition to insulin resistance, is a characteristic of DM2 [6]. Overproduction of IAPP in insulin resistance may occur due to common transcription regulatory elements in the promoter regions of the IAPP and insulin genes [7], and this might underly the enhanced amyloid formation in DM2 [3]. This in turn may induce impairment of beta cell function since aggregation of hIAPP has been demonstrated to be cytotoxic [8–10]. However, involvement of islet amyloid in development of DM2 is still not firmly established. Recent data, both for hIAPP and for other amyloidogenic proteins (notably the Alzheimer's disease-related Abeta peptide), indicate that the degree of amyloid formation does not correspond with the severity of disease [11, 12]. In addition, prefibrillar aggregates of amyloidogenic proteins seem to be more cytotoxic than mature amyloid fibrils [13, 14]. To explore the potential diabetogenic effects of hIAPP and islet amyloid, we have generated transgenic mice overproducing biologically active hIAPP in the islet beta cells [15–17]

(mouse IAPP does not form islet amyloid). We previously showed that hIAPP overexpression in itself does not induce hyperglycemia, hyperinsulinemia, or obesity in these mice [15]. However, when the hIAPP transgenic mice were crossbred with leptin-deficient and insulin-resistant ob/ob mice, extensive islet amyloid formation with worsening of the diabetes was observed [18]. In the present paper, we describe two experimental studies. In an in vivo experiment, we examined the influence of transgenic hIAPP expression on glucose tolerance of mice on a high-fat diet for a long period of time. Previous studies had shown that long-term, high-fat diet induces hyperglycemia, hyperinsulinemia, and obesity in mice [19, 20]. Furthermore, high-fat diet may be involved in islet amyloid formation in hIAPP transgenic mice [21]. We, thus, administered a high-fat diet for 14 months to hIAPP transgenic and nontransgenic (control) mice and report here the islet amyloid formation, glucose tolerance, and islet GLUT-2 mRNA expression. In addition, we describe the development of an ex vivo model system for islet amyloidosis, using pancreatic islets isolated from the hIAPP transgenic mice. When such islets were cultured in high-glucose medium, amyloid formation occurs more rapidly as compared to the in vivo situation. Thus, this ex vivo model system will enable to study the process and effects of islet amyloid formation more specifically and conveniently.

2. MATERIALS AND METHODS

2.1. Animals

The generation of C57Bl/6J hIAPP transgenic mice with a rat insulin-2 gene promoter fragment (position −695 to +8 relative to the transcription start site) linked to the hIAPP gene has previously been described [15]. The hIAPP transgenic mice were maintained by breeding heterozygous transgenic mice with mates of the C57BL/6J strain. Transgenic mice were differentiated from nontransgenic (NT) littermates by dot blot Southern hybridization, using a 588 bp hIAPP-specific DNA probe [15]. Mice were housed on hardwood bedding in polypropylene cages and maintained in air-conditioned rooms at 20–22°C with a photoperiod of 12 hours light, 12 hours dark. Water was available continuously and the mice received ad libitum a regular diet until 2.5 months of age. This diet contained 4,500 kcal/kg and included 22.5% protein and 4.8% fat (Hope Farms, Woerden, The Netherlands). At 2.5 months of age, the diet was switched to a high-fat diet for 14 months containing 5,600 kcal/kg, 20.8% protein, and 36.0% fat (30.0% cocoa oil, 6.0% corn oil; Hope Farms).

2.2. Glucose tolerance test

At 14 months after the start of the high-fat diet, non-fasted mice were anaesthetized with an i.p. injection of midazolam (0.4 mg/mouse) (Dormicum, Hoffman-La-Roche, Basel, Switzerland), and a combination of fluanison (0.9 mg/mouse), and fentanyl (0.02 mg/mouse) (Hypnorm, Janssen, Beerse, Belgium). D-glucose (British Drug Houses, Poole, UK) was injected i.p. (1 g/kg) and blood was sampled from the retrobulbar, intraorbital, capillary plexus before glucose administration and after 10, 30, 60, and 120 minutes. The samples were taken in heparinized tubes and stored on ice. Following centrifugation, plasma was separated and stored at −20°C until analysis. After the 120-minute blood sample, tissue was sampled (see below), and trunk blood was obtained for measurement of IAPP levels. The blood was collected in EDTA-tubes and kept on ice until centrifugation at 1500 g for 5 minutes at 4°C. Plasma was stored at −80°C.

All animal experiments were approved by the Animal Welfare Committee of Utrecht University/University Medical Center Utrecht, The Netherlands.

2.3. Plasma measurements

IAPP levels were measured in 25–100 ul plasma by RIA as described [15], using a rabbit, polyclonal hIAPP antiserum (K1338) that shows full cross-reactivity with synthetic amidated rat/mouse IAPP [22]. Free and bound radioactivity was separated by use of double antibody immunoprecipitation. The sensitivity of the assay is 3.5 pmol/l and the coefficiency of variation <10% at both low and high levels. Insulin levels were measured in 20 ul plasma by RIA using guinea pig anti-rat insulin antibody, ^{125}I-labelled human insulin as tracer and rat insulin as standard (Linco Research, St. Charles, Mo, USA). Free and bound radioactivity was separated by use of an anti-IgG antibody (Linco). The sensitivity of the assay is 12 pmol/l and the coefficiency of variation <3% at both low and high levels. Glucose was determined in 10 ul plasma by the glucose oxidase method.

2.4. Histological analysis of pancreatic tissue

Pancreatic tissue samples were fixed in 3.7% phosphate-buffered formalin (pH 7.4) for 24–48 hours and paraffin embedded. Sections of 5 μm were stained with Congo red for detection of islet amyloid by polarized light microscopy ("apple-green" birefringence) and fluorescence light microscopy (red-coloured autofluorescence). At least 10 islets per mouse were examined. The percentage of individual islet areas occupied by amyloid, as indicated by Congo red positive staining, was visually estimated and scored as follows: 0% = score 0, between 0 and 26% = score 1, 26–50% = score 2, 51–75% = score 3, and 76–100% = score 4. The Amyloid Index (range: 0–100) of an individual mouse was calculated as $(1 \times N1 + 2 \times N2 + 3 \times N3 + 4 \times N4) \times 25/n$, where $N1$ is the number of islets with score 1, $N2$ the number with score 2, and so on, and n is the total number of islets investigated. The degree of islet amyloid formation was determined with the investigator being unaware of the genetic status of the animals (i.e., "blind").

To examine the cellular expression of GLUT-2 mRNA, paraffin sections were subjected to in situ hybridization using a previously described protocol [23] and a ^{35}S-labelled oligonucleotide probe covering the nucleotide sequence 247–276 of mouse GLUT-2 cDNA [24]. In order to confirm beta cell expression of hIAPP mRNA in the transgenic mice,

sections were also hybridized with a ^{35}S-labelled oligonucleotide probe specific for hIAPP mRNA [25].

2.5. Image analysis and morphometry

In situ hybridization radiolabelling was examined in a bright field microscope (Olympus, BX60), and images were captured with a digital camera (Olympus, DP50). To quantify the density of labelling for GLUT-2 mRNA within islets, areas of in situ hybridization radiolabelling were calculated. Islets (n = 5–8 per animal) were randomly selected from different parts of the sections from 4 mice, 2 males and 2 females in each group. The transgenic mice analyzed were rated as negative for amyloid. The labelled area, that is, grain density within an islet, and total islet area were measured, using NIH-image software, and the density of labelling was expressed as percentage of the total islet area [23, 26]. All sections used were hybridized simultaneously and under identical conditions.

2.6. Isolation of pancreatic islets

For islet isolation, transgenic mice were bred to homozygosity for the hIAPP transgenic locus. Homozygotes were discriminated from heterozygous and nontransgenic littermates by dot blot Southern hybridization of tail DNA using a human-specific IAPP probe [15] and quantification of the hybridization signal using phosphor imaging and Image-Quant software (Molecular Dynamics, Inc. Krefeld, Germany).

Islets were isolated from the pancreas of 6-month-old hIAPP transgenic male mice, essentially as previously described [27]. Briefly, under halothane anaesthesia, the abdomen was opened. The pancreas was excised starting from the spleen site to the duodenum. Subsequently, the pancreas was brougth in 10 mL sterile Krebs-Ringer-buffer supplemented with 25 mmol/L Hepes (KRH) and containing 10% Bovine Serum Albumin (BSA) at 4°C. Next, the pancreas was chopped, digested using a two-stage incubation of 20 minutes at 37°C with successively 1.0 and 0.7 mg/mL collagenase (Sigma type XI, Sigma, St Louis, MO, USA). Islets were separated from exocrine tissue by centrifugation over a discontinuous dextran gradient [28] and further purified by handpicking into 9 cm petridishes with 12 mL KRH buffer, pH = 7.4, supplemented with 10% BSA penicillin (100 units/mL)/streptomycin (0.1 mg/mL) (KRH 10% BSA P/S) and glucose to a concentration of 11 mM. Two days after isolation, the islets from 12 mice were pooled, mixed and split into portions. Four portions of 75 islets each were fixed and embedded for amyloid quantification. Eight portions of approximately 90 islets were transferred to culture medium with 28 mM glucose. Medium was changed every 2-3 days, switching between 11 mM and 28 mM of glucose (to prevent possible desensitization of the beta cells). Islets were counted, while being picked into the dishes with fresh medium. At 3 weeks after islet isolation, the cultured islets were fixed and embedded for amyloid quantification.

2.7. Fixation and embedding of pancreatic islets

Islets were washed with phosphate buffered saline (PBS), and fixed in 0.5 mL islets fixative (2% paraformaldehyde, 0.2% glutaraldehyde in 0.1 M Sörensen buffer) for 2 hours at room temperature. Fixative was removed and islets were washed with 0.5 mL 0.1 M Sörensen buffer. Sörensen buffer was removed and islets were resuspended in 30 μl 37°C heated 12% gelatin, cooled on ice and stored at −20°C.

2.8. Amyloid quantification in cultured islets

From the gelatin-embedded islet blocks, 5 μm frozen sections were cut onto Superfrost Plus microscope slides (Menzel-Gläser) and stored at −20°C until further use. Sections were fixed in acetone for 1′, rehydrated in PBS for 15′, stained with heamatoxylin for 1′, washed in running tap water for 5′, and stained with Congo red (1 g/liter saturated sodium chloride 80% ethanol, into which 10 mL/liter 1% sodium hydroxide was added just before staining) for 30′. After dehydration in an augmenting ethanol series (70%, 96%, 100%) and xylene (twice), sections were enclosed with Depex. Amyloid-containing paraffin sections of hIAPP transgenic mouse pancreatic tissue were used as positive control for the Congo red staining.

For the detection of amyloid, Congo red-stained islet sections were examined using a fluorescence microscope. Amyloid deposits were visible as bright red autofluorescent areas without cells, which showed a green birefringence upon visualization with polarized light. An islet was scored as amyloid positive if at least 2 successive sections of that islet contained Congo red-positive amyloid deposits. The scoring was performed in a "blind" fashion, that is, with the investigator unaware of the source of the islets.

2.9. Statistical analysis

Values are means ±SEM, unless stated otherwise. P-values indicate the probability level of random difference between groups, or of random correlation, respectively. P-values <.05 were considered to represent statistical significance. Nonparametric T-tests were used to compare 2 independent samples (Mann-Whitney-U test: hIAPP versus NT, male versus female). Data of the mRNA in situ hybridizations were analyzed by Student's unpaired t-test. Differences in percentage of amyloid-positive islets between 2 days and 3 weeks of culture were analyzed by use of one-way analysis of variance (ANOVA). Probability values of less than .01 were considered significant.

3. RESULTS

3.1. Body weight and plasma IAPP levels

Body weight after 14 months on the high-fat diet did not differ between the groups, being 57 ± 0.8 g versus 58 ± 0.9 g in male hIAPP (n = 8) and NT (n = 5) mice, and 59 ± 1.1 g versus 64 ± 3 g in female hIAPP (n = 11) and NT (n = 6) mice. Plasma IAPP levels were 462 ± 78 pmol/L in male hIAPP mice versus 195 ± 32 pmol/L in male NT mice,

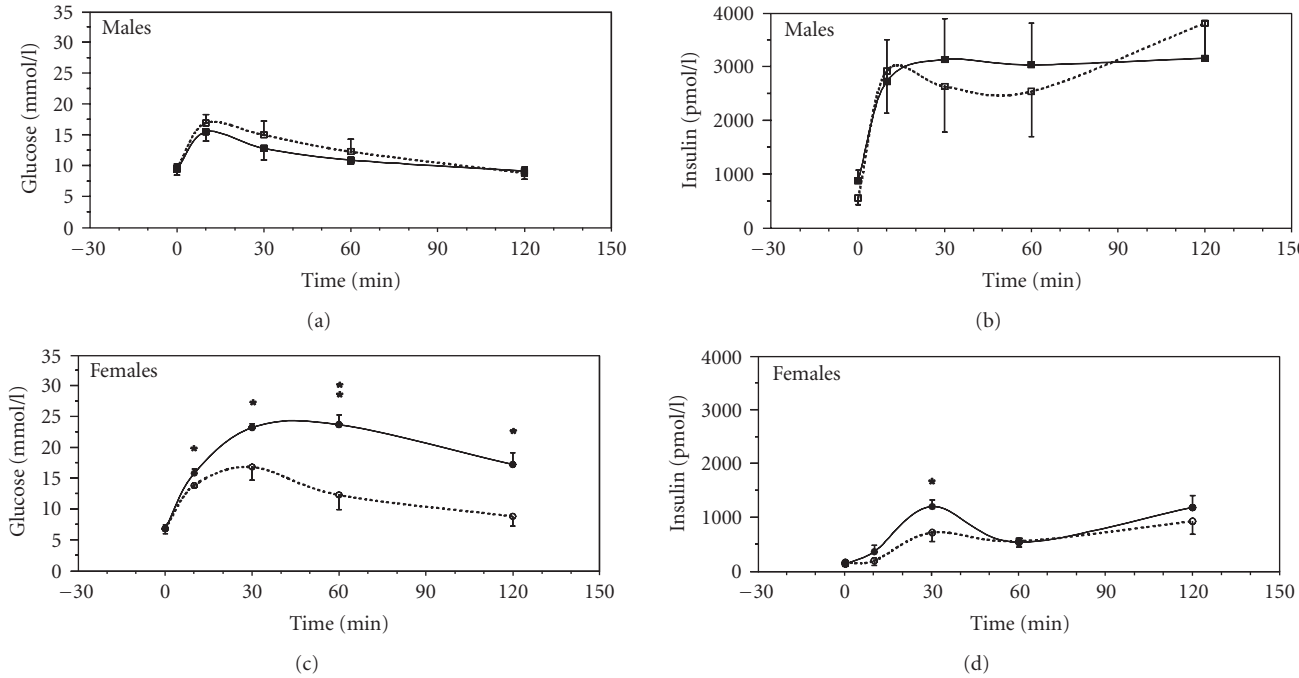

Figure 1: Plasma insulin and glucose levels immediately before and at different timepoints after an intraperitoneal injection of glucose (1 g/kg body weight) in anaesthetized, nonfasted nontransgenic (NT, dotted line), and hIAPP transgenic mice (solid line) on a high-fat diet for 14 months. Mean values and SEM are shown; $n = 5$–11 per group of mice; statistically significant changes between hIAPP and NT mice are indicated by $^{*}(P < .05)$ and $^{**}(P < .01)$.

and 346 ± 81 pmol/L in female hIAPP mice versus 130 ± 21 pmol/L in female NT mice, being significantly higher in hIAPP mice of both genders ($P < .01$) without any gender difference.

3.2. Glucose tolerance test

After 14 months on the high-fat diet, nonfasted plasma glucose and insulin levels were not different between hIAPP and NT mice of the same gender. However, both for the hIAPP and NT mice, plasma insulin levels were higher in males as compared to females (Figure 1). When glucose was administered i.p. (1 g/kg), the insulin response to glucose and the glucose elimination were similar in hIAPP and NT male mice. In contrast, in female hIAPP mice, plasma glucose levels after the i.p. glucose challenge were markedly higher at all time points as compared to female NT mice ($P < .05$ or $P < .01$) in association with increased insulin levels 30 minutes after glucose administration ($P < .01$). Hence, hIAPP overproduction was associated with severe impairment of glucose elimination in female but not in male mice after high-fat diet.

3.3. Pancreatic islet amyloid formation

Islet amyloid was detected in 4/19 hIAPP mice on high-fat diet but in none of the 11 NT mice. The Amyloid Index for these 4 mice was 11.0 ± 6.2 (average and SD). There was no gender difference in islet amyloid formation in hIAPP transgenic mice (3/8 in males versus 1/11 in females).

3.4. Islet GLUT-2 mRNA expression

As expected, a strong hIAPP mRNA labeling was observed in the islets of all transgenic mice, while it was lacking in all NT mice (Figures 2(a), 2(b)). GLUT-2 mRNA labeling of weak to moderate density was observed in the islets of NT mice (Figure 2(c)), with no overt difference between female and male mice. In the transgenic mice, however, the GLUT-2 mRNA labeling was generally weaker, and even barely detectable in some female mice (Figure 2(d)). The GLUT-2 mRNA signal was reduced in all transgenic mice, regardless of the presence or absence of islet amyloid. Image analysis revealed a significant reduction of GLUT-2 mRNA labeling of islets in hIAPP transgenic versus NT mice ($P = .02$, Figure 3).

3.5. Ex vivo survival and amyloid formation in cultured hIAPP transgenic pancreatic islets

The percentage of 3-week survival of hIAPP transgenic islets was 83.8 ± 1.0% ($n = 8$). Of all islet cultures, 22–30 islets were scored for the presence of amyloid. The percentage of amyloid-positive islets significantly increased ($P < .001$) from 5.5±3.4% ($n = 4$) after 2 days of culture to 70 ± 3.1% ($n = 8$) at the end of the culture period. Thus, the percentage of amyloid-positive islets increased more than 10 times in three weeks of culture at high glucose conditions in this ex vivo islet amyloidosis system. An example of a cultured hIAPP transgenic islet containing amyloid is shown in Figure 4.

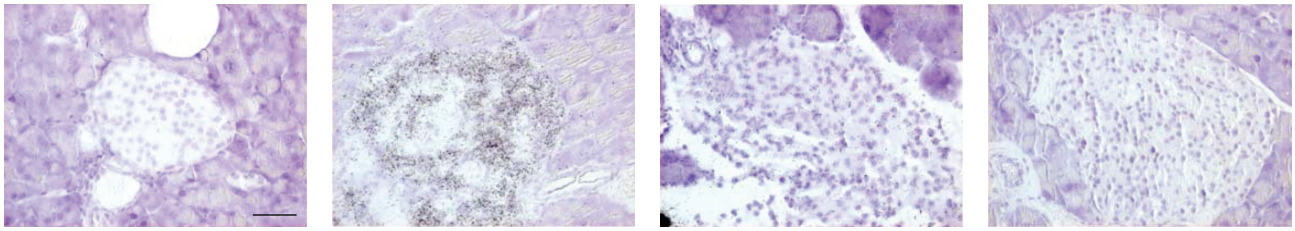

(a) (b) (c) (d)

Figure 2: In situ mRNA hybridization (using radiolabeled oligoprobes) for hIAPP (a), (b), and GLUT-2 (c), (d) in islets of nontransgenic (a), (c), and hIAPP transgenic (b), (d) female mice after 14 months on high-fat diet. Note that hIAPP mRNA expression is absent in the nontransgenic islet, and that GLUT-2 mRNA expression is reduced in the transgenic islet. Scale bar = 30 μm.

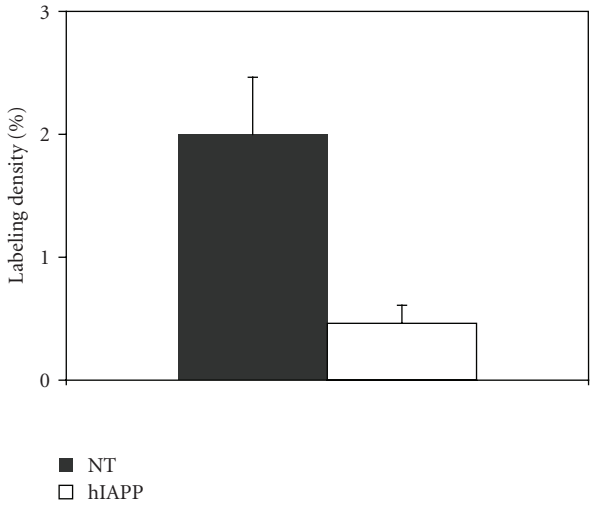

Figure 3: Comparison of the average labeling density of GLUT-2 mRNA in situ hybridization in pancreatic islets from nontransgenic (NT) and hIAPP transgenic (hIAPP) mice (P = .02). For both groups 4 mice were analysed, 2 males, and 2 females. The 4 transgenic mice did not have amyloid.

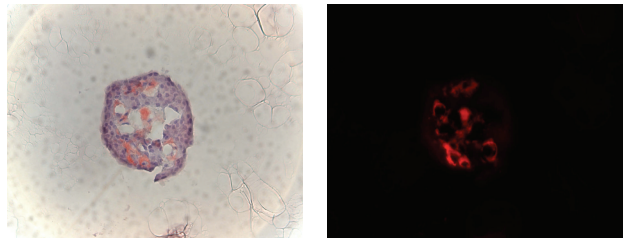

(a) (b)

Figure 4: Detection of islet amyloid in islet of Langerhans isolated from an hIAPP transgenic mouse, and cultured in medium with a high glucose concentration. Frozen section of a gelatine-embedded islet was stained with the amyloid-specific dye Congo red and visualized with light microscopy (a) and fluorescence microscopy (b), respectively.

4. DISCUSSION

4.1. High-fat diet and amyloid formation

In this study, transgenic mice overproducing the amyloidogenic hIAPP in their pancreatic islet beta cells, as well as NT control mice, were fed a high-fat diet for 14 months, in order to evaluate the impact on islet amyloid formation and glucose homeostasis when combining these two potentially diabetogenic factors. We anticipated a marked islet amyloid formation in the hIAPP transgenic mice on the high-fat diet because we previously observed that crossbreeding the hIAPP transgenic mice with the Obese mouse (being severly insulin resistant) resulted in extensive islet amyloid formation [18]. Also, when insulin resistance was induced in hIAPP mice by crossbreeding with the obese Agouti viable yellow mice [29] or by exogenous growth hormone and glucocorticoids [30], islet amyloid formation was promoted. In addition, high-fat feeding induced islet amyloid formation in approximately 80% of male mice in another hIAPP transgenic colony [21]. However, we found that only four out of the 19 hIAPP mice (approx. 40% of the males) that were followed for 14 months on the high-fat diet did develop islet amyloid. This lower frequency might be due to differences in the genetic background and/or the composition of the diet, influencing insulin resistance and IAPP expression. The amyloid index in those four high-fat fed mice was higher than in six of 33 similarly aged hIAPP mice (approx. 30% of the males) which developed amyloid on a regular diet (11.0 ± 6.2 versus 4.2 ± 2.9, P = .024) [18]. This indicates that although long-term, high-fat diet indeed has the capacity to promote islet amyloid formation in these hIAPP transgenic mice, the efficiency is not high. Crossbreeding the hIAPP mice with leptin-deficient Obese mice introduced more severe obesity and insulin resistance [18] as compared to the high-fat diet. Consequently, these other factors seem of importance for the promotion of islet amyloid formation. Another factor might be hyperglycemia, which is more severe in the hIAPP ob/ob mice as compared to the hIAPP mice on high-fat diet. Such a hypothesis is supported by the finding that in isolated pancreatic islets of our hIAPP mice, islet amyloid was detected by electron microscopy after culture in high-glucose medium but not in low-glucose medium [31]. Other mechanisms may, however, also be of importance.

4.2. High fat diet and glucose tolerance

In this study, we also observed severe glucose intolerance in female but not in male hIAPP transgenic mice. The finding that in all groups of mice plasma insulin levels failed to return to basal within 2 hours after the glucose load is in accordance with high-fat diet inducing insulin resistance [32]. Also, the higher insulin levels in male mice versus female mice is well known from previous studies [33]. Thus, our data indicate that the overproduction of insulin in response to insulin resistance after high-fat diet was adequate in hIAPP males but not in hIAPP females. Since there was no gender difference in the amyloid formation in high-fat fed hIAPP mice, these results suggest that a metabolic impact of high levels of circulating IAPP underlies the gender difference in glucose tolerance of hIAPP transgenic mice after high-fat diet. IAPP has, thus, been shown to inhibit insulin secretion [34, 35] as well as to inhibit glycogen synthesis in rat muscle tissue [36] through inhibition of glycogen synthase and stimulation of glycogen phosphorylase [37]. In addition, it has been observed that IAPP administration induces insulin resistance in rats [38], although no such effect was evident in humans [39]. IAPP has also in some studies [40] but not in others [41] been shown to increase liver glucose production. Whether these actions show gender differences, and thus may explain the remarkable glucose intolerance observed in female but not in male hIAPP transgenic mice on the high-fat diet, is not known. Indeed, it is striking that although male rodents generally are more prone to insulin resistance than females, the hIAPP transgenic females on high-fat diet are more glucose intolerant than their male littermates. Since insulin levels are not lower in the hIAPP females compared to the NT females, these data suggest that insulin sensitivity is impaired in the female hIAPP mice.

4.3. High-fat diet and GLUT-2 expression

Islet GLUT-2 mRNA expression was reduced in hIAPP transgenic versus NT mice, and this reduction appeared more severe in female than in male mice. Beta cell GLUT-2 expression is known to correlate with glucose responsiveness of the cells [42]. However, insulin levels were not reduced in the male or female hIAPP mice. Therefore, it is presently not known if and how the reduced GLUT-2 mRNA expression among the transgenic mice might be related to the glucose intolerance in the female hIAPP mice. Also, the mechanism of hIAPP mediated downregulation of islet GLUT-2 mRNA expression is unknown, but our data indicate that in addition to inhibition of insulin action in muscle [33, 34] IAPP can (in) directly inhibit glucose responsiveness of islet beta cells by affecting GLUT-2 expression.

In conclusion, this in vivo study shows that promoting insulin resistance over a long period of time by giving a high-fat diet for 14 months promotes islet amyloid formation in hIAPP transgenic mice, although less extensively than in the severe insulin-resistant Obese, leptin-deficient hIAPP mice. This suggests that the degree of insulin resistance is important for extensive development of islet amyloid. In addition, we observed a remarkable gender difference in that severe glucose intolerance was observed only in female hIAPP transgenic mice given high-fat diet and not in males. We suggest that this gender difference is due to the high level of circulating IAPP rather than to islet amyloid formation. If and how this glucose intolerance might be mediated by downregulation of beta cell GLUT-2 gene expression, as observed in the hIAPP mice, is presently unknown.

4.4. Ex vivo islet amyloidosis model

The rationale for the ex vivo study was to examine if amyloid would be formed in isolated and cultured pancreatic islets from hIAPP mice, to such a degree that it would be detectable with light microscopy. Since both the present and previous [18] in vivo data indicated the development of islet amyloid notably in male hIAPP mice, we decided to investigate amyloid formation in such islets specifically from male mice. To increase the potential for amyloid formation, we bred the mice to homozygosity for the hIAPP transgene. At an age of 6 months, homozygous transgenic hIAPP males had islet amyloid in about 5% of their pancreatic islets, at 2 days after islet isolation. Previously, we detected amyloid fibrils by electron microscopy in islets from 4–10 months old heterozygous hIAPP transgenic mice, cultured for 1 week in medium with 11 or 28 mM glucose [31]. With the present model, using islets from 6-month-old homozygous hIAPP transgenic males, cultured in medium with high glucose (switching between 11 and 28 mM), we can detect amyloid deposits with Congo red staining and light microscopy, thus enabling quantification of the degree of islet amyloidosis. The number of amyloid-positive islets increased more than 10 fold (from 5.5 to 70%) after 3 weeks of culture in medium containing a high glucose concentration. Although an accurate comparison between the degrees of islet amyloid formation in vivo and ex vivo was not made, our data certainly indicate stronger islet amyloid formation in hIAPP islets cultured ex vivo as compared to in vivo. This might be explained by the higher glucose concentrations in the ex vivo system. hIAPP transgenic mice in vivo have normal plasma glucose concentrations [15, 18], whereas ex vivo the glucose concentration in the medium switched between 11 and 28 mM. It is known that a high glucose concentration triggers both insulin and IAPP secretion, and the hIAPP transgene is under control of an insulin promoter. In addition, macrophages have been implicated in in vivo removal of (beginning) amyloid deposits [43] and such macrophages are absent in the ex vivo system, potentially allowing increased amyloid formation. When combined with a more accurate amyloid quantification procedure involving image analysis, this ex vivo system may present a fast and convenient model to study the process (and factors involved) of islet amyloidosis, as well as the detrimental consequences for individual beta cells (apoptosis) and islet function (insulin producing capacity). In addition, such a model system might be used as an amyloidosis assay to assess the potency of known and novel therapeutic strategies, aimed at reducing, or even preventing, islet amyloid formation, and its effects on beta cell and islet function.

ACKNOWLEDGMENTS

The authors wish to thank Lena Kvist (Lund University, Lund), Bart de Haan (University of Groningen), Gerard Graad (Department of Endocrinology, UMC Utrecht), Renske Luneborg-Van Netten (Department of Pathology, UMC Utrecht), Herma Boere and Toon Hesp (Animal House Utrecht University) for expert technical assistance and Dr. P. Westers (Center for Biostatistics, Utrecht University) for advice on statistical analyses. This study was supported by grants from the Dutch Diabetes Fund (Grant DFN 92.133) as well as from the Swedish Medical Research Council (Grants no. 14X-6834 and 72X-4499), Albert Påhlsson, Novo Nordic and Crafoord Foundations, Swedish Diabetes Association.

REFERENCES

[1] P. Westermark, C. Wernstedt, E. Wilander, D. W. Hayden, T. D. O'Brien, and K. H. Johnson, "Amyloid fibrils in human insulinoma and islets of Langerhans of the diabetic cat are derived from a neuropeptide-like protein also present in normal islet cells," *Proceedings of the National Academy of Sciences of the United States of America*, vol. 84, no. 11, pp. 3881–3885, 1987.

[2] S. E. Kahn, S. Andrikopoulos, and C. B. Verchere, "Islet amyloid: a long-recognized but underappreciated pathological feature of type 2 diabetes," *Diabetes*, vol. 48, no. 2, pp. 241–253, 1999.

[3] J. W. M. Höppener, B. Ahrén, and C. J. M. Lips, "Islet amyloid and type 2 diabetes mellitus," *The New England Journal of Medicine*, vol. 343, no. 6, pp. 411–419, 2000.

[4] P. Westermark, "Fine structure of islets of Langerhans in insular amyloidosis," *Virchows Archiv*, vol. 359, no. 1, pp. 1–18, 1973.

[5] A. Clark, C. A. Wells, I. D. Buley, et al., "Islet amyloid, increased A-cells, reduced B-cells and exocrine fibrosis: quantitative changes in the pancreas in type 2 diabetes," *Diabetes Research*, vol. 9, no. 4, pp. 151–159, 1988.

[6] C. J. Rhodes, "Type 2 diabetes-a matter of β-cell life and death?" *Science*, vol. 307, no. 5708, pp. 380–384, 2005.

[7] M. German, L. G. Moss, J. Wang, and W. J. Rutter, "The insulin and islet amyloid polypeptide genes contain similar cell-specific promoter elements that bind identical B-cell nuclear complexes," *Molecular Cell Biology*, vol. 12, no. 4, pp. 1777–1788, 1992.

[8] A. Lorenzo, B. Razzaboni, G. C. Weir, and B. A. Yankner, "Pancreatic islet cell toxicity of amylin associated with type-2 diabetes mellitus," *Nature*, vol. 368, no. 6473, pp. 756–760, 1994.

[9] J. Janson, R. H. Ashley, D. Harrison, S. McIntyre, and P. C. Butler, "The mechanism of islet amyloid polypeptide toxicity is membrane disruption by intermediate-sized toxic amyloid particles," *Diabetes*, vol. 48, no. 3, pp. 491–498, 1999.

[10] J. W. M. Höppener and C. J. M. Lips, "Role of islet amyloid in type 2 diabetes mellitus," *International Journal of Biochemistry and Cell Biology*, vol. 38, no. 5-6, pp. 726–736, 2006.

[11] J. S. Jacobsen, C.-C. Wu, J. M. Redwine, et al., "Early-onset behavioral and synaptic deficits in a mouse model of Alzheimer's disease," *Proceedings of the National Academy of Sciences of the United States of America*, vol. 103, no. 13, pp. 5161–5166, 2006.

[12] A. E. Butler, J. Janson, W. C. Soeller, and P. C. Butler, "Increased β-cell apoptosis prevents adaptive increase in β-cell mass in mouse model of type 2 diabetes: evidence for role of islet amyloid formation rather than direct action of amyloid," *Diabetes*, vol. 52, no. 9, pp. 2304–2314, 2003.

[13] M. Bucciantini, G. Calloni, F. Chiti, et al., "Prefibrillar amyloid protein aggregates share common features of cytotoxicity," *Journal of Biological Chemistry*, vol. 279, no. 30, pp. 31374–31382, 2004.

[14] R. Kayed, E. Head, J. L. Thompson, et al., "Common structure of soluble amyloid oligomers implies common mechanism of pathogenesis," *Science*, vol. 300, no. 5618, pp. 486–489, 2003.

[15] J. W. M. Höppener, J. S. Verbeek, E. J. P. de Koning, et al., "Chronic overproduction of islet amyloid polypeptide/amylin in transgenic mice: lysosomal localization of human islet amyloid polypeptide and lack of marked hyperglycaemia or hyperinsulinaemia," *Diabetologia*, vol. 36, no. 12, pp. 1258–1265, 1993.

[16] K. L. van Hulst, W. Born, R. Muff, et al., "Biologically active human islet amyloid polypeptide/amylin in transgenic mice," *European Journal of Endocrinology*, vol. 136, no. 1, pp. 107–113, 1997.

[17] B. Ahrén, C. Oosterwijk, C. J. M. Lips, and J. W. M. Höppener, "Transgenic overexpression of human islet amyloid polypeptide inhibits insulin secretion and glucose elimination after gastric glucose gavage in mice," *Diabetologia*, vol. 41, no. 11, pp. 1374–1380, 1998.

[18] J. W. M. Höppener, C. Oosterwijk, M. G. Nieuwenhuis, et al., "Extensive islet amyloid formation is induced by development of type II diabetes mellitus and contributes to its progression: pathogenesis of diabetes in a mouse model," *Diabetologia*, vol. 42, no. 4, pp. 427–434, 1999.

[19] R. S. Surwit, C. M. Kuhn, C. Cochrane, J. A. McCubbin, and M. N. Feinglos, "Diet-induced type II diabetes in C57BL/6J mice," *Diabetes*, vol. 37, no. 9, pp. 1163–1167, 1988.

[20] B. Ahrén, E. Simonsson, A. J. W. Scheurink, H. Mulder, U. Myrsén, and F. Sundler, "Dissociated insulinotropic sensitivity to glucose and carbachol in high-fat diet-induced insulin resistance in C57 BL/6J mice," *Metabolism*, vol. 46, no. 1, pp. 97–106, 1997.

[21] C. B. Verchere, D. A. D'Alessio, R. D. Palmiter, et al., "Islet amyloid formation associated with hyperglycemia in transgenic mice with pancreatic β-cell expression of human islet amyloid polypeptide," *Proceedings of the National Academy of Sciences of the United States of America*, vol. 93, no. 8, pp. 3492–3496, 1996.

[22] K. L. van Hulst, W. H. L. Hackeng, J. W. M. Höppener, et al., "An improved method for the determination of islet amyloid polypeptide levels in plasma," *Annals of Clinical Biochemistry*, vol. 31, no. 2, pp. 165–170, 1994.

[23] H. Mulder, B. Ahrén, M. Stridsberg, and F. Sundler, "Non-parallelism of islet amyloid polypeptide (amylin) and insulin gene expression in rat islets following dexamethasone treatment," *Diabetologia*, vol. 38, no. 4, pp. 395–402, 1995.

[24] B. Thorens, H. K. Sarkar, H. R. Kaback, and H. F. Lodish, "Cloning and functional expression in bacteria of a novel glucose transporter present in liver, intestine, kidney, and β-pancreatic islet cells," *Cell*, vol. 55, no. 2, pp. 281–290, 1988.

[25] H. Y. Wong, B. Ahrén, C. J. M. Lips, J. W. M. Höppener, and F. Sundler, "Postnatally disturbed pancreatic islet cell distribution in human islet amyloid polypeptide transgenic mice," *Regulatory Peptides*, vol. 113, no. 1–3, pp. 89–94, 2003.

[26] N. Wierup, M. J. Kuhar, B. O. Nilsson, H. Mulder, E. Ekblad, and F. Sundler, "Cocaine- and amphetamine-regulated transcript (CART) is expressed in several islet cell types during rat development," *Journal of Histochemistry & Cytochemistry*, vol. 52, no. 2, pp. 169–177, 2004.

[27] B. J. de Haan, M. M. Faas, H. Spijker, J. W. van Willigen, A. de Haan, and P. de Vos, "Factors influencing isolation of functional pancreatic rat islets," *Pancreas*, vol. 29, no. 1, pp. e15–e22, 2004.

[28] P. T. R. van Suylichem, G. H. J. Wolters, and R. van Schilfgaarde, "The efficacy of density gradients for islet purification: a comparison of seven density gradients," *Transplant International*, vol. 3, no. 3, pp. 156–161, 1990.

[29] W. C. Soeller, J. Janson, S. E. Hart, et al., "Islet amyloid-associated diabetes in obese A(vy)/a mice expressing human islet amyloid polypeptide," *Diabetes*, vol. 47, no. 5, pp. 743–750, 1998.

[30] M. Couce, L. A. Kane, T. D. O'Brien, et al., "Treatment with growth hormone and dexamethasone in mice transgenic for human islet amyloid polypeptide causes islet amyloidosis and β-cell dysfunction," *Diabetes*, vol. 45, no. 8, pp. 1094–1101, 1996.

[31] E. J. P. de Koning, E. R. Morris, F. M. A. Hofhuis, et al., "Intra- and extracellular amyloid fibrils are formed in cultured pancreatic islets of transgenic mice expressing human islet amyloid polypeptide," *Proceedings of the National Academy of Sciences of the United States of America*, vol. 91, no. 18, pp. 8467–8471, 1994.

[32] B. Ahrén and A. J. W. Scheurink, "Marked hyperleptinemia after high-fat diet associated with severe glucose intolerance in mice," *European Journal of Endocrinology*, vol. 139, no. 4, pp. 461–467, 1998.

[33] B. Ahrén, "Diurnal variation in circulating leptin is dependent on gender, food intake and circulating insulin in mice," *Acta Physiologica Scandinavica*, vol. 169, no. 4, pp. 325–331, 2000.

[34] H. Ohsawa, A. Kanatsuka, T. Yamaguchi, H. Makino, and S. Yoshida, "Islet amyloid polypeptide inhibits glucose-stimulated insulin secretion from isolated rat pancreatic islets," *Biochemical and Biophysical Research Communications*, vol. 160, no. 2, pp. 961–967, 1989.

[35] A. Ar'Rajab and B. Ahrén, "Effects of amidated rat islet amyloid polypeptide on glucose-stimulated insulin secretion in vivo and in vitro in rats," *European Journal of Pharmacology*, vol. 192, no. 3, pp. 443–445, 1991.

[36] B. Leighton and G. J. Cooper, "Pancreatic amylin and calcitonin gene-releted peptide cause resistance to insulin in skeletal muscle in vitro," *Nature*, vol. 335, no. 6191, pp. 632–635, 1988.

[37] R. O. Deems, R. W. Deacon, and D. A. Young, "Amylin activates glycogen phosphorylase and inactivates glycogen synthase via a cAMP-independent mechanism," *Biochemical and Biophysical Research Communications*, vol. 174, no. 2, pp. 716–720, 1991.

[38] J. M. Molina, G. J. S. Cooper, B. Leighton, and J. M. Olefsky, "Induction of insulin resistance in vivo by amylin and calcitonin gene-related peptide," *Diabetes*, vol. 39, no. 2, pp. 260–265, 1990.

[39] J. P. H. Wilding, N. Khandan-Nia, W. M. Bennet, et al., "Lack of acute effect of amylin (islet associated polypeptide) on insulin sensitivity during hyperinsulinaemic euglycaemic clamp in humans," *Diabetologia*, vol. 37, no. 2, pp. 166–169, 1994.

[40] T. P. Ciaraldi, M. Goldberg, R. Odom, and M. Stolpe, "In vivo effects of amylin on carbohydrate metabolism in liver cells," *Diabetes*, vol. 41, no. 8, pp. 975–981, 1992.

[41] T. W. Stephens, W. F. Heath, and R. N. Hermeling, "Presence of liver CGRP/amylin receptors in only nonparenchymal cells and absence of direct regulation of rat liver glucose metabolism by CGRP/amylin," *Diabetes*, vol. 40, no. 3, pp. 395–400, 1991.

[42] B. Thorens, "Molecular and cellular physiology of GLUT-2, a high-Km facilitated diffusion glucose transporter," *International Review of Cytology*, vol. 137, pp. 209–238, 1992.

[43] E. J. P. de Koning, J. J. G. van den Brand, V. L. Mott, et al., "Macrophages and pancreatic islet amyloidosis," *Amyloid*, vol. 5, no. 4, pp. 247–254, 1998.

Hindawi Publishing Corporation
Experimental Diabetes Research
Volume 2008, Article ID 304513, 4 pages
doi:10.1155/2008/304513

Research Article

Disturbed α-Cell Function in Mice with β-Cell Specific Overexpression of Human Islet Amyloid Polypeptide

Bo Ahrén and Maria Sörhede Winzell

Department of Clinical Sciences, Lund University, 22184 Lund, Sweden

Correspondence should be addressed to Bo Ahrén, bo.ahren@med.lu.se

Received 5 February 2008; Revised 20 March 2008; Accepted 6 May 2008

Recommended by Per Westermark

Exogenous administration of islet amyloid polypeptide (IAPP) has been shown to inhibit both insulin and glucagon secretion. This study examined α-cell function in mice with β-cell specific overexpression of human IAPP (hIAPP) after an oral protein gavage (75 mg whey protein/mouse). Baseline glucagon levels were higher in transgenic mice (41±4.0 pg/mL, $n = 6$) than in wildtype animals (19±5.1 pg/mL, $n = 5$, $P = .015$). In contrast, the glucagon response to protein was impaired in transgenic animals (21±2.7 pg/mL in transgenic mice versus 38±5.7 pg/mL in wildtype mice at 15 minutes; $P = .027$). Baseline insulin levels did not differ between the groups, while the insulin response, as the glucagon response, was impaired after protein challenge ($P = .018$). Glucose levels were not different between the groups and did not change significantly after protein gavage. Acetaminophen was given through gavage to the animals (2 mg/mouse) to estimate gastric emptying. The plasma acetaminophen profile was similar in the two groups of mice. We conclude that disturbances in glucagon secretion exist in mice with β-cell specific overexpression of human IAPP, which are not secondary to changes in gastric emptying. The reduced glucagon response to protein challenge may reflect a direct inhibitory influence of hIAPP on glucagon secretion.

1. INTRODUCTION

Islet amyloid polypeptide is a 37-amino-acid peptide, which is produced in the β-cells in the pancreatic islets [1–3]. It is coreleased with insulin [4], and exogenous administration of IAPP inhibits insulin secretion [2, 3, 5–7]. Several studies have also shown that exogenous administration of IAPP at supraphysiological doses inhibits glucagon secretion [8–11]. IAPP of the human form may lead to fibril formation, which causes amyloid deposition in the islets resulting in β-cell dysfunction and diabetes [12–14]. We have previously shown that mice with β-cell specific overexpression of the human form of IAPP (hIAPP) have defective insulin secretion and disturbed islet topography with centrally located glucagon producing α-cells [15, 16]. Whether these mice in addition have disturbed glucagon secretion is, however, not known. Therefore, the aim of the present study was to examine the glucagon response to an oral protein load in these mice compared to wildtype mice. Since IAPP has been shown to inhibit gastric emptying [11], also the gastric emptying rate in the transgenic and wildtype mice was evaluated with the previously described acetaminophen-test [17], to control for any differences in gastric emptying between the groups.

2. METHODS

2.1. Animals

Hemizygous transgenic mice with islet β-cell expression of hIAPP on a C57BL/6J/6xDBA/2 background were generated as previously described [18]. Transgenic status was determined by PCR using oligonucleotide primers directed against the hIAPP transgene [19]. The transgenic mice and their wildtype controls were kind gifts of Dr Steven E Kahn, University of Washington, Seattle, Wash, USA. Transgenic and wildtype mice were transported from the animal facility of the University of Washington, Seattle, to the In Vivo Department, Biomedical Center, Lund University, Lund, Sweden, after embryo transfer performed at Taconic A/S, Ry, Denmark. The animals were cross-bred for >16 generations to C57BL/6J mice. The animals were kept in a 12-hour light

schedule (lights on at 0600 am) and given a standard pellet diet (fat 11.4%, carbohydrate 62.8%, protein 25.8% on an energy base, total energy 12.6 kJ/g) and tap water ad libitum. The Ethics Committee in Lund/Malmö approved the study.

2.2. Experiments

Following a four-hour period after removal of food from the cage, female transgenic and wildtype animals were anesthetized with an intraperitoneal injection of midazolam (Dormicum, Hoffman-La-Roche, Basel, Switzerland, 0.2 mg/mouse) as well as a combination of fluanison (0.4 mg/mouse) and fentanyl (0.02 mg/mouse; Hypnorm, Janssen, Beerse, Belgium). Thirty minutes later, a blood sample was taken from the retrobulbar, intraorbital, capillary plexus in heparinized tubes. Then, whey protein (100% Anywhey, 75 mg, Optimum Nutrition, Lindesberg, Sweden) and acetaminophen (paracetamol; Sigma Chemical Co, St Louis, Mo, 2 mg) dissolved in saline (total volume 500 μL) were administered through a gastric tube (outer diameter 1.2 mm). After 15, 30, 60, and 120 minutes, blood samples, 75 μL each, were collected. Blood was kept in heparinized tubes containing 5 μL Trasylol (aprotinin; 10000 KIE/mL; Bayer HealthCare AG, Leverkusen, Germany), immediately centrifuged whereupon plasma was separated and stored at -20°C until analysis for glucose, glucagon, insulin, and acetaminophen.

2.3. Analyses

Plasma glucagon was determined with radioimmunoassay (Linco Res, St Charles, Mo, USA) with a guinea pig antiglucagon antibody, radioiodine labelled glucagon as tracer and glucagon standard. CV of the assay is 8% and the sensitivity of the assay is 10 pg/mL. The antibodies do not cross-react with GLP-1. Plasma insulin was determined with radioimmunoassay (Linco) with a guinea pig antirat insulin antibody, radioiodine labelled human insulin as tracer and rat insulin as standard. Plasma acetaminophen was determined with a colorimetric assay (Cambridge Life Science, Ely, Cambridgeshire, UK). Plasma glucose was determined with the glucose oxidase method.

2.4. Calculations and statistics

Means ± SEM are shown. Statistical comparisons were performed with the Student's t-test. For estimation of glucagon secretion, the increase in plasma glucagon levels during the first 15 minutes after protein gavage was estimated by subtracting baseline glucagon values from the 15-minute glucagon values. The area under the glucagon and insulin curves (AUCs) were also calculated using the trapezoid rule.

3. RESULTS

3.1. Glucagon response to oral protein

Figure 1 (upper left panel) shows plasma glucagon levels during the oral protein challenge. Baseline glucagon levels were higher in the transgenic animals (41 ± 4.0 pg/mL, n = 6) than in the wildtype animals (19 ± 5.1 pg/mL, n = 5, P = .015). Glucagon levels at 15, 30, and 60 minutes after protein administration did not differ significantly between the groups, whereas the levels after 120 minutes were, again, significantly, higher in the transgenic animals (P = .008). Glucagon secretion was estimated as the change in glucagon levels during the first 15 minutes after protein gavage. This 15-minute glucagon response to protein administration was impaired in the transgenic animals, being 21 ± 2.7 pg/mL in transgenic mice versus 38 ± 5.7 pg/mL in wildtype mice (P = .027). The suprapasal AUC for glucagon for the entire 120-minute study period did not differ significantly between the groups, being 4.3 ± 1.1 μg/mL × 120 minutes in wildtype mice versus 3.9 ± 0.9 μg/mL × 120 minutes in transgenic mice.

3.2. Insulin and glucose responses to oral protein

Baseline insulin levels were 50 ± 5.1 påmol/L in wildtype animals and 46 ± 4.9 pmol/L in transgenic mice (NS). The insulin response to protein ingestion was impaired in transgenic mice; the suprabasal AUC for insulin for the 120-minute study period was 27.2 ± 3.1 nmol/L × 120 minutes in wildtype animals versus 16.5 ± 3.9 nmol/L × 120 minutes in transgenic animals (P = .018) (Figure 1, upper right). Baseline glucose levels were 7.2 ± 0.3 mmol/L in wildtype animals and 7.8 ± 0.2 mmol/L in transgenic mice (NS); glucose levels did not change significantly during the test (Figure 1, lower left panel).

3.3. Acetaminophen response to acetaminophen administration

Figure 1 (lower right) shows the acetaminophen concentrations during test. Plasma acetaminophen increased to a maximum level at 15 minutes after administration, thereafter it gradually fell. There was no significant difference between the groups in plasma acetaminophen.

4. DISCUSSION

This study evaluated the islet hormone responses to oral protein ingestion in mice with β-cell specific overexpression of human IAPP. It was found that the insulin response to protein was impaired in transgenic mice. This confirms that these mice have impaired insulin secretion, as previously was reported also after oral glucose challenge [15]. The main novel finding in this report is, however, that the transgenic mice have also changes in the glucagon levels. Thus, the mice were found to have higher baseline glucagon levels than their wildtype counterparts and yet they have a reduced glucagon response to protein administration. The mechanism of the high-baseline glucagon remains to be established. It is, however, consistent with the disturbance in islet topography in these mice. Thus, we have previously shown that the islets of these mice have enlarged population of glucagon producing α cells as opposed to the reduced β-cell immunostaining in these animals which is associated

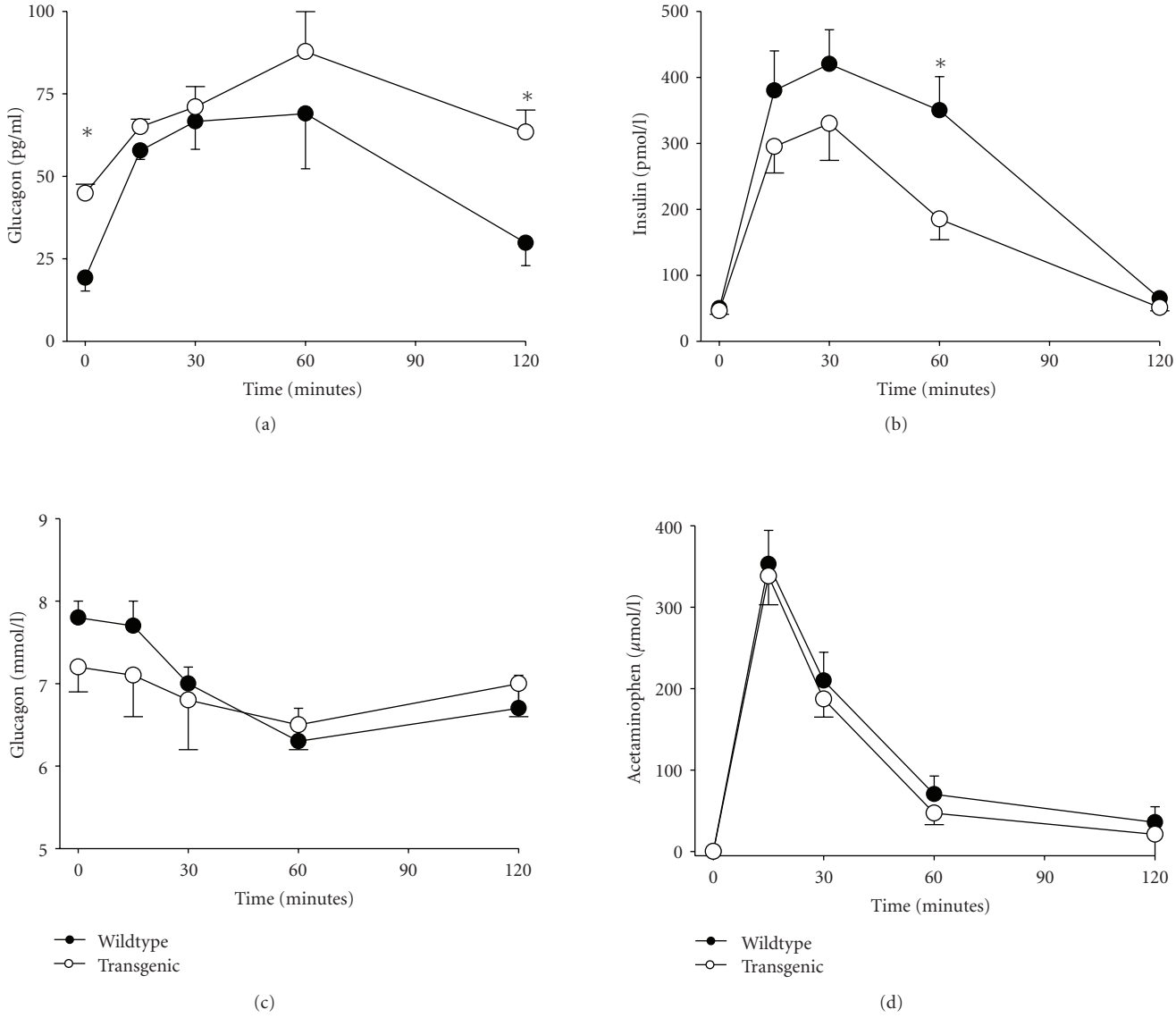

Figure 1: Plasma levels of glucagon, insulin, glucose, and acetaminophen following administration of whey protein (75 mg) and acetaminophen (2 mg) in female wildtype mice ($n = 5$) and transgenic mice with β-cell specific overexpression of hIAPP ($n = 6$). Means ± SEM are shown. Asterisks indicate probability level of random difference between the two groups ($^*P < .05$).

with significantly reduced islet insulin content [16]. This hyperglucagonemia may be the result of the reduced islet insulin, in view of the inhibitory influence of insulin on glucagon secretion. At the same time, the glucagon response to the protein administration was impaired, which may be explained by the transgene, because IAPP is known to inhibit glucagon secretion [8–11]. Hence, high-baseline glucagon and impaired glucagon response to stimulation are two characteristics of the hIAPP transgene, and may have different mechanisms.

In this study, we also determined the acetaminophen concentration after acetaminophen administration to determine whether gastric emptying had been altered in the transgenic mice. Previously, inhibition by IAPP of gastric emptying has been demonstrated [11] and changes in gastric emptying would be a mechanism for changes in glucagon secretion after protein administration. The acetaminophen test has previously been validated in humans [20] and used in a previous study in mice [17]. It is based on the poor absorption of acetaminophen from the stomach and the rapid and almost complete absorption from the small intestine. This implies that plasma acetaminophen profiles give an estimation of gastric emptying, which also has been verified as good correlation with isotopic technique measurements of gastric emptying [21, 22]. We found that there was no difference in plasma acetaminophen profiles between transgenic and wildtype mice. This shows that the increase in β-cell IAPP expression does not affect gastric

emptying, and, therefore, the inhibited glucagon response to oral protein in these mice is not due to impaired gastric emptying.

In conclusion, this study has shown that β-cell specific overexpression of human IAPP increases baseline glucagon levels and impairs the glucagon response to oral protein in association with impaired insulin response. This shows that a disturbed α-cell function in these mice is evident in association with the previously described disturbed β-cell function [15, 16].

ACKNOWLEDGMENTS

The authors are grateful to Kristina Andersson, Lilian Bengtsson, and Lena Kvist for expert technical assistance. This study was supported by the Swedish Research Council (Grants 6834), The Swedish Diabetes Foundation, Albert Påhlsson Foundation, The Swedish Diabetes Association, Region Skåne, and the Faculty of Medicine, Lund University.

REFERENCES

[1] P. Westermark, C. Wernstedt, E. Wilander, D. W. Hayden, T. D. O'Brien, and K. H. Johnson, "Amyloid fibrils in human insulinoma and islets of Langerhans of the diabetic cat are derived from a neuropeptide-like protein also present in normal islet cells," *Proceedings of the National Academy of Sciences of the United States of America*, vol. 84, no. 11, pp. 3881–3885, 1987.

[2] B. Ahrén and M. Pettersson, "Calcitonin gene-related peptide (CGRP) and amylin and the endocrine pancreas," *International Journal of Pancreatology*, vol. 6, no. 1, pp. 1–15, 1990.

[3] E. Karlsson, "IAPP as a regulator of glucose homeostasis and pancreatic hormone secretion (review)," *International Journal of Molecular Medicine*, vol. 3, no. 6, pp. 577–584, 1999.

[4] H. Larsson and B. Ahrén, "Effects of arginine on the secretion of insulin and islet amyloid polypeptide in humans," *Pancreas*, vol. 11, no. 2, pp. 201–205, 1995.

[5] A. Ar'Rajab and B. Ahrén, "Effects of amidated rat islet amyloid polypeptide on glucose-stimulated insulin secretion in vivo and in vitro in rats," *European Journal of Pharmacology*, vol. 192, no. 3, pp. 443–445, 1991.

[6] P. Dégano, R. A. Silvestre, M. Salas, E. Peiró, and J. Marco, "Amylin inhibits glucose-induced insulin secretion in a dose-dependent manner. Study in the perfused rat pancreas," *Regulatory Peptides*, vol. 43, no. 1-2, pp. 91–96, 1993.

[7] C. Fürnsinn, H. Leuvenink, M. Roden, et al., "Islet amyloid polypeptide inhibits insulin secretion in conscious rats," *American Journal of Physiology*, vol. 267, no. 2, pp. E300–E305, 1994.

[8] B. R. Gedulin, T. J. Rink, and A. A. Young, "Dose-response for glucagonostatic effect of amylin in rats," *Metabolism*, vol. 46, no. 1, pp. 67–70, 1997.

[9] F. Wang, T. E. Adrian, G. T. Westermark, X. Ding, T. Gasslander, and J. Permert, "Islet amyloid polypeptide tonally inhibits β-, α-, and δ-cell secretion in isolated rat pancreatic islets," *American Journal of Physiology*, vol. 276, no. 1, pp. E19–E24, 1999.

[10] B. Åkesson, G. Panagiotidis, P. Westermark, and I. Lundquist, "Islet amyloid polypeptide inhibits glucagon release and exerts a dual action on insulin release from isolated islets," *Regulatory Peptides*, vol. 111, no. 1–3, pp. 55–60, 2003.

[11] B. R. Gedulin, C. M. Jodka, K. Herrmann, and A. A. Young, "Role of endogenous amylin in glucagon secretion and gastric emptying in rats demonstrated with the selective antagonist, AC187," *Regulatory Peptides*, vol. 137, no. 3, pp. 121–127, 2006.

[12] K. H. Johnson, T. D. O'Brien, C. Betsholtz, and P. Westermark, "Islet amyloid polypeptide: mechanisms of amyloidogenesis in the pancreatic islets and potential roles in diabetes mellitus," *Laboratory Investigation*, vol. 66, no. 5, pp. 522–535, 1992.

[13] J. W. M. Höppener, B. Ahrén, and C. J. M. Lips, "Islet amyloid and type 2 diabetes mellitus," *The New England Journal of Medicine*, vol. 343, no. 6, pp. 411–419, 2000.

[14] R. A. Ritzel, J. J. Meier, C.-Y. Lin, J. D. Veldhuis, and P. C. Butler, "Human islet amyloid polypeptide oligomers disrupt cell coupling, induce apoptosis, and impair insulin secretion in isolated human islets," *Diabetes*, vol. 56, no. 1, pp. 65–71, 2007.

[15] B. Ahrén, C. Oosterwijk, C. J. M. Lips, and J. W. M. Höppener, "Transgenic overexpression of human islet amyloid polypeptide inhibits insulin secretion and glucose elimination after gastric glucose gavage in mice," *Diabetologia*, vol. 41, no. 11, pp. 1374–1380, 1998.

[16] B. Ahrén, M. Sörhede Winzell, N. Wierup, F. Sundler, B. Burkey, and T. E. Hughes, "DPP-4 inhibition improves glucose tolerance and increases insulin and GLP-1 responses to gastric glucose in association with normalized islet topography in mice with β-cell-specific overexpression of human islet amyloid polypeptide," *Regulatory Peptides*, vol. 143, no. 1–3, pp. 97–103, 2007.

[17] P. T. Gunnarsson, M. Sörhede Winzell, C. F. Deacon, et al., "Glucose-induced incretin hormone release and inactivation are differently modulated by oral fat and protein in mice," *Endocrinology*, vol. 147, no. 7, pp. 3173–3180, 2006.

[18] C. B. Verchere, D. A. D'Alessio, R. D. Palmiter, et al., "Islet amyloid formation associated with hyperglycemia in transgenic mice with pancreatic beta cell expression of human islet amyloid polypeptide," *Proceedings of the National Academy of Sciences of the United States of America*, vol. 93, no. 8, pp. 3492–3496, 1996.

[19] S. Andrikopoulos, C. B. Verchere, Y. Terauchi, T. Kadowaki, and S. E. Kahn, "β-Cell glucokinase deficiency and hyperglycemia are associated with reduced islet amyloid deposition in a mouse model of type 2 diabetes," *Diabetes*, vol. 49, no. 12, pp. 2056–2062, 2000.

[20] E. Näslund, J. Bogefors, P. Grybäck, H. Jacobsson, and P. M. Hellström, "Gastric emptying: comparison of scintigraphic, polyethylene glycol dilution, and paracetamol tracer assessment techniques," *Scandinavian Journal of Gastroenterology*, vol. 35, no. 4, pp. 375–379, 2000.

[21] J. A. Clements, R. C. Heading, W. S. Nimmo, and L. F. Prescott, "Kinetics of acetaminophen absorption and gastric emptying in man," *Clinical Pharmacology & Therapeutics*, vol. 24, no. 4, pp. 420–431, 1978.

[22] A. W. Medhus, C. M. Lofthus, J. Bredesen, and E. Husebye, "Gastric emptying: the validity of the paracetamol absorption test adjusted for individual pharmacokinetics," *Neurogastroenterology & Motility*, vol. 13, no. 3, pp. 179–185, 2001.

Hindawi Publishing Corporation
Experimental Diabetes Research
Volume 2008, Article ID 429274, 7 pages
doi:10.1155/2008/429274

Research Article

Transthyretin and Amyloid in the Islets of Langerhans in Type-2 Diabetes

Gunilla T. Westermark[1] and Per Westermark[2]

[1] *Department of Clinical and Experimental Medicine, Linköping University, 581 85 Linköping, Sweden*
[2] *Department of Genetics and Pathology, Uppsala University, 751 85 Uppsala, Sweden*

Correspondence should be addressed to Per Westermark, per.westermark@genpat.uu.se

Received 31 January 2008; Revised 7 May 2008; Accepted 3 July 2008

Recommended by Steven E. Kahn

Transthyretin (TTR) is a major amyloid fibril protein in certain systemic forms of amyloidosis. It is a plasma protein, mainly synthesized by the liver but expression occurs also at certain minor locations, including the endocrine cells in the islets of Langerhans. With the use of immunohistochemistry and in situ hybridization, we have studied the distribution of transthyretin-containing cells in islets of Langerhans in type-2 diabetic and nondiabetic individuals. TTR expression was particularly seen in alpha (glucagon) cells. Islets from type-2 diabetic patients had proportionally more transthyretin-reactive islet cells, including beta cells. A weak transthyretin immunoreaction in IAPP-derived amyloid occurred in some specimens. In seeding experiments in vitro, we found that TTR fibrils did not seed IAPP while IAPP fibrils seeded TTR. It is suggested that islet expression of transthyretin may be altered in type-2 diabetes.

1. INTRODUCTION

Deposition of amyloid is the single, most common, and characteristic morphological lesion in islets of Langerhans in individuals with type-2 diabetes. Some degree of islet amyloidosis is found in at least 95% of such patients [1]. In about two thirds of the cases, more than 50% of the islets are affected. As the amyloid amount increases, the percentage of beta cells decreases [2, 3]. The amount of amyloid can be considerable in a single islet, more or less converting it into amyloid.

The islet amyloid fibril consists of islet amyloid polypeptide (IAPP; amylin) which is a 37-amino acid residues beta cell hormone, stored together with insulin in secretory vesicles and released with this hormone. The normal molar ratio between IAPP and insulin in human is less than 5%. Although IAPP is a very fibrillogenic peptide in vitro, it does not fibrillize in normal islets, possibly due to interaction with insulin which is a potent inhibitor of IAPP fibril formation [4–6].

It is not understood why IAPP forms amyloid deposits in conjunction with type-2 diabetes. An overexpression of IAPP does exist in obese type-2 diabetic patients [7], but this alone is most probably not sufficient for amyloid formation. Thus, transgenic mice, highly overexpressing human IAPP, do not develop islet amyloidosis unless manipulated in other ways, for example, feeding a diet high in fat [8–10]. Therefore, additional factors may operate in the amyloidogenesis.

The amyloid diseases constitute a biochemically and clinically diverse group of disorders. Each amyloid disease is characterized by one specific amyloid fibril protein and until now, more than 25 proteins have been found in human amyloidosis [11]. Aggregation of a peptide to amyloid-like fibrils in vitro is a nucleation-dependent process in which a nucleus is formed before fibrils start to grow [12–14]. The nature of this nucleus is not fully understood and the time it takes for its formation, known as the lag phase, varies depending on protein, concentration, temperature, and other factors. As soon as a nucleus is present, the growth of amyloid-like fibrils can occur rapidly. Seeding a solution with preformed fibrils greatly enhances the fibrillogenesis and reduces the lag phase sometimes close to zero. It is assumed that protein monomers add to the free end of the fibrils. This mechanism is believed not only to work in vitro

but also in vivo and may be an important reason why amyloid infiltration in systemic amyloidoses spreads rapidly as soon as it has started. Seeding capability is generally very specific and already minor variations in the protein efficiently block the addition of new monomers [15]. However, in vitro experiments have shown that preformed fibrils made from heterologous amyloid fibril proteins sometimes can act as seed [16]. Heterologous amyloid fibrils may also act as efficient seed in two different murine models of systemic amyloidosis [17, 18]. That means, at least in theory, that fibrils of one biochemical nature may be a risk factor for the formation of amyloid deposits of another kind of amyloidosis.

In addition to IAPP, another major amyloid fibril protein, transthyretin (TTR), is expressed in considerable amount in the pancreas [19, 20]. TTR is the major amyloid fibril protein in several systemic familial forms of amyloidosis and in the prevalent senile systemic amyloidosis [21]. Similar to other types of systemic amyloidosis, most of the fibril protein in these amyloidoses is derived from the plasma pool and the major expression site of TTR is the liver [22, 23]. There are, however, a few minor sites of TTR gene expression and one of them is the endocrine pancreas [24, 25]. The function of TTR in these localized cells is not known. Furthermore, the possible effect on amyloidogenesis by these additional expression sites has not yet been studied.

Against this background, we questioned whether IAPP-amyloid could induce TTR-fibril formation, and also whether deposition of TTR-amyloid in the pancreas leads to islet amyloidosis, either by deposition of fibrils from TTR or from IAPP. Since we were not aware of any study of islet TTR in type-2 diabetes, another aim was to study the immunoreactivity of islet alpha (glucagon) and beta (insulin) cells in diabetic and nondiabetic individuals.

2. MATERIAL AND METHODS

Paraffin-embedded pancreatic material (corpus or cauda) from 6 individuals with type-2 diabetes and from 10 nondiabetic individuals was available in the laboratory files. The inclusion criterion was that specimens had been taken within 12 hours after death. They were fixed in buffered neutral 4% formaldehyde solution and embedded in paraffin. Formalin-fixed and paraffin-embedded tissue from the pancreatic body was also obtained from two patients with long history of familial TTR-amyloidosis associated with a V30M-mutation in the TTR gene. Adjacent 5 μm sections were taken for alkaline Congo red staining [26] and for immunohistochemistry. The study was approved by the Ethical Committee at Uppsala University Hospital.

Antibodies against insulin (guinea pig) and glucagon (rabbit) were purchased from DAKO (Glostrup, Denmark). Rabbit antisera (A110) against rat/mouse IAPP, which shows complete cross-reactivity with human IAPP [27] and against a recombinant C-terminal fragment (aa 50–127; antiserum # A1898) of human TTR, have been characterized previously [28]. A rabbit antiserum, A1899, was raised against a high-molecular fraction from a gel separation of ATTR fibrils from an individual with senile systemic amyloidosis. This antiserum recognizes TTR amyloid, but is unreactive with AL and AA amyloid in Western blot analysis. Immunohistochemistry was performed with the antisera diluted 1 : 2000 using the biotin-streptavidin system. Sections were developed with 3,3′-diaminobenzidine-tetrahydrochloride (DAB). Double immunolabeling was performed with antibodies against glucagon and TTR or insulin and TTR, visualized with rabbit, mouse, or Guinea pig secondary antibodies conjugated to Alexa 488 (analyzed in blue light) or Alexa 546 (analyzed in green light) (Molecular Probes, Eugene, Ore, USA).

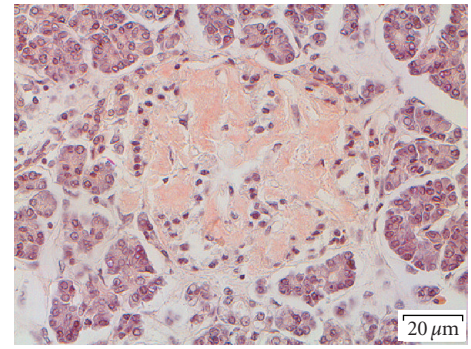

Figure 1: Islet in a type-2 diabetic patient. Most of the islet has been converted into amyloid; Congo red, bar 20 μm.

For controls, sections were treated with antiserum preabsorbed with TTR. Cross-reactivity between TTR or IAPP and glucagon was ruled out by dot blot analysis for which TTR, IAPP, and glucagon were dissolved at 3 μg/well in 0.1 M sodium carbonate buffer, pH 9.8, spotted on a nitrocellulose membrane and incubated with the antisera and developed with biotin-streptavidin followed by DAB. This showed that no cross-reactivity existed between IAPP and TTR or glucagon and TTR.

In order to test the specificity of the two TTR antisera, sections from an "amyloid array" were used. In this, 1 mm thick cylinders from amyloid-containing tissues had been embedded in one block. The array contained the following types of amyloid: AA-amyloid (7 cases, 9 tissues), AL-amyloid (7 cases, 9 tissues), ATTR-amyloid (6 cases, 3 tissues), Aβ-amyloid (1 case, brain), and IAPP-amyloid (3 cases, pancreas).

2.1. Degree of islet amyloidosis

The number of islets with and without amyloid deposits was determined in Congo red stained sections, analyzed in polarized light. Usually, at least 50 islets were scrutinized in each section.

2.2. Localization of TTR in islets of langerhans

A cDNA library was constructed from human liver with the aid of a cDNA synthesis kit (Amersham Bioscience, Uppsala, Sweden). A 237-nucleotide long fragment corresponding to amino acid residues 2–106 of TTR was amplified by polymerase chain reaction. The achieved fragment was ligated

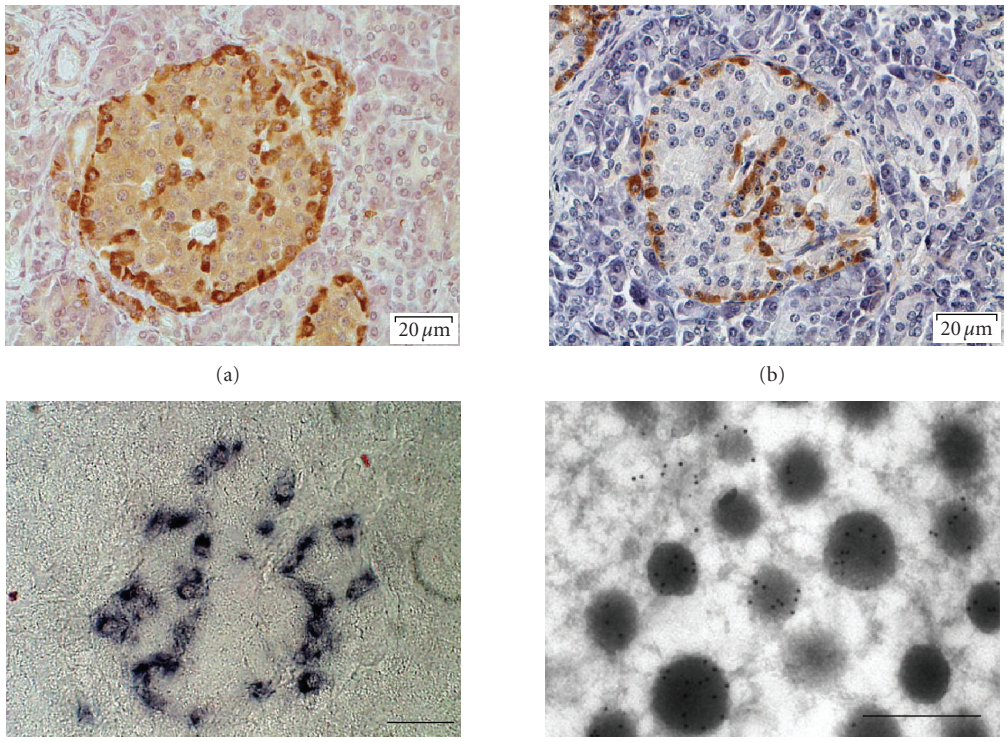

Figure 2: Normal human islets immunolabeled with antisera against: (a) transthyretin and (b) glucagon. In (c) is shown a normal human islet, subjected to in situ hybridization with a TTR probe, visualized with immunohistochemistry. Note that positive cells have a distribution indicative of glucagon cells. Bar 20 μm. (d) shows a part of a glucagon cell with typical granules. The section was double immunolabeled for glucagon (10 nm gold particles) and TTR (5 nm gold particles). Immunolabeling for both these substances is seen on the granules, bar 500 nm.

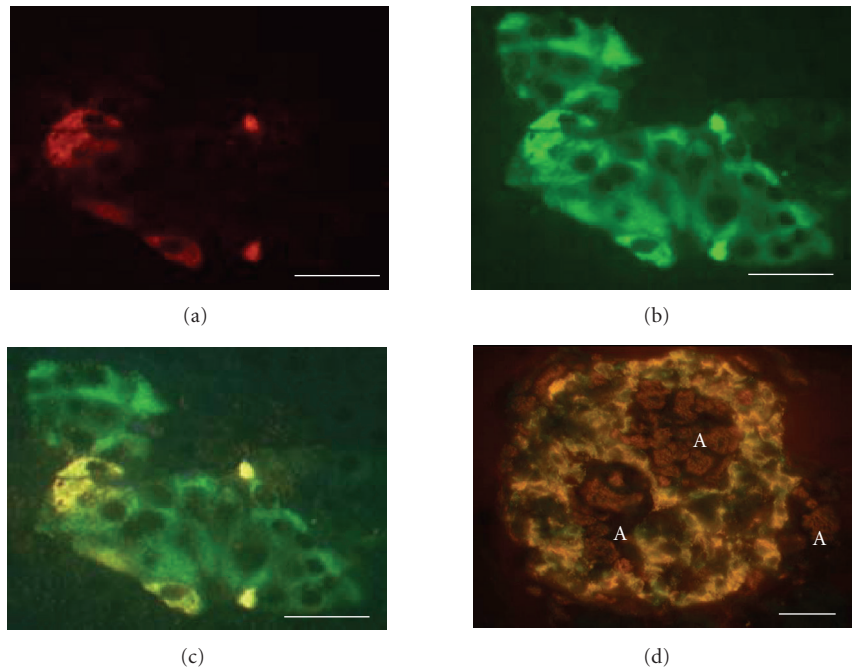

Figure 3: In (a), (b), and (c), an islet double labeled for glucagon (red) and TTR (green). Yellow color indicates colocalization. A large number of islet cells show TTR but not glucagon content. The islet in (d) is double labeled for insulin (green) and TTR (red). Many beta cells exhibit both TTR and insulin immunoreactivity (yellow). The amyloid (A) is weakly labeled for TTR. Bar (a)–(c) 25 μm, (d) 200 μm.

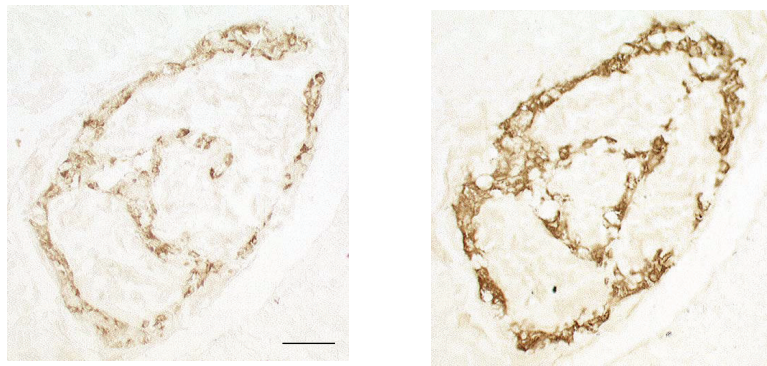

Transthyretin (a) Insulin (b)

Figure 4: Amyloid-rich islet from a type-2 diabetic individual, in (a) immunolabeled for TTR, and in (b) for insulin. Note virtually identical distribution of immune reactive cells. No nuclear staining, bar 20 μm.

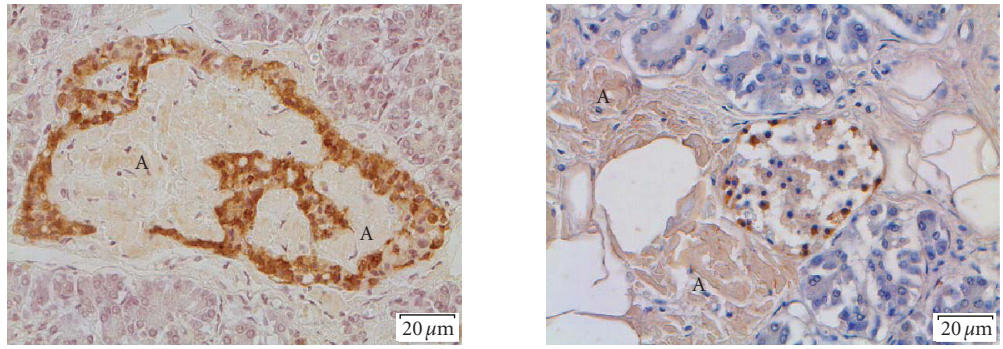

(a) (b)

Figure 5: In (a) is shown an islet from a type-2 diabetic individual. There is pronounced IAPP amyloid infiltration, weakly labeled with antibodies against TTR. (b) shows a small islet in a nondiabetic individual with familial TTR-amyloidosis. There are heavy deposits of TTR-amyloid outside the islet but no islet amyloid. A = amyloid. Immunolabeled with antiserum against TTR.

into the multiple cloning site of pGEM4Z (Promega, SDS-Biosciences, Falkenberg, Sweden). The vector was linearized in front of the SP6 or T7 promoters and digoxigenin-labelled RNA probes were produced according to the manufacturer (Roche, Bromma, Sweden). In situ hybridization was performed as described [29].

For ultrastructural studies, pancreatic tissue was available from one patient with type-2 diabetes and one normal control, fixed in 2% glutaraldehyde in phosphate buffer and embedded in epon. For double immunolabeling, ultrathin sections on formvar-coated nickel grids, were incubated with the primary antibodies (rabbit anti TTR50-127) and mouse antiglucagon (DAKO). TTR was visualized with 5 nm gold particles and glucagon with 10 nm gold particles (British Biocell, Cardiff, UK).

2.3. Seeding experiments

Full length human TTR was a kind gift from Dr. Tom Pettersson (Danderyd, Sweden) and human IAPP was synthesized by Keck Laboratory, New Haven, Connecticut. TTR (0.5 mg) and IAPP (0.125 mg) were dissolved separately in 25 μl methyl sulfoxide (DMSO). To the solutions, 100 μl distilled water was added. After incubation for 2 days at room temperature, 0.5 μl samples were taken from each and studied electron microscopically (negative contrast) for presence of amyloid-like fibrils. Since typical fibrils were seen in both solutions, they were diluted to 2 ml with 0.05 M sodium phosphate buffer, pH 7.2. To wells of a 96-well plate with either 25 μl of TTR or IAPP fibrils, 50 μm newly dissolved TTR or IAPP in 0.05 M phosphate buffer containing 2% DMSO was added, followed by thioflavin T to 10 μM. The final volume was 100 μl. Fluorescence was measured every 20 minutes in a fluoroscan as described [28].

2.4. Statistics

Values are given as mean $\pm$ SD. Comparison between groups was performed with Mann Whitney test.

3. RESULTS

In the pancreata of all individuals with type-2 diabetes and in 7 out of 10 individuals without diabetes, amyloid

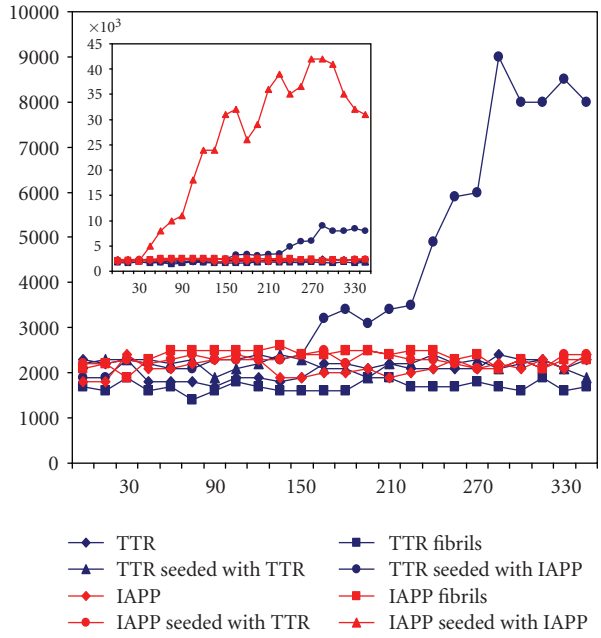

Figure 6: In vitro seeding and cross-seeding experiments with TTR and IAPP measured with thioflavin T. Preformed fibrils of IAPP seeded TTR (blue circles) and IAPP (red triangles, insert). No other increase in signals occurred. Thus, TTR fibrils did not seed IAPP (red circles).

was found in islets of Langerhans. All of the diabetic individuals had a very pronounced islet amyloidosis with some islets with little remaining endocrine cells (Figure 1). In the nondiabetic patients, usually only small amyloid deposits were detected but in three individuals amyloid affected more than 20% and in one as much as 38% of the islets. Comparison of the percentage of affected islets in the two groups when only individuals with some degree of islet amyloidosis were included, showed that significantly more islets contained deposits in the diabetic individuals ($98 \pm 3\%$ and $13 \pm 14\%$, $P = 0.001$). The islet amyloid had typical staining properties with Congo red and was strongly labeled with antiserum against IAPP (not shown).

3.1. Hormone and transthyretin reactivity in islet cells of non-diabetic individuals

In sections of pancreata without amyloid from nondiabetic individuals, both antisera A1898 and A1899 labeled islet cells in a similar way. A strong reaction was seen in all islets with cells with a preferentially peripheral distribution (Figure 2(a)) When compared with sections immunostained for glucagon, an identical distribution was seen (Figure 2(b)). In addition, the majority of remaining islet cells, mainly beta cells, were also labeled but only weakly (Figure 2(a)). In situ hybridization exhibited clear expression of TTR in cells which had a distribution of alpha cells only and no certain reactivity was found with beta cells (Figure 2(c)). Electron microscopically glucagon cells are characterized by secretory vesicles with a rounded electron dense core often situated somewhat eccentrically on the rest of the granule. Glucagon immunoreactivity occurred in both these areas of the granules while TTR labeling was mainly seen in the less electron dense parts of the alpha cell granules (Figure 2(d)). Small gold particles were also seen in the translucent areas of beta cells but only to a small extent (not shown.). Antisera against insulin and IAPP labeled normal beta cells as described [30].

Double labeling for glucagon and TTR showed that all glucagon cells also exhibited TTR immunoreactivity (Figures 3(a) and 3(b)). In addition, a large number of islet cells, negative for glucagon, showed an evident TTR-reactivity (Figure 3(c)). Colocalization of insulin and TTR was seen in many, but not all, beta cells (Figure 3(d)).

3.2. Endocrine cells in islets with amyloid

Both insulin and glucagon immunoreactive cells were identified in islets will all degrees of amyloid deposits. As described earlier [31, 32], beta cells in amyloid-laden islets generally were devoid of IAPP-immunoreactivity. Many cells showed a strong labeling with antibodies against TTR. From adjacent sections, stained for TTR, insulin, and glucagon, it was obvious that not only alpha cells but also beta cells were strongly TTR-positive (Figure 3).

3.3. Transthyretin reactivity in islet amyloid

Islet amyloid from diabetic and nondiabetic individuals exhibited a strong immunolabeling with antiserum against IAPP (not shown). Since we have shown previously that commercially available antibodies against TTR often do not recognize TTR in fibrillar (i.e., amyloid) form, we developed two different rabbit antisera which both strongly labeled cellular TTR and TTR in amyloid. The two TTR antisera labeled islet amyloid weakly in some cases (Figures 3(d) and 5(a)). This staining was even and no areas with strong reaction were seen. In the electron microscopic study, IAPP antiserum labeled amyloid in the diabetic case, but no certain binding of TTR antibodies to fibrils was seen. In order to study the specificity of the reaction in amyloid, we used an amyloid array with tissues from several patients in one block. The two TTR antisera showed reaction only with amyloid of known TTR origin (i.e., Swedish familial amyloidosis and SSA) but not with amyloid of AA, AL, AMed, or Aβ nature, showing that TTR-immunoreactivity is not a general feature of amyloid deposits.

The pancreatic tissue from the individuals with familial TTR-amyloidosis contained varying amounts of amyloid, irregularly distributed in the exocrine parenchyma and surrounding connective tissue. Although amyloid was seen very close to some pancreatic islets, TTR-amyloid did not occur within these islets (Figure 5(b)). Neither was IAPP-amyloid seen here.

3.4. IAPP fibrils seed fibril formation from TTR

Fibril formation of many amyloid proteins, including TTR and IAPP, occurs spontaneously in vitro after a lag phase

which varies in length depending on protein. Seeding with preformed fibrils can shorten the lag phase considerably, which was seen most evidently when a solution of IAPP was seeded with IAPP fibrils (Figure 6, inserted). TTR fibrils did not induce any increase in fluorescence signal when incubated with newly dissolved TTR or solubilized IAPP (Figure 6). However, IAPP fibrils had a clear effect on TTR after a lag phase of about 3 hours (Figure 6).

4. DISCUSSION

This study confirms that TTR is normally expressed by pancreatic alpha (glucagon) cells. As earlier suggested [33], beta cells may also produce TTR but at a low degree, not detectable by in situ hybridization. TTR is stored in the secretory vesicles and is therefore most likely released together with hormones at exocytosis. TTR in plasma is a transporter of thyroxine and indirectly of retinol, but the function of the protein in the secretory granules is unknown. One can only speculate about the possibility that TTR binds to the glucagon precursor and may affect its processing.

IAPP and TTR are both well-known amyloid fibril proteins. Formation of amyloid fibrils is a nucleation dependent phenomenon which can be shown in vitro [14]. After a lag phase, which can last for several days, generation of fibrils usually is rapid. Seeding a fibrillogenic protein solution with preformed fibrils shortens or abolishes this lag phase. Cross-seeding, that is, the same effect achieved by addition of fibrils of a different biochemical nature, can occur with some proteins [16]. In this study, IAPP fibrils seeded IAPP efficiently. This was not seen with TTR which is in accordance with a previous report [34]. TTR fibrils did not seed IAPP but, interestingly, IAPP fibrils evidently induced fibril formation from TTR. Therefore, the weak immunoreaction of IAPP amyloid with antibodies against TTR in some cases may indicate existence of mixed fibrils in islet deposits as a result of a specific interaction between IAPP and TTR, although a passive diffusion of the latter molecule into the amyloid cannot be ruled out. While insulin is an inhibitor of IAPP fibril formation, effects of TTR is not known. It has been suggested that molecules may exist that lead to pathological protein folding and aggregation and these have been called "pathological chaperones" [35]. Therefore, the possible interaction between TTR and IAPP has to be studied further.

In the present study, we also evaluated the TTR immunoreactivity in alpha and beta cells in conjunction with type-2 diabetes. No such studies seem to have been published. Generally, islets in type-2 diabetic patients contained proportionally more strongly TTR-reactive cells in accordance with the known loss of beta cells in that disease [2, 3]. In addition, an interesting and unexpected finding was an increased TTR immunoreactivity of beta cells in pancreatic islets with heavy amyloid deposits. What this means is presently not understood but we have shown previously that IAPP in beta cells in islets with amyloid obtains altered immunoreactive properties [32]. Thus, IAPP immunoreactivity with a polyclonal IAPP antiserum was lost, although labeling with a monoclonal antibody was retained. This finding was interpreted as a sign of modification of the beta cell IAPP in type-2 diabetes. The finding here that IAPP fibrils interact with TTR is interesting in this respect. The observation in the present study that beta cells in amyloidotic islets are strongly TTR immunoreactive may indicate that the intragranular milieu is altered which may affect the ability of IAPP to aggregate.

ACKNOWLEDGMENTS

This work is supported by the Swedish Research Council, the Swedish Diabetes Association, the patient's associations FAMY, FAMY-Norrbotten, the AMYL Foundation, the Family Ernfors Foundation, the Östergötland County Council, and the European Union FP6 Program.

REFERENCES

[1] P. Westermark, "Islet amyloid polypeptide and amyloid in the islets of Langerhans," in *Diabetes: Clinical Science in Practice*, R. D. G. Leslie and D. Robbins, Eds., pp. 189–199, Cambridge University Press, Cambridge, UK, 1995.

[2] P. Westermark and L. Grimelius, "The pancreatic islet cells in insular amyloidosis in human diabetic and non diabetic adults," *Acta Pathologica et Microbiologica Scandinavica A*, vol. 81, no. 3, pp. 291–300, 1973.

[3] A. Clark, C. A. Wells, I. D. Buley, et al., "Islet amyloid, increased A-cells, reduced B-cells and exocrine fibrosis: quantitative changes in the pancreas in type 2 diabetes," *Diabetes Research*, vol. 9, no. 4, pp. 151–159, 1988.

[4] P. Westermark, Z.-C. Li, G. T. Westermark, A. Leckström, and D. F. Steiner, "Effects of beta cell granule components on human islet amyloid polypeptide fibril formation," *FEBS Letters*, vol. 379, no. 3, pp. 203–206, 1996.

[5] S. Janciauskiene, S. Eriksson, E. Carlemalm, and B. Ahrén, "B cell granule peptides affect human islet amyloid polypeptide (IAPP) fibril formation in vitro," *Biochemical and Biophysical Research Communications*, vol. 236, no. 3, pp. 580–585, 1997.

[6] Y. C. Kudva, C. Mueske, P. C. Butler, and N. L. Eberhardt, "A novel assay in vitro of human islet amyloid polypeptide amyloidogenesis and effects of insulin secretory vesicle peptides on amyloid formation," *Biochemical Journal*, vol. 331, part 3, pp. 809–813, 1998.

[7] T. Sanke, T. Hanabusa, Y. Nakano, et al., "Plasma islet amyloid polypeptide (Amylin) levels and their responses to oral glucose in type 2 (non-insulin-dependent) diabetic patients," *Diabetologia*, vol. 34, no. 2, pp. 129–132, 1991.

[8] C. B. Verchere, D. A. D'Alessio, R. D. Palmiter, et al., "Islet amyloid formation associated with hyperglycemia in transgenic mice with pancreatic beta cell expression of human islet amyloid polypeptide," *Proceedings of the National Academy of Sciences of the United States of America*, vol. 93, no. 8, pp. 3492–3496, 1996.

[9] J. W. M. Höppener, C. Oosterwijk, M. G. Nieuwenhuis, et al., "Extensive islet amyloid formation is induced by development of type II diabetes mellitus and contributes to its progression: pathogenesis of diabetes in a mouse model," *Diabetologia*, vol. 42, no. 4, pp. 427–434, 1999.

[10] G. T. Westermark, S. Gebre-Medhin, D. F. Steiner, and P. Westermark, "Islet amyloid development in a mouse strain lacking endogenous islet amyloid polypeptide (IAPP) but

expressing human IAPP," *Molecular Medicine*, vol. 6, no. 12, pp. 998–1007, 2000.

[11] P. Westermark, M. D. Benson, J. N. Buxbaum, et al., "A primer of amyloid nomenclature," *Amyloid*, vol. 14, no. 3, pp. 179–183, 2007.

[12] J. T. Jarrett and P. T. Lansbury Jr., "Seeding "one-dimensional crystallization" of amyloid: a pathogenic mechanism in Alzheimer's disease and scrapie?" *Cell*, vol. 73, no. 6, pp. 1055–1058, 1993.

[13] J.-C. Rochet and P. T. Lansbury Jr., "Amyloid fibrillogenesis: themes and variations," *Current Opinion in Structural Biology*, vol. 10, no. 1, pp. 60–68, 2000.

[14] C. M. Dobson, "Principles of protein folding, misfolding and aggregation," *Seminars in Cellular and Developmental Biology*, vol. 15, no. 1, pp. 3–16, 2004.

[15] M. R. H. Krebs, L. A. Morozova-Roche, K. Daniel, C. V. Robinson, and C. M. Dobson, "Observation of sequence specificity in the seeding of protein amyloid fibrils," *Protein Science*, vol. 13, no. 7, pp. 1933–1938, 2004.

[16] B. O'Nuallain, A. D. Williams, P. Westermark, and R. Wetzel, "Seeding specificity in amyloid growth induced by heterologous fibrils," *Journal of Biological Chemistry*, vol. 279, no. 17, pp. 17490–17499, 2004.

[17] K. Johan, G. T. Westermark, U. Engström, Å. Gustavsson, P. Hultman, and P. Westermark, "Acceleration of amyloid protein A amyloidosis by amyloid-like synthetic fibrils," *Proceedings of the National Academy of Sciences of the United States of America*, vol. 95, no. 5, pp. 2558–2563, 1998.

[18] Y. Xing, A. Nakamura, T. Chiba, et al., "Transmission of mouse senile amyloidosis," *Laboratory Investigation*, vol. 81, no. 4, pp. 493–499, 2001.

[19] B. Jacobsson, T. Pettersson, B. Sandstedt, and A. Carlström, "Prealbumin in the islets of Langerhans," *IRCS Medical Science*, vol. 7, no. 12, p. 590, 1979.

[20] C. Cras-Méneur, H. Inoue, Y. Zhou, et al., "An expression profile of human pancreatic islet mRNAs by serial analysis of gene expression (SAGE)," *Diabetologia*, vol. 47, no. 2, pp. 284–299, 2004.

[21] L. H. Connors, A. Lim, T. Prokaeva, V. A. Roskens, and C. E. Costello, "Tabulation of human transthyretin (TTR) variants, 2003," *Amyloid*, vol. 10, no. 3, pp. 160–184, 2003.

[22] P. Felding and G. Fex, "Cellular origin of prealbumin in the rat," *Biochimica et Biophysica Acta*, vol. 716, no. 3, pp. 446–449, 1982.

[23] P. W. Dickson, G. J. Howlett, and G. Schreiber, "Rat transthyretin (prealbumin). Molecular cloning, nucleotide sequence, and gene expression in liver and brain," *Journal of Biological Chemistry*, vol. 260, no. 13, pp. 8214–8219, 1985.

[24] M. Kato, K. Kato, W. S. Blaner, B. S. Chertow, and D. S. Goodman, "Plasma and cellular retinoid-binding proteins and transthyretin (prealbumin) are all localized in the islets of Langerhans in the rat," *Proceedings of the National Academy of Sciences of the United States of America*, vol. 82, no. 8, pp. 2488–2492, 1985.

[25] B. Jacobsson, "In situ localization of transthyretin-mRNA in the adult human liver, choroid plexus and pancreatic islets and in endocrine tumours of the pancreas and gut," *Histochemistry*, vol. 91, no. 4, pp. 299–304, 1989.

[26] H. Puchtler, F. Sweat, and M. Levine, "On the binding of Congo red by amyloid," *Journal of Histochemistry and Cytochemistry*, vol. 10, no. 6, pp. 355–364, 1962.

[27] L. Christmanson, C. Betsholtz, A. Leckström, et al., "Islet amyloid polypeptide in the rabbit and European hare: studies on its relationship to amyloidogenesis," *Diabetologia*, vol. 36, no. 3, pp. 183–188, 1993.

[28] J. Bergström, C. Murphy, M. Eulitz, et al., "Codeposition of apolipoprotein A-IV and transthyretin in senile systemic (ATTR) amyloidosis," *Biochemical and Biophysical Research Communications*, vol. 285, no. 4, pp. 903–908, 2001.

[29] G. T. Westermark, L. Christmanson, G. Terenghi, et al., "Islet amyloid polypeptide: demonstration of mRNA in human pancreatic islets by in situ hybridization in islets with and without amyloid deposits," *Diabetologia*, vol. 36, no. 4, pp. 323–328, 1993.

[30] A. Lukinius, E. Wilander, G. T. Westermark, U. Engström, and P. Westermark, "Co-localization of islet amyloid polypeptide and insulin in the B cell secretory granules of the human pancreatic islets," *Diabetologia*, vol. 32, no. 4, pp. 240–244, 1989.

[31] P. Westermark, E. Wilander, G. T. Westermark, and K. H. Johnson, "Islet amyloid polypeptide-like immunoreactivity in the islet B cells of type 2 (non-insulin-dependent) diabetic and non-diabetic individuals," *Diabetologia*, vol. 30, no. 11, pp. 887–892, 1987.

[32] Z. Ma, G. T. Westermark, Z.-C. Li, U. Engström, and P. Westermark, "Altered immunoreactivity of islet amyloid polypeptide (IAPP) may reflect major modifications of the lapp molecule in amyloidogenesis," *Diabetologia*, vol. 40, no. 7, pp. 793–801, 1997.

[33] B. Jacobsson, V. P. Collins, L. Grimelius, T. Pettersson, B. Sandstedt, and A. Carlström, "Transthyretin immunoreactivity in human and porcine liver, choroid plexus, and pancreatic islets," *Journal of Histochemistry & Cytochemistry*, vol. 37, no. 1, pp. 31–37, 1989.

[34] A. R. Hurshman, J. T. White, E. T. Powers, and J. W. Kelly, "Transthyretin aggregation under partially denaturing conditions s a downhill polymerization," *Biochemistry*, vol. 43, no. 23, pp. 7365–7381, 2004.

[35] T. Wisniewski, A. A. Golabek, E. Kida, K. E. Wisniewski, and B. Frangione, "Conformational mimicry in Alzheimer's disease: role of apolipoproteins in amyloidogenesis," *American Journal of Pathology*, vol. 147, no. 2, pp. 238–244, 1995.

Hindawi Publishing Corporation
Experimental Diabetes Research
Volume 2008, Article ID 256954, 8 pages
doi:10.1155/2008/256954

Research Article

The Role of the 14–20 Domain of the Islet Amyloid Polypeptide in Amyloid Formation

Sharon Gilead and Ehud Gazit

Department of Molecular Microbiology and Biotechnology, George S. Wise Faculty of Life Sciences, Tel Aviv University, Tel Aviv 69978, Israel

Correspondence should be addressed to Ehud Gazit, ehudg@post.tau.ac.il

Received 7 September 2007; Revised 19 March 2008; Accepted 2 May 2008

Recommended by Per Westermark

The molecular mechanism of amyloid formation by the islet amyloid polypeptide (IAPP) has been intensively studied since its identification in the late 1980s. The IAPP(20–29) region is considered to be the central amyloidogenic module of the polypeptide. This assumption is mainly based on the amyloidogenic properties of the region and on the large sequence diversity within this region between the human and mouse IAPP, as the mouse IAPP does not form amyloids. A few years ago, another region within IAPP was identified that seems to be at least as important as IAPP(20–29) in facilitation of molecular recognition that leads to amyloid formation. Here, we reinforce our and others' previous findings by analyzing supporting evidence from the recent literature. Moreover, we provide new proofs to our hypothesis by comparing between the amyloidogenic properties of the two regions derived from the IAPP of cats, which is also known to form amyloid fibrils.

1. INTRODUCTION

The islet amyloid polypeptide (IAPP) is a 37 amino acid hormone, which is colocalized with insulin in the pancreatic β-cells. The two polypeptides are cosecreted in response to β-cell stimulation [1–4]. In 1986 and 1987, Westermark et al. and Cooper et al. identified IAPP (also designated as *Amylin*) as the major component of pancreatic amyloid deposits, a characteristic pathological feature of type II diabetes [5, 6]. As other amyloid-related proteins and polypeptides, the IAPP identified in these deposits is the wild-type polypeptide in most type II diabetes cases. In its physiological role, IAPP acts as a regulator of glucose homeostasis [7–9].

The formation of amyloid fibrils, which is the hallmark of a group of more than twenty diseases, among them some of the most devastating disorders of the 20th century, is a highly specific self-assembly process [10–14]. The accumulation of IAPP, as well as of amyloidogenic proteins found in other amyloid-related diseases, into amyloid fibrils proceeds via a self-recognition mechanism. The process involves a structural transition from the protein native structure, which is considered to be random coil in the case of IAPP, into a cross-β-pleated-sheet secondary structure conformation.

The exact conditions that stimulate the aggregation of amyloidogenic proteins are yet to be fully understood. However, comprehension of the molecular traits of the amyloidogenic process may be highly valuable in the attempts to understand and prevent this world affecting phenomenon. The identification of IAPP in the late 1980s paved the way for vast investigation regarding the molecular mechanism of IAPP self-assembly process. A central issue addressed was the search for the molecular elements that make IAPP highly prone to amyloid formation. One of the first observations regarding IAPP amyloidogenicity was the specie specificity of this process [15, 16]. Although more than 80% of the IAPP sequence is conserved in mammalians, only a few species such as humans, primates, and cats develop islet amyloid and suffer from type II diabetes, while mice, rats, and dogs do not develop islet amyloid deposits.

The most noticeable sequence diversity is the one between human and mouse/rat IAPP. The sequence of rodent IAPP (rIAPP) differs from that of human IAPP (hIAPP) in 6 out of 37 amino acids, 5 of them are located in a defined region between residues 20 and 29 [hIAPP(20–29) is SNNFGAILSS and rIAPP(20–29) is SNNLGPVLPP] [15–17]. Moreover, the rodent IAPP contains within this region 3

proline residues, which are absent in the human sequence. The proline residue is known to strongly unfavor β-sheet structures. Therefore, the hIAPP(20–29) has been suggested to be responsible for the amyloidogenic propensities of full-length hIAPP.

The decapeptide sequence of hIAPP(20–29) was shown to be able to aggregate into amyloids, whereas the corresponding rIAPP(20–29) did not [15–17]. Furthermore, shorter peptide fragments derived from this region, the penta- and hexapeptides sequences hIAPP(23–27) (FGAIL) and hIAPP(22–27) (NFGAIL), were found to be sufficient for the formation of amyloid-like structures [18]. Hence, the hIAPP(20–29) has been used as a model to study intermolecular interactions and β-sheet formation and was considered to be the only recognition region of IAPP.

In 2001, Fraser et al. identified a previously unrecognized amyloidogenic domain of IAPP located within residues 8–20. Synthetic peptides corresponding to this region assembled into fibrils with typical amyloid-like morphology [19]. Thereafter, we identified, using an unbiased peptide array analysis, a domain comprising the same region that showed even higher affinity recognition to IAPP as compared to the hIAPP(20–29) region [20]. IAPP was incubated with a SPOT membrane containing consecutive overlapping sequences of the full-length hIAPP. Indeed, IAPP was found to bind to the 20–29 region, however a substantially stronger interaction to a region within residues 11–20 was found. Moreover, peptide fragments within this region were shown to readily form amyloid-like structures, some of which are as short as pentapeptides, corresponding to hIAPP(14–18) and hIAPP(15–19). Thus, we suggested that this new identified region plays a central role in the recognition as well as the self-assembly of IAPP amyloid formation process.

During the last few years, accumulating data has supported our previous assumption, both directly and indirectly. However, the hIAPP(20–29) has still remained the major studied amyloidogenic region. Here, we pinpoint these supporting evidences from the recent literature in order to emphasize the relevance of the new recognition and self-assembling region. Furthermore, we provide new proofs for our hypothesis by investigating and comparing the amyloidogenic propensity of the two regions derived from the amyloidogenic cat IAPP (cIAPP).

2. MATERIALS AND METHODS

2.1. Peptide solutions

Peptides were purchased from Peptron, Inc. (Taejeon, Korea). Lyophilized peptides were dissolved in dimethyl sulfoxide (DMSO) at a concentration of 100 mM. To avoid any preaggregation, fresh stock solutions were prepared for each experiment. Peptide stock solutions were diluted into 10 mM Tris buffer, pH 7.2 to a final concentration of 2 or 5 mM and 2% or 5% DMSO, respectively.

2.2. Congo Red staining and birefringence

A 10 μL suspension of 5 mM peptide solution aged for 1 day was allowed to dry overnight on a glass microscope slide. Staining was performed by the addition of a 10 μL suspension of saturated Congo Red (CR) and NaCl in 80% ethanol (v/v) solution. Birefringence was determined with an SZX-12 stereoscope (Olympus, Hamburg, Germany) equipped with cross polarizers.

2.3. Transmission electron microscopy

A 10 μL sample of 2 or 5 mM peptide solution aged for 1 to 3 days was placed on a 400-mesh copper grid covered by carbon-stabilized formvar film (SPI supplies, West Chester PA). After 1 minute, excess fluid was removed, and the grid was then negatively stained with 2% uranyl acetate in water for another 2 minutes. Samples were viewed in a JEOL 1200EX electron microscope operating at 80 kV.

2.4. Fourier-transform infrared spectroscopy

A 30 μL sample of 2 mM peptide solution aged for 2 days was suspended on a polytetrafluoroethylene (PTFE) card and dried by vacuum. Peptide deposit was resuspended with D_2O and subsequently dried. The resuspension procedure was repeated twice to ensure maximal hydrogen to deuterium exchange. Infrared spectra were recorded using a Nicolet Nexus 470 FT-IR spectrometer with a DTGS detector.

3. RESULTS AND DISCUSSION

3.1. Identification of other amyloidogenic regions within IAPP

The hIAPP(20–29) region was considered to be the central amyloidogenic domain within hIAPP. In 1999 and 2001, two other amyloidogenic regions, hIAPP(30–37) and hIAPP(8–20), were identified to be able to form amyloid-like fibrils in aqueous medium as well [19, 21]. Sequence examination of these regions reveals a single amino acid variation between the rodent and human sequences at position 18, displaying Arg or His, respectively. At the C-terminus part, rIAPP(30–37) and hIAPP(30–37) are completely homologous. Thus, it was suggested that in the rodent molecule, two potentially amyloidogenic domains exist but are separated by the proline rich domain, residues 20–29, which prevent β-sheet formation [4].

Shortly after the publication of our results regarding the identification of very short amyloid-forming peptides within the IAPP(14–19) region [20], another study has shown the presence of short amyloidogenic peptides within the 8–20 region [22]. By scanning a series of overlapping peptides from the 8–20 region, two peptide fragments, IAPP(12–17) and IAPP(15–20), were found to form amyloid-like structures. This study gave a strong independent support to our findings. All together these findings provided clear evidence of the presence of more than one amyloidogenic domain within IAPP.

3.2. Contribution of individual residues to amyloid formation by full-length IAPP

The contribution of specific residues from different regions to hIAPP fibrillization was also investigated in the context

of full-length IAPP by performing single and multiple amino acid substitutions and assessing their influence on amyloid fibril formation. The ability of rIAPP variants of single-residue substitutions with amino acids from the corresponding positions of hIAPP was studied [23]. A single substitution of Arg to His at position 18 (R18H), in the full-length rIAPP, was found sufficient to render its competence for fibril formation at a small yield. Similar results were observed with the single substitutions L23F and V26I. In addition, the combination of two or three of these substitutions generally increased the ability to produce fibrils. These results show that the presence of the three proline residues in the rIAPP(20–29) domain is insufficient to abolish the ability to form fibrils. Moreover, the ability of the R18H variant of rIAPP to self-associate into amyloid fibrils suggests that other domains of IAPP except the 20–29 are involved in the self-recognition process.

The role of the histidine at position 18 in amyloid formation was further examined by assessing hIAPP fibrillization at various pH ranges [24]. The ionization state of His-18 was found to substantially affect the rate of assembly as well as the morphology of the amyloid fibrils formed by hIAPP. The aggregation process was faster at high pH (8.8), when the histidine is deprotonated, than at low pH (4.0). This fact may be physiologically relevant as mature hIAPP is stored in the β-cell granules at a pH of 5.5 and released into the extracellular matrix where the pH is of 7.4. Thus, the low pH in the pancreatic granules may protect hIAPP from aggregation.

Abedini and Raleigh, who performed the above-described study, further questioned the exclusive importance of the 20–29 region by designing a variant of the amyloidogenic hIAPP(8–37), containing three proline residues outside this region, at positions 17, 19, and 30 [25]. The 3×P variant had dramatically greater solubility and reduced tendency to form β-sheet structures compared to the wild-type polypeptide, as assayed by a variety of amyloid-detecting techniques. The authors concluded that models of IAPP fibrillization must take into account contributions of other regions within IAPP.

3.3. Inhibition of hIAPP amyloid formation

Based on our identification of the hIAPP(13–18) recognition site, we designed peptide inhibitors against IAPP fibrillization, which were targeted to this region. Using the previously exemplified method of incorporating β-breaker elements into amyloidogenic core peptides [26], we introduced a new inhibition strategy using the α-aminoisobutyric acid (Aib), a β-breaker element with extreme structural constrains [27]. Peptide fragments corresponding to the recognition domain were modified with Aib. The modified peptides completely lost their amyloidogenic potential. Furthermore, the Aib-modified peptide showed a powerful inhibitory effect on the formation of amyloid fibrils by the full-length hIAPP.

Evidently, the 20–29 region was also used as a template for inhibitor design and served as a target for inhibition. Kapurniotu et al. designed a nonamyloidogenic and bioactive mimic of hIAPP, which contains a double N-methylation of full-length hIAPP at positions G24 and I26, termed as IAPP-GI [28]. The presence of two N-methyl rests on the same side of a β-strand interferes with the interstrand amide hydrogen-bonding necessary for β-sheet formation [29]. The IAPP-GI analogue was shown to be a nanomolar affinity inhibitor of hIAPP fibrillization and cytotoxicity. However, although IAPP-GI did not form amyloid fibrils, it was found to have a "pronounced self-association propensity" and to form spheroids of up to 100 nm in diameter. Moreover, the Far-UV circular dichroism (CD) analysis of IAPP-GI indicated the presence of β-sheet and/or β-turn conformations. These insinuate the presence of another recognition and self-assembly domain besides the 20–29 region that enabled the formation of the observed structures. A reminiscent scenario exists in the study of peptide nanotubes and nanostructures, which was initiated from the search for a minimal amyloidogenic core domain of Alzheimer's β-amyloid polypeptide. While the Phe-Phe dipeptide was shown to form well-discrete peptide nanotubes [30], two other peptides, Cys-Phe-Phe and diphenylglycine, which are very similar to the diphenylalanine, formed closed-cage nanospheres [31]. We speculate that the remarkable inhibition ability of the IAPP-GI analogue is actually due to its high affinity recognition to the 3–18 site, as it is kept unmodified and thus provides maximal compatibility.

The search for inhibitors against amyloid formation led to the identification of insulin as an exceptional inhibitor of IAPP fibrillization [32–34]. This finding may be of high physiological importance as IAPP and insulin are costored and cosecreted from the pancreatic β-cell granules. Consequently, insulin is considered to form a complex with IAPP which stabilizes it and prevents it from aggregation within the granules [35, 36]. In order to reveal the molecular mechanism underlying the interaction between IAPP and insulin, we performed a molecular mapping of the interaction interface. Using a reductionist approach and peptide arrays, we located the cross-recognition sites within both polypeptides [37]. Interestingly, insulin was found to bind to the 13–18 region within IAPP. In addition, the identified recognition site within insulin, which resides within the insulin B chain, was previously shown to have sequence similarity to the hIAPP(13–18) region [35]. These findings reveal a typical amyloid inhibition mechanism for insulin and reinforce the central role of the 13–18 region: the binding of insulin to IAPP self-recognition site is mediated through sequence similarity, it interferes with IAPP self-association and prevents it from amyloid formation.

3.4. Interaction of IAPP with the membrane

As in the case of other amyloid-related disease, the mechanism by which IAPP causes cell destruction is assumed to involve interaction with the cell membrane. Different studies have investigated the possible interaction of IAPP with the membrane, mostly by the use of membrane mimetics such as liposomes and phospholipid assemblies. In a recent study, hIAPP was claimed to insert into phospholipid monolayer as a monomer [38]. Interestingly, it was suggested that the N-terminus of hIAPP is largely responsible for the insertion.

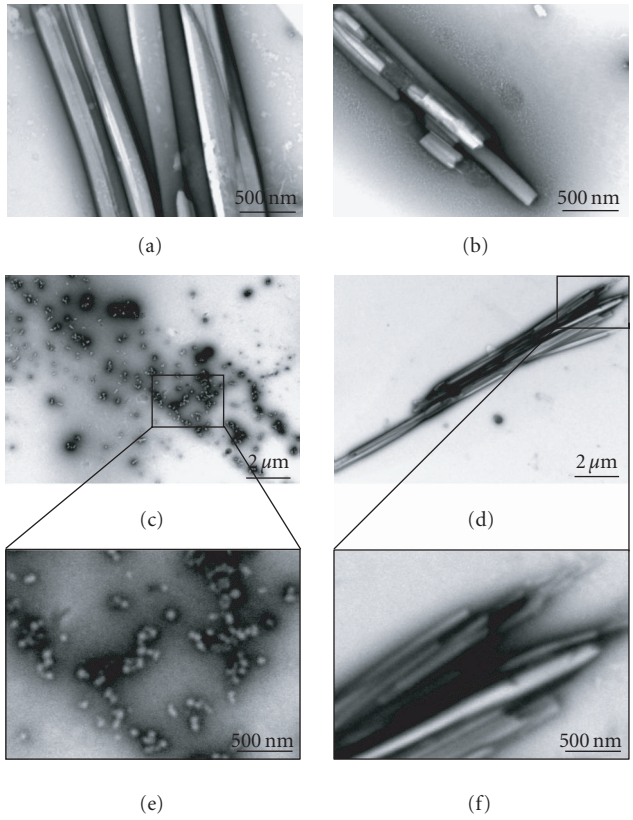

Figure 1: Morphology of the formed structures. Electron microscopic examination of negatively stained samples of the studied peptides: (a) C2, (b) H2, (c) C1, and (d) H1. The C1 peptide failed to form tubular structures as did the other peptides. (e) and (f) are high magnification micrographs of the marked rectangle areas of C1 and H1, respectively.

Experiments using fragments of hIAPP showed that a peptide consisting of the 19 N-terminal residues of hIAPP efficiently inserts into a phospholipids monolayer, whereas the 20–29 residue peptide inserts much less efficiently. These results offer a possible role for the N-terminal region also in the sense of interaction with the pancreatic β-cells which may be part of the mechanism underlying type II diabetes pathogenesis.

3.5. Comparison between the two amyloidogenic regions derived from the cat IAPP

Cats are among the few mammalian species that are known to suffer from type II diabetes and from accumulation of IAPP islet amyloid deposits [39, 40]. The cat IAPP (cIAPP) sequence differs from that of hIAPP in only four amino acids, at positions 17, 18, 23, and 29. The decapeptide corresponding to cIAPP(20–29) was previously shown to be able to aggregate into amyloidal structures as well [16, 41, 42], thus supporting the apparent fibrillization role of the 20–29 region. However, both the dog and cat IAPP are identical over the 20–29 region [43] and dogs are not known to develop type II diabetes.

Table 1: The studied peptides. Peptide fragments corresponding to regions within the human and cat IAPP were tested for the ability to form amyloid-like structures.

Name	Origin	Sequence	Residues
C1	cat	NLGAILSP	22–29
H1	human	NFGAILSS	22–29
C2	cat	NFLIRSS	14–20
H2	human	NFLVHSS	14–20

In order to re-evaluate the role of the two identified recognition sites of IAPP in the fibrillization process, we tested the self-assembly propensity of peptide fragments derived from the cat IAPP, cIAPP(22–29), and cIAPP(14–20). We also tested the aggregation of the corresponding human sequence peptides for reference. The peptide sequences are presented in Table 1. The peptides were dissolved into aqueous solution, under the exact same conditions, incubated for one to three days and tested for amyloid formation by electron microscopy (EM) and Congo Red (CR) birefringence. Their secondary conformation was also evaluated by Fourier-transform infrared spectroscopy (FTIR).

Differences between the peptides appeared already before applying the amyloid tests. Upon dilution of the peptides into aqueous solution, the H1 peptide immediately precipitated into eye-visible aggregates. The other peptide solutions appeared clear to the unarmed-eye. Examination of the peptide samples under the electron microscope revealed the presence of well-ordered tubular structures for all the peptides except the C1 peptide (Figure 1). Apparently, the peptides were found to form nanotubes rather than fibrils. The formation of tubular structures by H2 and H1 was previously shown [18, 20, 44]. Here we found that the C2 peptide can also form highly defined tubular structures. Thin fibrils were also detected in proximity with the nanotubes or in independent bundles (not shown). The C2 sample contained mostly nanotubes, the H2 sample contained nanotubes and fibrils, and the H1 sample contained also large aggregates. The C1 peptide however did not form fibrils or tubes, only less ordered spherical structures and aggregates were observed. The spherical structures may be reminiscing the ones observed for the IAPP analogue IAPP-GI [28], which were discussed above, however they are less ordered than the last ones.

Upon staining with the Congo Red dye, the C2 and H2 samples exhibited clear gold-green birefringence (Figure 2). In the H1 sample, the dye appears to be bound, however, no green color was detected. Possibly, the large amount of aggregates, which were present in addition to the fibrillar and tubular structures, were shielding over them. No birefringence or CR binding was shown in the C1 sample, the slide looked quite clean. Secondary structure analysis of the peptides by FTIR showed large β-sheet content for all the peptides (Figure 3). The β-sheet conformation is characteristic of amyloid-like structures, but is not exclusive for them. The C1 peptide, negatively detected for amyloid structures, also displayed β-sheet conformation which may

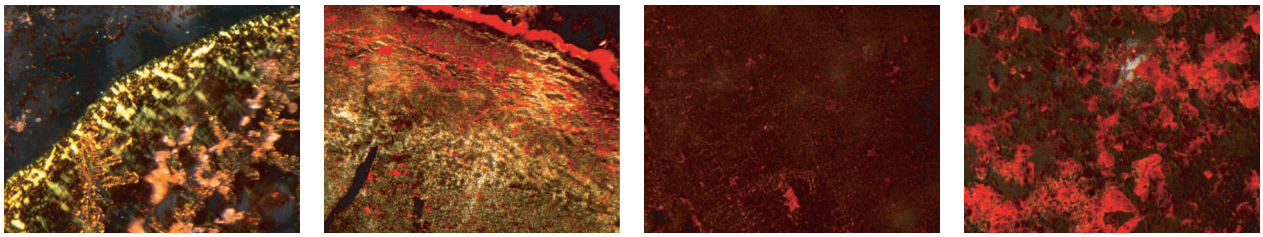

Figure 2: Congo Red binding and birefringence. Microscopic examination under cross-polerizers upon staining with Congo Red of samples of the studied peptides: (a) C2, (b) H2, (c) C1, and (d) H1. The C2 and H2 peptides exhibited green birefringence characteristic of amyloidal structures.

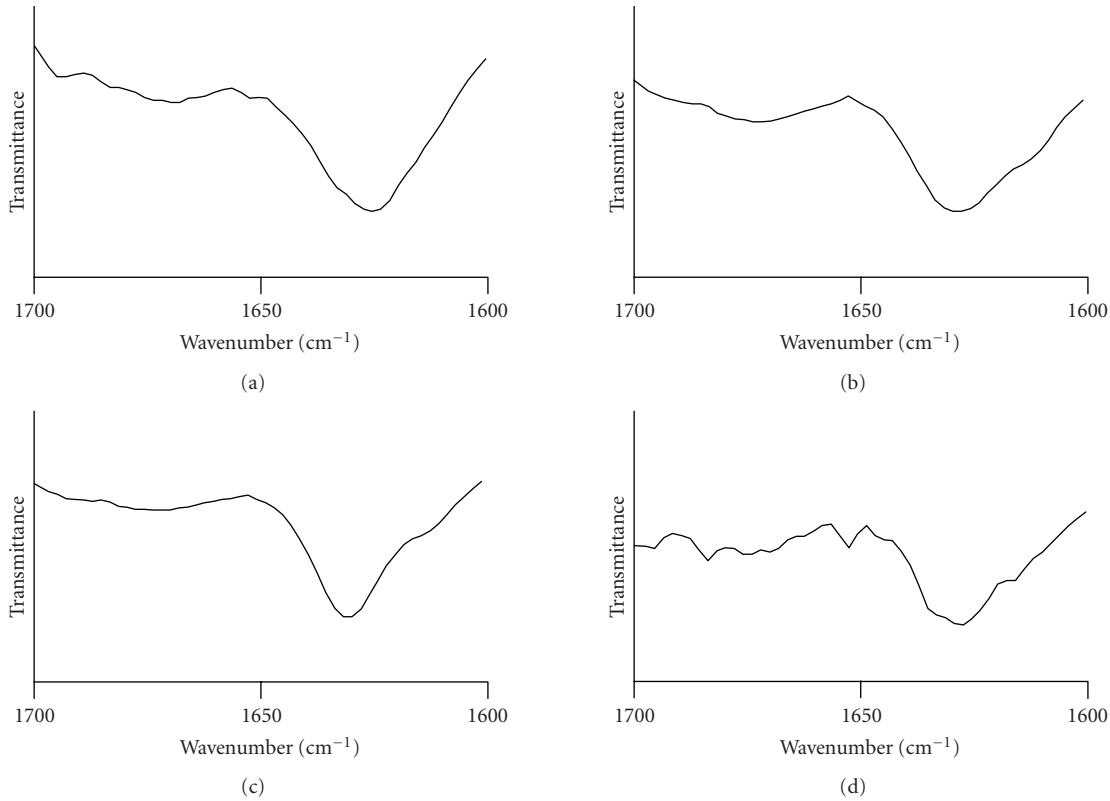

Figure 3: Secondary conformation of the formed structures. Fourier-transform infrared (FTIR) spectroscopy analysis of the secondary conformation of the peptides: (a) C2, (b) H2, (c) C1, and (d) H1. All the peptides exhibited spectra typical for β-sheet secondary structure.

be attributed to the spheroid structures observed by the EM or to its soluble form.

The comparison between the two cat derived peptides reveals that the C2 peptide, containing residues 14–20, is much more competent for self-assembly into amyloid-like structures than the C1 peptide, composed of residues 22–29. Although a longer version of the C1 peptide, composed of residues 20–29, was previously shown to form fibrillar structures [41, 42], in the present experimental setup it was unable to form such fibrils. We consider this diversity to result from the length of the peptide and different experimental conditions, which are in the present assay of more physiologically-relevant environment and of lower concentration. Nevertheless, when compared to the C2 peptide, C1 is dramatically less potent for fibril formation. While the C1 peptide may contain self-association properties as observed by the presence of spherical structures and β-sheet content, the C2 peptide exhibited self-assembly potency into well-ordered macromolecular fibrils, which were not displayed by the C1 peptide. This observation provides fresh supporting evidence for the central role of the 13–18 region within the IAPP molecule in amyloid formation: while in hIAPP both regions are highly amyloidogenic, in the cat IAPP, there is a clear difference between the two peptides.

Different behavior was also observed for the two human derived peptides H1 and H2, which may insinuate their diverse roles in the amyloidogenic process. The H1 peptide seems to be highly aggregative since visible precipitates were

observed upon dilution into aqueous solution as well as under the EM. The H2 peptide however seems to have higher ability to form well-ordered structures which requires specific recognition. Its solution was visibly clear and EM examination revealed only fibrilar and tubular structures without aggregates. In addition, green birefringence upon CR binding, which is characteristic of ordered structures, was observed in the H2 sample but not in the H1 sample. Consistent with this observation is the different recognition affinity of the two peptide fragments to the full-length IAPP as we have previously showed by the peptide array assay [20].

The C1 peptide is not as aggregative as the H1 peptide, although it contains some structural features as observed by the FTIR and EM analyses. A comparison between these two sequences in their longer versions of residues 20–29 was previously performed by Ashburn and Lansbury [42]. In this study, both peptides were found to form amyloid fibrils, however, with remarkably different kinetics. The cIAPP(20–29) peptide formed fibrils approximately 13-fold more slowly than its human version. This correlates with our results regarding the different potency for fibrillization of the two sequences. It is likely that with a longer incubation period, the cIAPP(22–29) would also fibrillate eventually.

The cIAPP sequence differs from the hIAPP sequence by a Leu instead of a Phe at position 23 and a Pro instead of a Ser at position 29. Both modifications were shown to separately influence the kinetics of the peptide fibrillization [42]. It seems obvious that a Ser to Pro substitution will decrease the fibrillization potency, since Pro is a strong β-breaker element. Regarding the Phe to Leu substitution, we speculate that the Phe residue facilitates the fibrillization process through aromatic interactions. According to our established hypothesis, aromatic residues and interactions largely enhance the process of amyloid formation by providing directionality and stability to the growing fibril [45–49].

3.6. *Intra-β-sheet mechanism for IAPP amyloid formation*

The accumulated data presented in this paper prove that none of the two amyloidogenic regions within IAPP can be ignored. A possible mechanism underlying the self-assembly of IAPP into amyloid fibrils includes a role for both regions. It was already suggested in 2001 by Jaikaran and Clark that the structural transition of IAPP into amyloid fibrils involves in interactions between β-stranded regions within the monomer [4]. According to their model, an intramolecular β-sheet is formed by three β-strands composed of the segments 8–20, 24–29, and 32–37. Earlier secondary structure prediction based on IAPP sequence provided support to their model by predicting β-turns at positions 20 and 31, as well as β-strands for residues 14–18 and 26–29 [50]. More recently, another model for the structure of IAPP within the amyloid fibril was proposed. Accordingly, the same three β-strands are present, however, arranged in a zigzag planar s-shaped β-sheet, instead of the previously proposed e-shaped structure [51].

The presence of an intramolecular β-sheet in the fibrillar structure of IAPP is supported by the identification of long-range interactions between distinct residues within the IAPP molecule. Using fluorescence resonance energy transfer (FRET), the tyrosine at position 37 was shown to be close in space to the two phenylalanine residues (F23 and F15) at the fibrillogenic state of hIAPP [52]. Another interesting point arises from the genetic background of type II diabetes. Although the disease is predominantly sporadic, a mutation in hIAPP sequence, the S20G mutation, which is identified among the Japanese population, was found to be related to early onset of the disease [53]. The S20G mutant was also shown to exhibit increased fibrillization and cytotoxicity compared to wild-type hIAPP [54]. Indeed, according to the intra-β-sheet models, the mutation is placed in a β-turn region, which is favorable for the glycine residue.

4. CONCLUSIONS

The formation of amyloid deposits by IAPP appears to play a central role in the pathogenesis of type II diabetes. Knowledge regarding the exact mechanism of this process may be highly relevant for the development of therapeutic agents for the treatment of the disease. Although it is clear that many environmental factors are involved in this process, understanding the amyloid formation route at the molecular level may be highly valued. In this paper, we have summarized results from several research groups which support the notion that the 20–29 region within IAPP cannot be considered as the sole amyloidogenic core of the polypeptide. By reviewing previously published data, by us and others, as well as providing experimental data regarding the amyloidogenicity of the 13–18 region derived from the cat IAPP, we emphasized the essential role of the 13–18 region in the fibrillization process of IAPP. We conclude that an intramolecular β-sheet structure, formed by at least the two discussed regions, may provide a very good mechanism to the discussed observations.

ACKNOWLEDGMENTS

The authors thank Yaacov Delarea for help with electron microscopy experiments and members of the Gazit laboratory for helpful discussions. The second author thanks the Deutsch-Israelische Projektkooperation (DIP) for financial support.

REFERENCES

[1] A. Lukinius, E. Wilander, G. T. Westermark, U. Engström, and P. Westermark, "Co-localization of islet amyloid polypeptide and insulin in the B cell secretory granules of the human pancreatic islets," *Diabetologia*, vol. 32, no. 4, pp. 240–244, 1989.

[2] P. Westermark, K. H. Johnson, T. D. O'Brien, and C. Betsholtz, "Islet amyloid polypeptide—a novel controversy in diabetes research," *Diabetologia*, vol. 35, no. 4, pp. 297–303, 1992.

[3] A. Kapurniotu, "Amyloidogenicity and cytotoxicity of islet amyloid polypeptide," *Peptide Science*, vol. 60, no. 6, pp. 438–459, 2001.

[4] E. T. A. S. Jaikaran and A. Clark, "Islet amyloid and type 2 diabetes: from molecular misfolding to islet pathophysiology,"

Biochimica et Biophysica Acta, vol. 1537, no. 3, pp. 179–203, 2001.

[5] P. Westermark, C. Wernstedt, E. Wilander, and K. Sletten, "A novel peptide in the calcitonin gene related peptide family as an amyloid fibril protein in the endocrine pancreas," *Biochemical and Biophysical Research Communications*, vol. 140, no. 3, pp. 827–831, 1986.

[6] G. J. S. Cooper, A. C. Willis, A. Clark, R. C. Turner, R. B. Sim, and K. B. M. Reid, "Purification and characterization of a peptide from amyloid-rich pancreases of type 2 diabetic patients," *Proceedings of the National Academy of Sciences of the United States of America*, vol. 84, no. 23, pp. 8628–8632, 1987.

[7] J. W. M. Höppener, C. Oosterwijk, K. L. Van Hulst, et al., "Molecular physiology of the islet amyloid polypeptide (IAPP)/amylin gene in man, rat, and transgenic mice," *Journal of Cellular Biochemistry*, vol. 55, supplement, pp. 39–53, 1994.

[8] S. J. Wimalawansa, "Amylin, calcitonin gene-related peptide, calcitonin, and adrenomedullin: a peptide superfamily," *Critical Reviews in Neurobiology*, vol. 11, no. 2-3, pp. 167–239, 1997.

[9] O. Schmitz, B. Brock, and J. Rungby, "Amylin agonists: a novel approach in the treatment of diabetes," *Diabetes*, vol. 53, supplement 3, pp. S233–S238, 2004.

[10] J.-C. Rochet and P. T. Lansbury Jr., "Amyloid fibrillogenesis: themes and variations," *Current Opinion in Structural Biology*, vol. 10, no. 1, pp. 60–68, 2000.

[11] C. Soto, "Protein misfolding and disease; protein refolding and therapy," *FEBS Letters*, vol. 498, no. 2-3, pp. 204–207, 2001.

[12] E. Gazit, "The "correctly folded" state of proteins: is it a metastable state?" *Angewandte Chemie International Edition*, vol. 41, no. 2, pp. 257–259, 2002.

[13] J. C. Sacchettini and J. W. Kelly, "Therapeutic strategies for human amyloid diseases," *Nature Reviews Drug Discovery*, vol. 1, no. 4, pp. 267–275, 2002.

[14] C. M. Dobson, "Protein folding and misfolding," *Nature*, vol. 426, no. 6968, pp. 884–890, 2003.

[15] C. Betsholtz, L. Christmansson, U. Engström, et al., "Sequence divergence in a specific region of islet amyloid polypeptide (IAPP) explains differences in islet amyloid formation between species," *FEBS Letters*, vol. 251, no. 1-2, pp. 261–264, 1989.

[16] P. Westermark, U. Engström, K. H. Johnson, G. T. Westermark, and C. Betsholtz, "Islet amyloid polypeptide: pinpointing amino acid residues linked to amyloid fibril formation," *Proceedings of the National Academy of Sciences of the United States of America*, vol. 87, no. 13, pp. 5036–5040, 1990.

[17] G. G. Glenner, E. D. Eanes, and C. A. Wiley, "Amyloid fibrils formed from a segment of the pancreatic islet amyloid protein," *Biochemical and Biophysical Research Communications*, vol. 155, no. 2, pp. 608–614, 1988.

[18] K. Tenidis, M. Waldner, J. Bernhagen, et al., "Identification of a penta- and hexapeptide of islet amyloid polypeptide (IAPP) with amyloidogenic and cytotoxic properties," *Journal of Molecular Biology*, vol. 295, no. 4, pp. 1055–1071, 2000.

[19] E. T. A. S. Jaikaran, C. E. Higham, L. C. Serpell, et al., "Identification of a novel human islet amyloid polypeptide β-sheet domain and factors influencing fibrillogenesis," *Journal of Molecular Biology*, vol. 308, no. 3, pp. 515–525, 2001.

[20] Y. Mazor, S. Gilead, I. Benhar, and E. Gazit, "Identification and characterization of a novel molecular-recognition and self-assembly domain within the islet amyloid polypeptide," *Journal of Molecular Biology*, vol. 322, no. 5, pp. 1013–1024, 2002.

[21] M. R. Nilsson and D. P. Raleigh, "Analysis of amylin cleavage products provides new insights into the amyloidogenic region of human amylin," *Journal of Molecular Biology*, vol. 294, no. 5, pp. 1375–1385, 1999.

[22] L. A. Scrocchi, K. Ha, Y. Chen, L. Wu, F. Wang, and P. E. Fraser, "Identification of minimal peptide sequences in the (8–20) domain of human islet amyloid polypeptide involved in fibrillogenesis," *Journal of Structural Biology*, vol. 141, no. 3, pp. 218–227, 2003.

[23] J. Green, C. Goldsbury, T. Mini, et al., "Full-length rat amylin forms fibrils following substitution of single residues from human amylin," *Journal of Molecular Biology*, vol. 326, no. 4, pp. 1147–1156, 2003.

[24] A. Abedini and D. P. Raleigh, "The role of His-18 in amyloid formation by human islet amyloid polypeptide," *Biochemistry*, vol. 44, no. 49, pp. 16284–16291, 2005.

[25] A. Abedini and D. P. Raleigh, "Destabilization of human IAPP amyloid fibrils by proline mutations outside of the putative amyloidogenic domain: is there a critical amyloidogenic domain in human IAPP?" *Journal of Molecular Biology*, vol. 355, no. 2, pp. 274–281, 2006.

[26] C. Soto, E. M. Sigurdsson, L. Morelli, R. A. Kumar, E. M. Castaño, and B. Frangione, "β-sheet breaker peptides inhibit fibrillogenesis in a rat brain model of amyloidosis: implications for Alzheimer's therapy," *Nature Medicine*, vol. 4, no. 7, pp. 822–826, 1998.

[27] S. Gilead and E. Gazit, "Inhibition of amyloid fibril formation by peptide analogues modified with α-aminoisobutyric acid," *Angewandte Chemie International Edition*, vol. 43, no. 31, pp. 4041–4044, 2004.

[28] L.-M. Yan, M. Tatarek-Nossol, A. Velkova, A. Kazantzis, and A. Kapurniotu, "Design of a mimic of nonamyloidogenic and bioactive human islet amyloid polypeptide (IAPP) as nanomolar affinity inhibitor of IAPP cytotoxic fibrillogenesis," *Proceedings of the National Academy of Sciences of the United States of America*, vol. 103, no. 7, pp. 2046–2051, 2006.

[29] A. Kapurniotu, A. Schmauder, and K. Tenidis, "Structure-based design and study of non-amyloidogenic, double N-methylated IAPP amyloid core sequences as inhibitors of IAPP amyloid formation and cytotoxicity," *Journal of Molecular Biology*, vol. 315, no. 3, pp. 339–350, 2002.

[30] M. Reches and E. Gazit, "Casting metal nanowires within discrete self-assembled peptide nanotubes," *Science*, vol. 300, no. 5619, pp. 625–627, 2003.

[31] M. Reches and E. Gazit, "Formation of closed-cage nanostructures by self-assembly of aromatic dipeptides," *Nano Letters*, vol. 4, no. 4, pp. 581–585, 2004.

[32] P. Westermark, Z.-C. Li, G. T. Westermark, A. Leckström, and D. F. Steiner, "Effects of beta cell granule components on human islet amyloid polypeptide fibril formation," *FEBS Letters*, vol. 379, no. 3, pp. 203–206, 1996.

[33] S. Janciauskiene, S. Eriksson, E. Carlemalm, and B. Ahrén, "B cell granule peptides affect human islet amyloid polypeptide (IAPP) fibril formation in vitro," *Biochemical and Biophysical Research Communications*, vol. 236, no. 3, pp. 580–585, 1997.

[34] Y. C. Kudva, C. Mueske, P. C. Butler, and N. L. Eberhardt, "A novel assay in vitro of human islet amyloid polypeptide amyloidogenesis and effects of insulin secretory vesicle peptides on amyloid formation," *Biochemical Journal*, vol. 331, part 3, pp. 809–813, 1998.

[35] E. T. A. S. Jaikaran, M. R. Nilsson, and A. Clark, "Pancreatic β-cell granule peptides form heteromolecular complexes which inhibit islet amyloid polypeptide fibril formation," *Biochemical Journal*, vol. 377, part 3, pp. 709–716, 2004.

[36] J. L. Larson and A. D. Miranker, "The mechanism of insulin action on islet amyloid polypeptide fiber formation," *Journal of Molecular Biology*, vol. 335, no. 1, pp. 221–231, 2004.

[37] S. Gilead, H. Wolfenson, and E. Gazit, "Molecular mapping of the recognition interface between the islet amyloid polypeptide and insulin," *Angewandte Chemie International Edition*, vol. 45, no. 39, pp. 6476–6480, 2006.

[38] M. F. M. Engel, H. Yigittop, R. C. Elgersma, et al., "Islet amyloid polypeptide inserts into phospholipid monolayers as monomer," *Journal of Molecular Biology*, vol. 356, no. 3, pp. 783–789, 2006.

[39] K. H. Johnson, D. W. Hayden, T. D. O'Brien, and P. Westermark, "Spontaneous diabetes mellitus-islet amyloid complex in adult cats," *American Journal of Pathology*, vol. 125, no. 2, pp. 416–419, 1986.

[40] P. Westermark, C. Wernstedt, E. Wilander, D. W. Hayden, T. D. O'Brien, and K. H. Johnson, "Amyloid fibrils in human insulinoma and islets of Langerhans of the diabetic cat are derived from a neuropeptide-like protein also present in normal islet cells," *Proceedings of the National Academy of Sciences of the United States of America*, vol. 84, no. 11, pp. 3881–3885, 1987.

[41] C. Betsholtz, L. Christmanson, U. Engström, et al., "Structure of cat islet amyloid polypeptide and identification of amino acid residues of potential significance for islet amyloid formation," *Diabetes*, vol. 39, no. 1, pp. 118–122, 1990.

[42] T. T. Ashburn and P. T. Lansbury Jr., "Interspecies sequence variations affect the kinetics and thermodynamics of amyloid formation: peptide models of pancreatic amyloid," *Journal of the American Chemical Society*, vol. 115, no. 23, pp. 11012–11013, 1993.

[43] K. Albrandt, E. Mull, G. J. S. Cooper, and M. J. Johnson, "Nucleotide sequence of a cDNA for canine amylin," *Biochimica et Biophysica Acta*, vol. 1130, no. 1, pp. 97–99, 1992.

[44] M. R. Sawaya, S. Sambashivan, R. Nelson, et al., "Atomic structures of amyloid cross-β spines reveal varied steric zippers," *Nature*, vol. 447, no. 7143, pp. 453–457, 2007.

[45] R. Azriel and E. Gazit, "Analysis of the minimal amyloid-forming fragment of the islet amyloid polypeptide. An experimental support for the key role of the phenylalanine residue in amyloid formation," *Journal of Biological Chemistry*, vol. 276, no. 36, pp. 34156–34161, 2001.

[46] E. Gazit, "A possible role for π-stacking in the self-assembly of amyloid fibrils," *The FASEB Journal*, vol. 16, no. 1, pp. 77–83, 2002.

[47] E. Gazit, "Global analysis of tandem aromatic octapeptide repeats: the significance of the aromatic-glycine motif," *Bioinformatics*, vol. 18, no. 6, pp. 880–883, 2002.

[48] M. Reches, Y. Porat, and E. Gazit, "Amyloid fibril formation by pentapeptide and tetrapeptide fragments of human calcitonin," *Journal of Biological Chemistry*, vol. 277, no. 38, pp. 35475–35480, 2002.

[49] Y. Porat, A. Stepensky, F.-X. Ding, F. Naider, and E. Gazit, "Completely different amyloidogenic potential of nearly identical peptide fragments," *Biopolymers*, vol. 69, no. 2, pp. 161–164, 2003.

[50] C. E. Higham, E. T. A. S. Jaikaran, P. E. Fraser, M. Gross, and A. Clark, "Preparation of synthetic human islet amyloid polypeptide (IAPP) in a stable conformation to enable study of conversion to amyloid-like fibrils," *FEBS Letters*, vol. 470, no. 1, pp. 55–60, 2000.

[51] A. V. Kajava, U. Aebi, and A. C. Steven, "The parallel superpleated beta-structure as a model for amyloid fibrils of human amylin," *Journal of Molecular Biology*, vol. 348, no. 2, pp. 247–252, 2005.

[52] S. B. Padrick and A. D. Miranker, "Islet amyloid polypeptide: identification of long-range contacts and local order on the fibrillogenesis pathway," *Journal of Molecular Biology*, vol. 308, no. 4, pp. 783–794, 2001.

[53] S. Sakagashira, T. Sanke, T. Hanabusa, et al., "Missense mutation of amylin gene (S20G) in Japanese NIDDM patients," *Diabetes*, vol. 45, no. 9, pp. 1279–1281, 1996.

[54] S. Sakagashira, H. J. Hiddinga, K. Tateishi, et al., "S20G mutant amylin exhibits increased in vitro amyloidogenicity and increased intracellular cytotoxicity compared to wild-type amylin," *American Journal of Pathology*, vol. 157, no. 6, pp. 2101–2109, 2000.

Hindawi Publishing Corporation
Experimental Diabetes Research
Volume 2008, Article ID 562985, 8 pages
doi:10.1155/2008/562985

Review Article

Amyloid Deposition in Transplanted Human Pancreatic Islets: A Conceivable Cause of Their Long-Term Failure

Arne Andersson,[1] Sara Bohman,[1] L. A. Håkan Borg,[1] Johan F. Paulsson,[2] Sebastian W. Schultz,[2] Gunilla T. Westermark,[1,2] and Per Westermark[3]

[1] *Department of Medical Cell Biology, Uppsala University, 751 23 Uppsala, Sweden*
[2] *Division of Cell Biology, Diabetes Research Centre, Linköping University, 581 83 Linköping, Sweden*
[3] *Department Genetics and Pathology, Uppsala University, 751 85 Uppsala, Sweden*

Correspondence should be addressed to Arne Andersson, arne.andersson@mcb.uu.se

Received 28 March 2008; Revised 30 June 2008; Accepted 1 December 2008

Recommended by Steven E. Kahn

Following the encouraging report of the Edmonton group, there was a rejuvenation of the islet transplantation field. After that, more pessimistic views spread when long-term results of the clinical outcome were published. A progressive loss of the β-cell function meant that almost all patients were back on insulin therapy after 5 years. More than 10 years ago, we demonstrated that amyloid deposits rapidly formed in human islets and in mouse islets transgenic for human IAPP when grafted into nude mice. It is, therefore, conceivable to consider amyloid formation as one potential candidate for the long-term failure. The present paper reviews attempts in our laboratories to elucidate the dynamics of and mechanisms behind the formation of amyloid in transplanted islets with special emphasis on the impact of long-term hyperglycemia.

1. INTRODUCTION

The discovery of insulin in the early 1920s greatly improved the prognosis for type 1 diabetes patients and by such means patients with diabetes could survive a previously fatal disease. Because of the substantial improvements in insulin therapy, most patients nowadays can handle their treatment themselves and risks for the crippling long-term complications have become extensively reduced. This, however, requires strict blood glucose control and life style restrictions. These latter insufficiencies of the present treatment together with the fact that a subgroup of patients is still disturbed by frequent hypoglycaemic attacks have meant that there is considerable interest in pancreatic islet transplantation. For long replacement of the destroyed β-cells in type 1 diabetes with new β-cells, this has attracted much attention. Paul Lacy's pioneering work with his collagenase-based method for rat islet isolation paved the way for islet transplantation experiments. Clinical trials were carried out in the 80s and 90s but only about 10% of islet recipients achieved normoglycemia without insulin therapy. However, in their report in the year 2000 James Shapiro et al. reported a handful of diabetes patients all of whom became normoglycemic after two or three intraportal implantations of noncultured human islets [1]. Given a steroid-free immunosuppression, these patients remained off insulin for at least one year. In an international trial of this so-called Edmonton protocol, 36 subjects with type 1 diabetes underwent this type of treatment at nine international sites [2]. While 16 of them (44%) were insulin free after one year only 5 (14%) remained so after one more year. It was concluded that there was a progressive loss of islet function in most subjects, who had all become insulin independent initially.

For long, it has been postulated that long-term hyperglycemia might influence β-cell function in a negative way. Numerous in vitro and in vivo studies have indicated that so is the case but the molecular mechanisms are still unclear. We, therefore, found it conceivable to consider amyloid formation as one potential candidate. This paper reviews attempts in our laboratory to elucidate the fate of transplanted human islets with a special view on their morphology and function and especially so under influence of prolonged hyperglycemic stress.

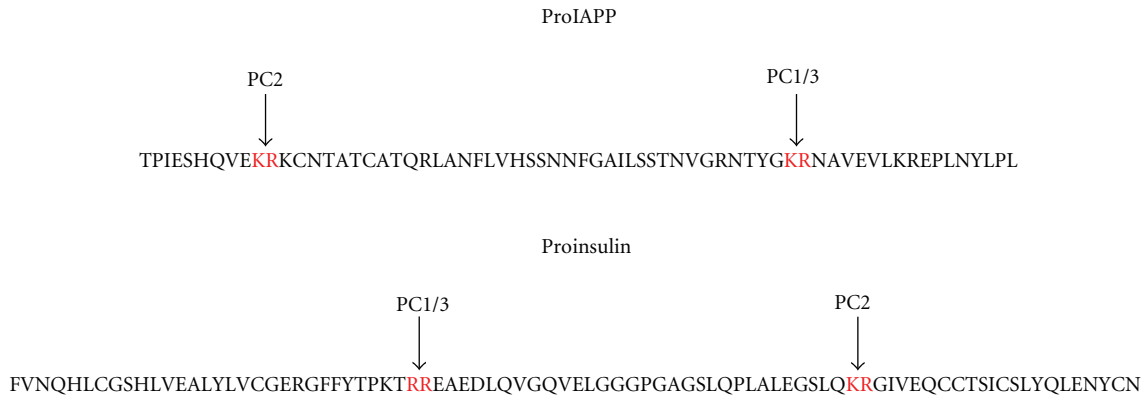

Figure 1: Processing at double basic amino acid residues of proinsulin and proIAPP by the prohormone convertases PC 1/3 and PC2.

2. ISLET AMYLOID POLYPEPTIDE AND ISLET AMYLOID

Although islet amyloid was discovered already in 1901 [3, 4], its impact in the pathogenesis of type 2 diabetes has been questioned for a long period of time. However, there are several lines of evidence for the importance of the amyloid formation for the β-cell lesion in type 2 diabetes (for reviews, see [5, 6]). The exact mechanisms are still not very well understood but aggregated IAPP is toxic to β-cells [7, 8].

IAPP was discovered by purification and analysis of amyloid, first from a human insulinoma [9, 10] and later from islets of Langerhans [11, 12]. The same peptide was found to form amyloid in apes [13, 14] and cats [11, 15]. Human IAPP is a 37-amino acid residue peptide, expressed as a prepromolecule. After removal of the signal peptide, the 67-amino acid propeptide is further processed at two double basic residues by the prohormone convertases PC2 and PC1/3 which remove two short peptides N- and C-terminally (Figure 1). The remaining peptide is C-terminally amidated and there is a disulfide bridge between residues 2 and 7.

IAPP is expressed by β-cells and is stored and released together with insulin. IAPP is very aggregation-prone in vitro and rapidly forms amyloid-like fibrils. This does not normally happen in vivo, where there must be mechanisms which hinder this. Binding to insulin may be such a mechanism [16, 17]. However, it is not understood why IAPP aggregates into amyloid in conjunction with type 2 diabetes. Experiments with transgenic mice, overexpressing human IAPP, clearly indicate that an increased production of IAPP is not the single explanation but that other factors must contribute.

2.1. *Transgenic animals overexpressing human IAPP*

Mice and rats do not develop islet amyloid, depending on differences in the IAPP sequence. Proline residues in the amyloid-forming core of IAPP abolish the fibril formation in both species [18]. Several groups have, therefore, created transgenic mouse lines expressing human IAPP under regulation of an insulin promoter. In spite of overexpression of human IAPP, islet amyloid generally does not develop. However, amyloid does appear when such animals are fed a diet high in fat [19, 20] or are crossed with ob/ob [21] or agouti [22] mice. We are working with a mouse line, overexpressing human IAPP behind rat insulin 1 promoter but devoid of mouse IAPP. Animals of this strain do not spontaneously develop islet amyloid at any age but in male mice, when fed a diet with high content of fat, amyloid deposits occur at an age of 11 months [20]. The amyloid is mainly found extracellularly but intracellular deposits do occur [23].

2.2. *Amyloid development in cultured human and transgenic mouse islets*

Interestingly, islets isolated from our transgenic mouse strain develop amyloid deposits rapidly when cultured in vitro [24]. A similar experience was obtained with another human IAPP transgenic mouse strain [25]. Furthermore, in contrast to what is found in islets in type 2 diabetes, where the amyloid is extracellular [26], intracellular aggregation of IAPP initially takes place in cultured human islets [27]. The exact compartmental position has been difficult to determine but is probably the endoplasmic reticulum or Golgi apparatus [28].

2.3. *Aberrant processing and amyloid formation*

There is evidence that the intracellular amyloid contains proIAPP and a defect processing of this precursor to mature IAPP may play a role in the pathogenesis of amyloid formation [23]. β-Cell stress that occurs in the initial phase of type 2 diabetes results in a disproportional secretion of unprocessed or partially processed proinsulin (des 32-33 C-peptide-A-chain fragment) [29]. This shift can mirror an increase in granule turnover, or, perhaps more interestingly is a sign of incomplete processing due to convertase deficiency. Also the prohormone convertases PC 1/3 and PC2 themselves must undergo cleavage to become active, and therefore, aberrant activation of convertases can

lead to incomplete processing. Proinsulin is processed by PC1/3 at the B-chain/C-peptide junction followed by PC2 cleavage at the C-peptide/A-chain junction while PC1/3 and PC2 processing of proIAPP results in the removal of the C-terminal and N-terminal flanking peptides, respectively [30]. In vitro, IAPP is one of the more aggregation-prone amyloid peptides known and insulin has been shown to exert a concentration-dependent inhibitory effect on IAPP fibril formation at neutral pH. We have produced human IAPP and partially processed proIAPP, lacking the C-terminal flanking peptide (NIAPP) with recombinant technology [31]. In the following, previously unpublished study, IAPP or NIAPP (20 μM) and insulin (40 μM) were dissolved in 25 mM phosphate buffer with 50 mM glycine at pH 7 and pH 5.2. Aliquots were analyzed for the presence of amyloid fibrils after Congo red staining. We conferred our earlier findings that addition of insulin to IAPP delays fibril formation at pH 7.0 and this was also true for NIAPP. However, at pH 5.2 the fibril formation was triggered for both IAPP and NIAPP. Semiquantitative analysis of amyloid amount, based on Congo red staining and electron microscopical analyses, showed that NIAPP was more prone to form amyloid-like fibrils than mature IAPP. Since both NIAPP and the des 32-33 C-peptide-A-chain proinsulin derivative are expected to appear in the secretory granules as a consequence of reduced PC2 processing, we also expressed des 32-33 C-peptide-A-chain proinsulin. NIAPP and 32-33 C-peptide-A-chain proinsulin were solubilized as described above and mixed 1:1 and 1:4. It was then shown that addition of 32-33 C-peptide-A-chain proinsulin to NIAPP promotes fibril formation. These previously unpublished results show that the intragranular composition of prohormones and processing metabolites is of importance and changes of the equilibrium can be a factor that causes IAPP to aggregate. Transfection of human proIAPP to cell lines missing one or both of the processing enzymes has supported this conclusion since the aberrant processing resulted in increased amyloid formation [32, 33].

3. INFLUENCE OF HYPERGLYCEMIA ON GRAFTED HUMAN ISLETS

3.1. Electron microscopical appearance

In general, the ultrastructure of human islets grafted into normoglycemic mice remains normal 4 weeks after implantation [34]. The β-cells are in great majority. A 4-week hyperglycaemic period induces well-known signs of β-cell hyperactivity such as marked degranulation and also signs of the development of an abundant rough endoplasmic reticulum (Figure 2). We also observed signs of glycogen particles accumulating in the β-cells. These glycogen depositions disappear when transferring the islets to a normoglycemic milieu by curing the recipient by means of implantation of a second islet graft. Interestingly, the mitochondria residing in the hyperglycaemic, noncured recipients are often swollen (Figure 2).

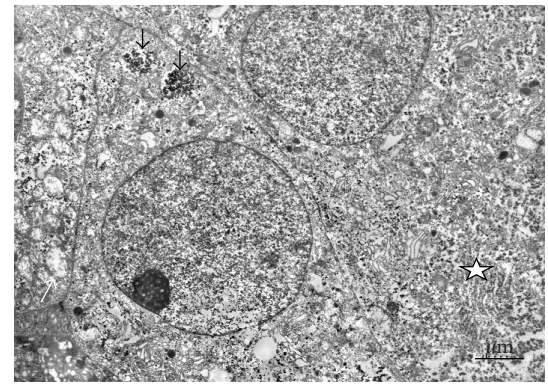

Figure 2: Electron micrograph of human islets transplanted under the kidney capsule of an alloxan-diabetic athymic nude mouse four weeks after implantation. Note the extensive degranulation, the abundant endoplasmic reticulum (star), glycogen particles (black arrows), and swollen mitochondria (white arrow).

Taken together, these previous ultrastructural investigations show that the transmission electron microscopical tool is of utmost importance when elucidating the impact of different functional loads put on human islets. Obviously, the knowledge on the classical "hydropic degeneration," later referred to as "ballooning degeneration" described by Weichelbaum and Stangl, Allen, Toreson, and Lazarus and Volk [35], in reality has become extended by the findings of the glycogen accumulations described above. Likewise, the very early reports on hyalinization of the islets of patients with diabetes by Opie, in 1901 [3], have formed the platform for extensive studies, both morphological and biochemical, on the formation of amyloid deposits (described below).

3.2. Functional properties

The ultrastructural findings were corroborated by measurements of the islet graft insulin content (Figure 3). Thus, the high glucose-exposed islet grafts contained about one tenth of the insulin found in the normoglycemic control grafts indicating a parallelism between low insulin content and extensive β-cell degranulation. In graft perfusion experiments, where test substances were infused via the renal artery and effluents collected from the ureter and renal vein [36], we found that a high glucose challenge in the test medium increased the insulin concentration of the effluent medium in a biphasic mode when the graft had resided in a normoglycemic recipient not treated with alloxan. Quite in contrast, islet grafts exposed to a high (more than 20 mM) glucose concentration in vivo for 4 weeks displayed a blunted insulin secretion. In fact, the integrated area under the curve, that is, the amount of insulin secreted during the 30-minute stimulation period, was less than 5% of that observed for the control, normoglycemic grafts (Figure 3). Interestingly, this extensively impaired glucose-stimulated insulin secretion was only marginally returned to normal after a 2-week period of normoglycemia effected by a second

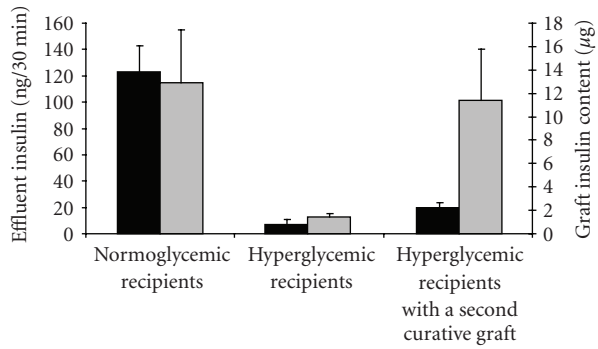

Figure 3: Total insulin secretion in effluent medium collected from human islet graft-bearing kidneys during 30-minute perfusion with 16.7 mM glucose (black bars), and insulin content of renal subcapsular islet grafts (grey bars). Values are means ± SEM.

intrasplenic mouse islet graft (Figure 3). This was despite a nearly total reconstitution of the insulin content of the graft.

In further studies of this defective glucose-induced insulin release of the human islet grafts, we found that also arginine-stimulated secretion was heavily impaired [37]. Neither impaired glucose metabolism nor decreased (pro)insulin biosynthesis could explain the deleterious effects of the diabetic state on human islet graft insulin secretion. It is tempting to speculate that formation of intracellular amyloid deposits might be one hitherto neglected reason for this functional impairment. With our present knowledge, attention should be paid to functional abnormalities also in IAPP biosynthesis and secretion. One process of particular interest in this context might be the enzymatic cleavage of pro-IAPP by the converting enzymes PC 2 and PC 1/3 [38].

4. AMYLOID DEPOSITS IN TRANSPLANTED PANCREATIC ISLETS INFLUENCE OF IMPLANTATION SITE, FUNCTIONAL ACTIVITY, AND MICROENCAPSULATION

In our first report on the rapid deposition of amyloid in human islets transplanted into nude mice, our primary aim was to study the occurrence of IAPP-positive cells in the grafts [39]. Not surprisingly, comparisons of adjacent human islet graft sections stained for insulin and IAPP, respectively, indicated that the antisera stained the same cells. However, while the insulin staining was fairly even, both strongly and weakly labelled cells occurred after staining for IAPP. Interestingly, we found a lower percentage of IAPP-positive cells in the grafts of hyperglycaemic mice, suggesting that the storage of the substance was decreased after hyperglycemia.

By means of Congo red staining, we found amyloid deposits in human islet transplants in six out of eight normoglycaemic and two out of four hyperglycaemic recipients. All these islet grafts had resided under the kidney capsule of the nude mice for no more than two weeks, demonstrating the rapidity of the process. Thus, no amyloid was found in sections of the donor pancreata collected before they were processed for islet isolation. The amyloid deposits were usually multiple and small and located extracellularly but some faintly stained deposits were also found in the cytoplasm of the islet cells.

Electron microscopical investigations showed explicitly that IAPP immunoreactivity normally was confined to the secretory granules of the β-cells, while α- and δ-cells were negative. Moreover, as in the light microscopical study, accumulation of amyloid material, strongly labelled with antisera to IAPP, was found in eight of the twelve grafted mice (Figures 4(a) and 4(b)). Large amounts of amyloid fibrils were easily recognized (Figure 4(c)) but sometimes the material also had a granular appearance.

It is worthy of note that in a comparative study elucidating the amyloid deposition in islets of transgenic mice expressing hIAPP and in human islets implanted into nude mice, we found considerable differences [27]. Thus, in human islets amyloid was mainly formed intracellularly (Figure 4), whilst in islets from transgenic mice the amyloid was exclusively deposited extracellularly. Later studies have shown, however, that also in these animals the first amyloid occurs within β-cells [38].

Descriptions of amyloid formation in grafted islets in this paper have all referred to studies using the subcapsular renal space as implantation site. Since essentially all clinical islet transplantations are performed by intraportal infusion, we were interested in investigating intraportally grafted islets as well. Again, nude mice were used as recipients and indeed amyloid exhibiting affinity for Congo red was found in 8 of 9 islet-containing livers (a total of 10 mice were implanted with human islets) [28]. Both quantitatively and qualitatively, the formation of amyloid seemed to occur to the same extent and similarly to that seen in the subcapsularly grafted islets. Separate studies of intrasplenic islet grafts showed that also such islets contained amyloid with the same appearance as in the intraportally implanted human islets.

While we were unable to demonstrate an effect of hyperglycemia on the amount of amyloid formed in our first study when using both normoglycemic and alloxan-diabetic recipients long-term (14 d) culture of the human islets prior to transplantation seemed to considerably enhance the amyloid formation [28]. At least this was the case in specimens observed for a short-time period—the grafts were evaluated already after 2 weeks. Taken together with results from studies of grafts kept under the kidney capsule for half a year [28] where rather large extracellular deposits were found, it appears that the first amyloid is formed intracellularly and that amyloid at a later stage acts as a nidus for further extracellular deposition. For some reason, however, the process halts and therefore the heavy amyloid deposition as seen in the islets of type 2 diabetes patients never develops. The reasons for this are still unknown but obviously the present experimental model offers unique opportunities for such studies.

One circumstance that might explain the rapid deposition of amyloid in the grafted islets is their fairly low vascular density as compared with the endogenous islets in the pancreas [40]. Such a relative lack of blood vessels providing

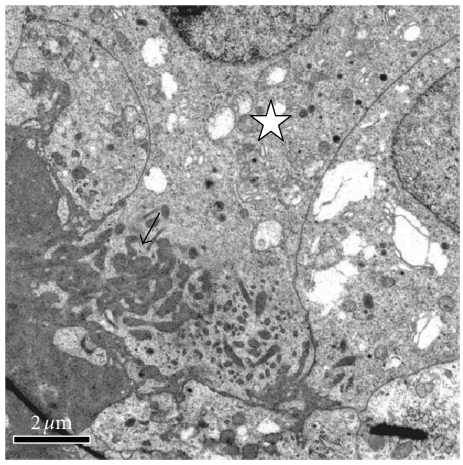

(a)

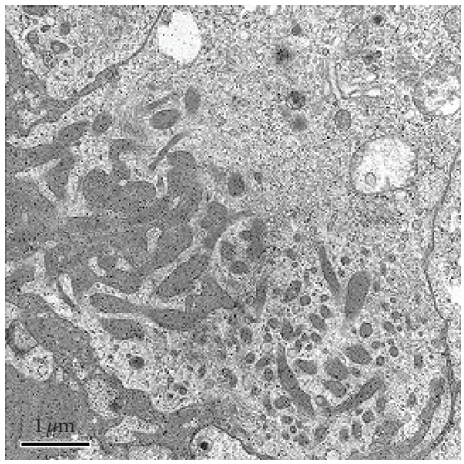

(b)

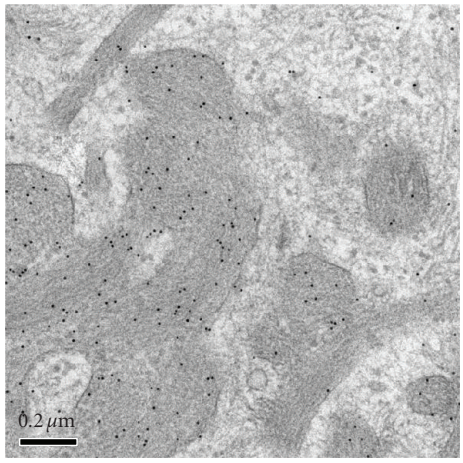

(c)

Figure 4: Intra- and extracellular amyloid in an islet graft implanted under the renal capsule of a nude mouse. (a) In the overview, it is seen that the amyloid (arrow) is present in the periphery of degranulated β-cells (star). (b) At higher magnification, it is obvious that the amyloid forms a network, presumably due to presence in the endoplasmic reticulum. (c) At high magnification, the fibrillar ultrastructure of the amyloid is evident as well as its specific immunolabelling with antibodies against IAPP, visualized with 10 nm gold particles.

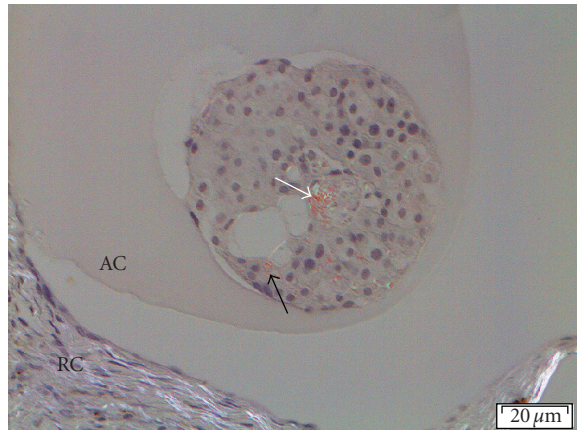

Figure 5: Polarized light microscopic image of a Congo red stained microencapsulated human islet residing in the renal subcapsular space of an athymic nude mouse for four weeks. The black arrow points out amyloid in and outside a normal islet cell, whereas the white arrow indicates amyloid in the central necrotic part of the islet. Surrounding the islet is the alginate capsule (AC), and in the lower part of the image the renal capsule (RC).

for an efficient export of the secretory products thus might facilitate the accumulation of IAPP and formation of amyloid. The ultimate test of that hypothesis would be to look for the presence of amyloid deposits in microencapsulated islets, which exemplify a totally nonvascularized islet graft. For that purpose, we encapsulated both human islets and hIAPP transgenic mouse islets in a high-guluronic alginate solution [41]. These capsules were subsequently transplanted into the renal subcapsular space of normoglycemic nude mice [42]. Indeed, preliminary results suggest that encapsulated human islet grafts that were retrieved one month after implantation contained considerable amounts of amyloid (Figure 5). Obviously, under these specific conditions amyloid deposits develop, thus demonstrating that a sustained blood supply is not a prerequisite for their formation. It also seems feasible to use the microencapsulated islets as a tool for more detailed studies of the amyloid formation process under forced circumstances.

5. CLINICAL IMPLICATIONS

At present, reports on the pathology of clinically grafted islets are very scarce and to our knowledge amyloid has not been looked for specifically except for our recent study [43]. There are methodological difficulties, one of which might be the fairly long ischemic periods before liver tissue can be harvested. Nevertheless, studies aiming at the localization and characterization of the implanted islets are highly warranted. Since the identification of the amyloid material is often laborious, consultations with groups experienced in this field of research might be desirable. During the final preparation of this manuscript, we published data indeed demonstrating widespread amyloid deposition in clinically transplanted human islets [43]. A patient with type 1 diabetes for more than 35 years died in a myocardial

infarction 5 years after the first of three intraportal islet infusions. In almost every second of a total of 89 islets found in the liver tissue blocks, amyloid deposits, most of them being extracellular, were identified. Immunoelectron microscopy demonstrated amyloid fibrils that were positive for antibodies against IAPP. Indeed, these findings highly strengthen the validity of our hypothesis.

6. FUTURE PERSPECTIVES

Long-term results with clinical islet transplantation are fairly discouraging. There is evidence to suggest that this is caused by a progressive loss of the grafted β-cells. Knowledge on the nature of that process is, however, meagre. Therefore, the importance of performing necropsies of as many as possible of deceased patients with islet grafts, functioning or nonfunctioning, cannot be enough underlined. Pathologists, experienced in different aspects of islet pathology, including islet amyloidosis, should be consulted when judging the harvested material. By such means, further insights on the nature of the destructive process(es) should be gained.

As regards, the pathogenic mechanisms of islet amyloidosis, islet transplantation models might offer unique possibilities to study them in more detail. We have very much focussed on the first intracellular IAPP aggregation and the role of proIAPP and proIAPP intermediates in that process. It remains to be established that under circumstances when concentrations of such molecules are high, there is an enhanced amyloid formation in vivo.

In the Edmonton protocol, preparative islet culture was not used perhaps because such manoeuvres might decrease the viability of the isolated islets. Although that view is controversial, it cannot be ruled out that amyloid develops during culture of human islets or mouse islets transgenic for hIAPP. Indeed, there is some evidence in support of that view [28, 44]. However, it has to be proven that such pretransplant deposits indeed stimulate a further and more extensive formation of amyloid in the islets once they have become transplanted.

Finally, it is still an open question as to whether enhanced insulin production, as under hyperglycemic conditions, promotes amyloid growth in the transplanted islets. A general suppression of β-cell function by means of insulin treatment or, at least under experimental conditions, drugs like somatostatin and its analogs or diazoxide might be of value to test. In this context, other types of medical intervention against IAPP aggregation should be of interest as well. One such substance is eprodisate, which recently was shown to slow the decline of renal function in patients with AA amyloidosis [45].

ACKNOWLEDGMENTS

This research was supported by the Swedish Research Council, the Swedish Diabetes Association, the Family Ernfors Fund, the Östergötland County Council, and the Juvenile Diabetes Research Foundation.

REFERENCES

[1] A. M. J. Shapiro, J. R. T. Lakey, E. A. Ryan, et al., "Islet transplantation in seven patients with type 1 diabetes mellitus using a glucocorticoid-free immunosuppressive regimen," *The New England Journal of Medicine*, vol. 343, no. 4, pp. 230–238, 2000.

[2] A. M. J. Shapiro, C. Ricordi, B. J. Hering, et al., "International trial of the Edmonton protocol for islet transplantation," *The New England Journal of Medicine*, vol. 355, no. 13, pp. 1318–1330, 2006.

[3] E. L. Opie, "On relation of chronic interstitial pancreatitis to the islands of Langerhans and to diabetes mellitus," *Journal of Experimental Medicine*, vol. 5, no. 4, pp. 397–428, 1901.

[4] A. Weichselbaum and E. Stangl, "Zur kenntnis der feineren veränderungen des pankreas bei diabetes mellitus," *Wiener Klinische Wochenschrift*, vol. 14, pp. 968–972, 1901.

[5] J. W. M. Höppener, B. Ahrén, and C. J. M. Lips, "Islet amyloid and type 2 diabetes mellitus," *The New England Journal of Medicine*, vol. 343, no. 6, pp. 411–419, 2000.

[6] R. L. Hull, G. T. Westermark, P. Westermark, and S. E. Kahn, "Islet amyloid: a critical entity in the pathogenesis of type 2 diabetes," *The Journal of Clinical Endocrinology & Metabolism*, vol. 89, no. 8, pp. 3629–3643, 2004.

[7] J. Janson, R. H. Ashley, D. Harrison, S. McIntyre, and P. C. Butler, "The mechanism of islet amyloid polypeptide toxicity is membrane disruption by intermediate-sized toxic amyloid particles," *Diabetes*, vol. 48, no. 3, pp. 491–498, 1999.

[8] L. Khemtémourian, J. A. Killian, J. W. Höppener, and M. F. E. Engel, "Recent insights in islet amyloid polypeptide-induced membrane disruption and its role in β-cell death in type 2 diabetes mellitus," *Experimental Diabetes Research*, vol. 2008, Article ID 421287, 9 pages, 2008.

[9] P. Westermark, C. Wernstedt, E. Wilander, and K. Sletten, "A novel peptide in the calcitonin gene related peptide family as an amyloid fibril protein in the endocrine pancreas," *Biochemical and Biophysical Research Communications*, vol. 140, no. 3, pp. 827–831, 1986.

[10] P. Westermark, C. Wernstedt, E. Wilander, D. W. Hayden, T. D. O'Brien, and K. H. Johnson, "Amyloid fibrils in human insulinoma and islets of Langerhans of the diabetic cat are derived from a neuropeptide-like protein also present in normal islet cells," *Proceedings of the National Academy of Sciences of the United States of America*, vol. 84, no. 11, pp. 3881–3885, 1987.

[11] P. Westermark, C. Wernstedt, T. D. O'Brien, D. W. Hayden, and K. H. Johnson, "Islet amyloid in type 2 human diabetes mellitus and adult diabetic cats contains a novel putative polypeptide hormone," *American Journal of Pathology*, vol. 127, no. 3, pp. 414–417, 1987.

[12] G. J. S. Cooper, A. C. Willis, A. Clark, R. C. Turner, R. B. Sim, and K. B. M. Reid, "Purification and characterization of a peptide from amyloid-rich pancreases of type 2 diabetic patients," *Proceedings of the National Academy of Sciences of the United States of America*, vol. 84, no. 23, pp. 8628–8632, 1987.

[13] S. Ohagi, M. Nishi, G. I. Bell, J. W. Ensinck, and D. F. Steiner, "Sequences of islet amyloid polypeptide precursors of an old world monkey, the pig-tailed macaque (*Macaca nemestrina*), and the dog (*Canis familiaris*)," *Diabetologia*, vol. 34, no. 8, pp. 555–558, 1991.

[14] E. J. P. de Koning, N. L. Bodkin, B. C. Hansen, and A. Clark, "Diabetes mellitus in *Macaca mulatta* monkeys is characterised by islet amyloidosis and reduction in beta-cell population," *Diabetologia*, vol. 36, no. 5, pp. 378–384, 1993.

[15] K. H. Johnson, C. Wernstedt, T. D. O'Brien, and P. Westermark, "Amyloid in the pancreatic islets of the cougar (*Felis concolor*) is derived from islet amyloid polypeptide (IAPP)," *Comparative Biochemistry and Physiology Part B*, vol. 98, no. 1, pp. 115–119, 1991.

[16] P. Westermark, Z.-C. Li, G. T. Westermark, A. Leckström, and D. F. Steiner, "Effects of beta cell granule components on human islet amyloid polypeptide fibril formation," *FEBS Letters*, vol. 379, no. 3, pp. 203–206, 1996.

[17] S. Janciauskiene, S. Eriksson, E. Carlemalm, and B. Ahrén, "B cell granule peptides affect human islet amyloid polypeptide (IAPP) fibril formation in vitro," *Biochemical and Biophysical Research Communications*, vol. 236, no. 3, pp. 580–585, 1997.

[18] C. Betsholtz, L. Christmansson, U. Engström, et al., "Sequence divergence in a specific region of islet amyloid polypeptide (IAPP) explains differences in islet amyloid formation between species," *FEBS Letters*, vol. 251, no. 1-2, pp. 261–264, 1989.

[19] C. B. Verchere, D. A. D'Alessio, R. D. Palmiter, et al., "Islet amyloid formation associated with hyperglycemia in transgenic mice with pancreatic beta cell expression of human islet amyloid polypeptide," *Proceedings of the National Academy of Sciences of the United States of America*, vol. 93, no. 8, pp. 3492–3496, 1996.

[20] G. T. Westermark, S. Gebre-Medhin, D. F. Steiner, and P. Westermark, "Islet amyloid development in a mouse strain lacking endogenous islet amyloid polypeptide (IAPP) but expressing human IAPP," *Molecular Medicine*, vol. 6, no. 12, pp. 998–1007, 2000.

[21] J. W. M. Höppener, C. Oosterwijk, M. G. Nieuwenhuis, et al., "Extensive islet amyloid formation is induced by development of type II diabetes mellitus and contributes to its progression: pathogenesis of diabetes in a mouse model," *Diabetologia*, vol. 42, no. 4, pp. 427–434, 1999.

[22] W. C. Soeller, J. Janson, S. E. Hart, et al., "Islet amyloid-associated diabetes in obese $A^{(vy)}$/a mice expressing human islet amyloid polypeptide," *Diabetes*, vol. 47, no. 5, pp. 743–750, 1998.

[23] G. T. Westermark, D. F. Steiner, S. Gebre-Medhin, U. Engström, and P. Westermark, "Pro islet amyloid polypeptide (ProIAPP) immunoreactivity in the islets of langerhans," *Upsala Journal of Medical Sciences*, vol. 105, no. 2, pp. 97–106, 2000.

[24] G. Westermark, M. B. Arora, N. Fox, et al., "Amyloid formation in response to β cell stress occurs in vitro, but not in vivo, in islets of transgenic mice expressing human islet amyloid polypeptide," *Molecular Medicine*, vol. 1, no. 5, pp. 542–553, 1995.

[25] E. J. P. de Koning, E. R. Morris, F. M. A. Hofhuis, et al., "Intra- and extracellular amyloid fibrils are formed in cultured pancreatic islets of transgenic mice expressing human islet amyloid polypeptide," *Proceedings of the National Academy of Sciences of the United States of America*, vol. 91, no. 18, pp. 8467–8471, 1994.

[26] P. Westermark, "Fine structure of islets of Langerhans in insular amyloidosis," *Virchows Archiv A*, vol. 359, no. 1, pp. 1–18, 1973.

[27] G. T. Westermark, P. Westermark, D. L. Eizirik, et al., "Differences in amyloid deposition in islets of transgenic mice expressing human islet amyloid polypeptide versus human islets implanted into nude mice," *Metabolism*, vol. 48, no. 4, pp. 448–454, 1999.

[28] G. T. Westermark, P. Westermark, A. Nordin, E. Törnelius, and A. Andersson, "Formation of amyloid in human pancreatic islets transplanted to the liver and spleen of nude mice," *Upsala Journal of Medical Sciences*, vol. 108, no. 3, pp. 193–204, 2003.

[29] S. E. Kahn and P. A. Halban, "Release of incompletely processed proinsulin is the cause of the disproportionate proinsulinemia of NIDDM," *Diabetes*, vol. 46, no. 11, pp. 1725–1732, 1997.

[30] R. S. Jackson, J. W. M. Creemers, S. Ohagi, et al., "Obesity and impaired prohormone processing associated with mutations in the human prohormone convertase 1 gene," *Nature Genetics*, vol. 16, no. 3, pp. 303–306, 1997.

[31] J. F. Paulsson, S. W. Schultz, M. Köhler, I. Leibiger, P. O. Berggren, and G. T. Westermark, "Real-time monitoring of apoptosis by caspase-3-like protease induced FRET reduction triggered by amyloid aggregation," *Experimental Diabetes Research*, vol. 2008, Article ID 865850, 12 pages, 2008.

[32] J. F. Paulsson and G. T. Westermark, "Aberrant processing of human proislet amyloid polypeptide results in increased amyloid formation," *Diabetes*, vol. 54, no. 7, pp. 2117–2125, 2005.

[33] L. Marzban, C. J. Rhodes, D. F. Steiner, L. Haataja, P. A. Halban, and C. B. Verchere, "Impaired NH_2-terminal processing of human proislet amyloid polypeptide by the prohormone convertase PC2 leads to amyloid formation and cell death," *Diabetes*, vol. 55, no. 8, pp. 2192–2201, 2006.

[34] L. Jansson, D. L. Elzirik, D. G. Pipeleers, L. A. Borg, C. Hellerström, and A. Andersson, "Impairment of glucose-induced insulin secretion in human pancreatic islets transplanted to diabetic nude mice," *Journal of Clinical Investigation*, vol. 96, no. 2, pp. 721–726, 1995.

[35] B. Volk, "Pathology of the diabetic pancreas," in *Diabetes Mellitus: Theory and Practice*, H. Rifkin and D. Porte Jr., Eds., pp. 341–345, Elsevier, Philadelphia, Pa, USA, 1990.

[36] O. Korsgren, L. Jansson, and A. Andersson, "Effects of hyperglycemia on function of isolated mouse pancreatic islets transplanted under kidney capsule," *Diabetes*, vol. 38, no. 4, pp. 510–515, 1989.

[37] D. L. Eizirik, L. Jansson, M. Flodström, C. Hellerström, and A. Andersson, "Mechanisms of defective glucose-induced insulin release in human pancreatic islets transplanted to diabetic nude mice," *The Journal of Clinical Endocrinology & Metabolism*, vol. 82, no. 8, pp. 2660–2663, 1997.

[38] J. F. Paulsson, A. Andersson, P. Westermark, and G. T. Westermark, "Intracellular amyloid-like deposits contain unprocessed pro-islet amyloid polypeptide (ProIAPP) in beta cells of transgenic mice overexpressing the gene for human IAPP and transplanted human islets," *Diabetologia*, vol. 49, no. 6, pp. 1237–1246, 2006.

[39] P. Westermark, D. L. Eizirik, D. G. Pipeleers, C. Hellerström, and A. Andersson, "Rapid deposition of amyloid in human islets transplanted into nude mice," *Diabetologia*, vol. 38, no. 5, pp. 543–549, 1995.

[40] P.-O. Carlsson, F. Palm, and G. Mattsson, "Low revascularization of experimentally transplanted human pancreatic islets," *The Journal of Clinical Endocrinology & Metabolism*, vol. 87, no. 12, pp. 5418–5423, 2002.

[41] S. Bohman, A. Andersson, and A. King, "No differences in efficacy between noncultured and cultured islets in reducing hyperglycemia in a nonvascularized islet graft model," *Diabetes Technology and Therapeutics*, vol. 8, no. 5, pp. 536–545, 2006.

[42] S. Bohman, P. Westermark, A. Andersson, and G.T. Westermark, "Amyloid formation in transplanted microencapsulated islets," in *Proceedings of the 18th EASD Islet Study Group Symposium*, p. 17, Rome, Italy, September 2008.

[43] G. T. Westermark, P. Westermark, C. Berne, and O. Korsgren, "Widespread amyloid deposition in transplanted human pancreatic islets," *The New England Journal of Medicine*, vol. 359, no. 9, pp. 977–979, 2008.

[44] S. Zraika, R. L. Hull, J. Udayasankar, et al., "Glucose- and time-dependence of islet amyloid formation in vitro," *Biochemical and Biophysical Research Communications*, vol. 354, no. 1, pp. 234–239, 2007.

[45] L. M. Dember, P. N. Hawkins, B. P. C. Hazenberg, et al., "Eprodisate for the treatment of renal disease in AA amyloidosis," *The New England Journal of Medicine*, vol. 356, no. 23, pp. 2349–2360, 2007.

Hindawi Publishing Corporation
Experimental Diabetes Research
Volume 2008, Article ID 865850, 12 pages
doi:10.1155/2008/865850

Methodology Report

Real-Time Monitoring of Apoptosis by Caspase-3-Like Protease Induced FRET Reduction Triggered by Amyloid Aggregation

Johan F. Paulsson,[1] Sebastian W. Schultz,[2] Martin Köhler,[3] Ingo Leibiger,[3] Per-Olof Berggren,[3] and Gunilla T. Westermark[2]

[1] *Department of Chemistry and The Skaggs Institute for Chemical Biology, The Scripps Research Institute, La Jolla, CA 92037, USA*
[2] *Division of Cell Biology, Diabetes Research Centre, Department of Clinical and Experimental Medicine, Linköping University, 58185 Linköping, Sweden*
[3] *The Rolf Luft Research Center for Diabetes and Endocrinology, Karolinska Institute, 17176 Stockholm, Sweden*

Correspondence should be addressed to Gunilla T. Westermark, gunwe@ibk.liu.se

Received 31 January 2008; Accepted 23 April 2008

Recommended by Per Westermark

Amyloid formation is cytotoxic and can activate the caspase cascade. Here, we monitor caspase-3-like activity as reduction of fluorescence resonance energy transfer (FRET) using the contstruct pFRET2-DEVD containing enhanced cyan fluorescent protin (EYFP) linked by the caspase-3 specific cleavage site residues DEVD. Beta-TC-6 cells were transfected, and the fluoorescence was measured at 440 nm excitation and 535 nm (EYFP) and 480 nm (ECFP) emission wavelength. Cells were incubated with recombinant pro lset Amyloid Polypeptide (*rec* prolAPP) or the processing metabolites of prolAPP; the N-terminal flanking peptide withIAPP (*rec*N+IAPP); IAPP with the C-terminal flanking peptied (*rec*IAPP+C) and lslet Amyloid Polypeptide (*rec*IAPP) . Peptides were added in solubilized from (50 μM) or as performed amyloid-like fibrils, or as a combination of these. FRET was measured and incubation with a mixture of solubilized peptide and performed fibrils resulted in loss of FRET and apoptosis was determined to occure in cells incubated with *rec*proIAPP (49%), *rec*N+IAPP (46%), *rec*IAPP (72%) and *rec*IAPP+C (59%). These results show that proIAPP and the processing intermediates reside the same cell toxic capacity as IAPP, and they can all have a central role in the reduction of beta-cell number in type 2 diabetes.

1. INTRODUCTION

If proteins misfold or lose their native fold, they are usually assisted to refold by molecular chaperons or they can be removed from the system and be degraded [1]. However, under certain circumstances this system seems to fail and proteins escape degradation. Instead, they can aggregate into fibrils with a high degree of beta-pleated secondary structure, and if these fibrils are stained by Congo red and exert green birefringence when viewed in polarised light they are referred to as amyloid [2–5]. Amyloid deposition is associated with loss of organ function and cell death. Hitherto, at least 25 different proteins have been characterised from systemic or localised amyloid deposits in humans [4].

The amyloid formation process can be divided into two phases. The first is a nucleation forming process where monomers of the amyloid peptide form prefibrillar oligomeric species and this is referred to as the lag phase [6, 7]. The second phase is the extension phase where rapid elongation of amyloid fibrils occurs which will reach a plateau when most of the molecules are converted into the fibrillar form. A dramatic reduction of the lag phase will occur if mature amyloid fibrils of the same origin are added and this is called the seeding effect. There is growing evidence that the cytotoxic species of the amyloid forming process are early oligomers consisting of 15–40 monomers forming a ring shaped structure [8–10]. These prefibrillar assemblies are able to incorporate and form pores in cellular membranes causing cell leakage and influx of cations which triggers the apoptosis cascade. According to this, the amyloid fibril itself is a nontoxic end product of a cytotoxic aggregation process.

Amyloid deposits in the islets of Langerhans are a pathological characteristic of type 2 diabetes, and the amyloid aggregates consist of islet amyloid polypeptide (IAPP)

[11, 12]. IAPP is a product of the endocrine beta-cell and as amyloid deposition occurs a large reduction of beta-cell mass has been observed [13–15]. IAPP has also been shown to form spherical structures with the capacity to incorporate into lipid bilayers [16–18]. In vitro studies of different cell lines show that amyloid formation of IAPP is cytotoxic and triggers the apoptotic pathway by activation of the caspase cascade [19–21].

IAPP is expressed as a precursor molecule (proIAPP) which is posttranslationally modified by the processing enzymes prohormone convertase (PC) 2 and 1/3 [22–25]. In the secretory granule, proIAPP is cleaved between dibasic residues at the N- and C-termini by PC2 and PC1/3, respectively. We and others have previously shown in cell lines that if aberrant processing of human proIAPP occurs, intracellular amyloid-like aggregates arise with cell death as a result [26, 27]. Also intracellular amyloid-like aggregates consisting of proIAPP have been described in both transgenic mice expressing human IAPP and in human beta-cells [28]. Cells with intracellular amyloid-like material are also positive for M30 cyto-death antibody which binds to an early neoepitope that becomes accessible during caspase activation.

Here, we describe a novel system for monitoring beta-cell apoptosis. The system uses two fluorophores linked together with a caspase 3-like cleavage site, and when cleavage occurs a reduction of fluorescence resonance energy transfer (FRET) can be measured as an indicator of apoptosis. Since measurements of the same cells can be done repeatedly, real-time monitoring of beta-cell apoptosis can be performed. Also, we used the established assay to compare the apoptotic properties of recombinant proIAPP (*rec*proIAPP) and proIAPP processing intermediates, N-terminal flanking peptide with IAPP (*rec*N+IAPP), IAPP with the C-terminal flanking peptide (*rec*IAPP+C), and recombinant IAPP (recIAPP).

2. EXPERIMENTAL PROCEDURES

2.1. Cell transfection

Beta-TC-6 (B-TC-6) cells obtained from American Type Culture Collection (Manassas, VA, USA) were cultured to 80% confluency in 10 cm diameter Petri dishes (Falcon: Labora, Stockholm, Sweden) in RPMI-1640 medium with 11 mM D-glucose containing 10% fetal bovine serum (FBS) (Sigma, Stockholm, Sweden), 100 IU/ml penicillin, 100 μg/ml streptomycin, 50 μM β-mercaptoethanol. One hour prior to transfection, medium was changed to RPMI-1640 medium without serum. A total volume of 175 μL with 20 μg pFRET2-DEVD, 20 μg pcDNA3, 10 mM polyethyleneimine, and 5% sucrose was added to 9 mL of RPMI-1640 medium without serum. After 6 hours of incubation, FBS was added to a final concentration of 10%. After 24 hours, 0.4 mg/mL G-418 antibiotics was added to the medium for selection of stabile B-TC-6 clones.

2.2. Assay buffer

The following solutions were investigated for autofluorescence: (1) Krebs-Ringer with hepes and glucose (KRHG) (120 mM NaCl, 4.7 mM KCl, 2.5 mM $CaCl_2$, 1.2 mM $MgSO_4$, 0.5 mM KH_2PO_4, pH 7.4 with 2 mM D-glucose, 20 mM Hepes, and 200 nM adenosine). (2) Hank's balanced salt solution (HBSS) (5.4 mM KCl, 0.3 mM $NaHPO_4$, 0.4 mM KH_2PO_4, 4.2 mM $NaHCO_3$, 1.3 mM $CaCl_2$, 0.5 mM $MgCl_2$, 0.6 mM $MgSO_4$, 137 mM NaCl, 5.6 mM D-glucose, pH 7.4). (3) RPMI-1640 medium without FBS (Sigma). (4) RPMI-1640 medium with 10% FBS. (5) Dulbeccoçs medium without phenol red (Invitrogen, Carlsbad, Calif, USA). (6) Schneiderçs Drosophila medium without phenol red (Invitrogen). (7) H_20.

2.3. Real-time monitoring of apoptosis

pFRET2-DEVD vector is driven by the insulin promoter and can only be expressed in insulin producing cells. When expressed, a product consisting of enhanced cyan fluorescent protein (ECFP) and enhanced yellow fluorescent protein (EYFP) linked by the amino acid residues DEVD will be dispersed throughout cytoplasm. The sequence DEVD is a specific substrate for caspase-3-like proteases and when ECFP and EYFP are connected by the DEVD residues FRET will occur. If the transfected B-TC-6 cells undergo apoptosis, the DEVD is cleaved and the two fluorophores will be separated and a loss of FRET can be monitored as a decrease of the 535 nm/480 nm fluorescence ratio. The pFRET2-DEVD vector has previously been characterised by Köhler et al. [29]. B-TC-6 cells with stable expression pFRET2-DEVD were cultured for 48 hours in black 96 well plates (Labsystems) to 80% confluency and washed once in KRHG-buffer prior to experimental procedures. Sample volume was set to 100 μL and both synthetic and recombinant peptides were kept as stock solution of 5 mM in dimethyl sulfoxide (DMSO) and diluted to a final concentration of 50 μM with a final DMSO concentration of 1%. Synthetic human and rat IAPP were analysed in solubilised form at final concentrations of 25 and 50 μM. Negative control was 1% DMSO in KRHG-buffer and when seeded assays were performed a final concentration of 30 nM synthetic IAPP fibrils was included in the negative control. Positive control for apoptosis contained 2 μM staurosporine and 1% DMSO in KRHG-buffer. Negative and positive controls were included in each individual assay. Mature recombinant amyloid-like fibrils were washed in H_2O and centrifuged at 16.000 g for 15 minutes and resuspended in KRHG-buffer, sonicated and diluted to an estimated concentration of 50 μM.

Loss of FRET was measured in a Wallac 1420 multilabel counter (Perkin Elmer, Turku, Finland) with WorkOut software version 1.5 (Perkin Elmer). Excitation was set to 440 nm, and emitted fluorescence was measured at 535 nm (EYFP) and 480 nm (ECFP). Data are presented as mean ratio ±SEM of 535 nm/480 nm ratio. Each point represents at least five individual measurements.

2.4. Confocal microscopy

B-TC-6 cells with stabile expression of pFRET2-DEVD and untransfected B-TC-6 cells were cultured on 19 mm cover

Table 1: Forward and reverse primers for amplification of IAPP fragments.

proIAPP forward	5′-GAT GAC ACC CAT TGA AAG TCA TCA GG-3′
proIAPP reverse	5′-CTA CTA AAG GGG CAA GTA ATT CAG TGG-3′
N-terminal+IAPP forward	5′-GAT GAC ACC CAT TGA AAG TCA TCA GG-3′
N-terminal+IAPP reverse	5′-CTA CTA GCC ATA TGT ATT GGA TCC CAC G-3′
IAPP forward	5′-GAT GAA ATG CAA CAC TGC CAC ATG-3′
IAPP reverse	5′-CTA CTA GCC ATA TGT ATT GGA TCC CAC G-3′
IAPP+C-terminal forward	5′-GAT GAA ATG CAA CAC TGC CAC ATG-3′
IAPP+C-terminal reverse	5′-CTA CTA AAG GGG CAA GTA ATT CAG TGG-3′

slips and rinsed in PBS (137 mM NaCl, 2.7 mM KCl, 4.3 mM Na_2HPO_4, and 1.4 mM, KH_2PO_4) before fixation in 2% paraformaldehyde in PBS for 30 minutes. For visualisation, cells were incubated with the nuclear stain TO-PRO-3 (Molecular probes, Eugene, Ore, USA) diluted 1 : 1000 in PBS for 15 minutes and then mounted with 50/50 glycerol/PBS. Cells were studied in a Nikon eclipse E600 microscope with a Nikon C1 confocal unit with argon 488 nm and HeNe 633 nm lasers (Nikon Kawasaki, Japan). Digital pictures were taken with an EZ-C1 digital camera and software version 1.0 for Nikon confocal microscopy.

2.5. Production of recombinant peptides

Human preproIAPP cloned into the pBluescript II vector was used as template for generation of PCR amplified DNA fragments corresponding to human proIAPP, N-terminal flanking peptide+IAPP, IAPP and IAPP+C-terminal flanking peptide. Forward and reverse primers used for this purpose are described in Table 1. The amplified IAPP fragments were blunt end ligated in expression vector pGEX 2TK (GE healthcare, Uppsala, Sweden). Constructs were confirmed by sequencing to be in correct reading frame and without mutations. The pGEX 2TK vector has glutathione S-transferase (GST) in front of the multiple cloning site and the peptide will be expressed as a GST fusion protein. Y1090 bacteria were transformed and cultured in Luria broth at +37°C until OD A_{600} reached 0.8, and protein synthesis was induced with 3 mM isopropyl β-D-1 thiogalactopyranoside (IPTG) (Fermentas, St Lenon Rot, Germany) for 3 hours at +25°C. Bacteria were spun down and resuspended in TEDG buffer (50 mM TRIS-HCl pH 7.4, 1.5 mM EDTA, 10% glycerol, 400 mM NaCl) and sonicated three times for 20 seconds. The bacteria lysate was centrifuged at 100.000 g in a SW41 Ti rotor for 30 minutes at +4°C, and the supernatant was transferred to Sepharose-4B beads (GE healthcare) and incubated 2 hours end over end at +4°C. Sepharose beads were spun down at 3000 g for one minute, and the lysate was decanted and the beads were washed three times in NET-N buffer (50 mM TRIS-HCl pH 7.4, 150 mM NaCl, 5 mM EDTA and 0.5% NONIDET-NP 40 (USB, Cleveland, Ohio, USA) followed by three times wash in PBS. The GST-tag was cleaved off with thrombin protease (GE healthcare) 20 U/mg expected peptide in PBS end over end overnight. Removal of the 27 kDa GST-tag resulted in rapid amyloid formation and aggregates were collected. The amyloid-like fibrils were washed in ddH_2O and solved in 50%/50% 1,1,1,3,3,3-hexafluoro-2-propanol (HFIP)/trifluoroacetic acid (TFA) for 24 hours. Solubilised peptides were centrifuged at 16.000 g for 15 minutes, and the supernatant was recovered. For assays with IAPP recombinant peptides in complete monomeric form, the supernatant was filtered trough a Millex-FG syringe filter 0.2 μm for hydrophobic solvents. Samples were dried in vacuum and redisolved in 100% DMSO. Peptide concentrations for *rec*proIAPP and *rec*N+IAPP were determined using A_{280} extinction coefficient 1615 $M^{-1}\,cm^{-1}$and for *rec*IAPP and *rec*IAPP+C 3105 $M^{-1}\,cm^{-1}$ in a nanodrop ND-1000 spectrophotometer (NanoDrop Technologies, Wilmington, Del, USA). Theoretical molecular masses were as follow: *rec*proIAPP 8358 Da, *rec*N+IAPP 6224 Da, *rec*IAPP 4918 Da, and *rec*IAPP+C 7053 Da. Synthetic human IAPP used in the study was synthesized by KEX Laboratories, Yale University (New Haven, Conn, USA), and synthetic rat IAPP was purchased from Bachem (Heidelberg, Germany).

2.6. Tricine-sodium dodecyl sulfate-polyacrylamide gel electrophoresis

Tricine-SDS-PAGE was performed as described by Schägger and von Jagow [30]. Samples were dissolved in sample buffer containing 0.1 M Tris-HCl at pH 6.8, 30% (wt/vol) glycerol, 8% (wt/vol) SDS, 0.2 M dithiothreitol (DTT), and 0.02% Coomassie blue G-250 and boiled for 5 minutes prior to loading onto the gel. The separation condition was 30 mV for 20 hours.

2.7. Silver staining and trypsin digestion

The tricine-SDS gel was sensitised in 1.4 mM $Na_2S_2O_4$ and incubated in 0.2% $AgNO_3$ solution containing 7.5 μL formaldehyde (37%)/100 mL water for 25 minutes and developed in 6% Na_2CO_3, 25 μM $Na_2S_2O_3$, and 50 μL formaldehyde (37%)/100 mL water.

Silver stained bands corresponding to the expected masses of the recombinant IAPP peptides were excised from the gel and dried. Each sample was incubated with 60 μL reducing agent consisting of 10 mM dithiothreitol (DTT) in 25 mM NH_4HC_3 for one hour at +56°C, after which the peptides were alkylated in 70 μL 55 mM iodoacetamide (IAA) at room temperature in dark for 45 minutes. Rehydrated gel pieces were digested in 100 μL trypsin solution containing

1.5 μg/mL trypsin (Promega, Madison, Wis, USA) and 25 mM NH_4HCO_3 and incubated 24 hours at +37°C.

2.8. Electro spray ionisation tandem mass spectrometry

Full scan mass spectra for peptide mass fingerprinting and TOF product scans for sequencing of amino acids were acquired on a hybrid mass spectrometer (API QSTAR Pulsar, Applied Biosystems, Foster city, Calif) equipped with a nanoelectrospray ion source (MDS Protana, Odense, Denmark).

2.9. Amyloid staining

Samples were dried onto glass slides and incubated for 20 minutes in A solution (NaCl saturated 80% ethanol with 0.01% NaOH) and were directly transferred to B solution (solution A saturated with Congo red). Samples were rinsed in 100% ethanol and xylen and mounted. Amyloid specific green birefringence was studied in an Olympus X51 microscope (Olympus, Tokyo, Japan) with two polarising filters connected to an Olympus DP 50 digital camera run by Studio Lite v 1.0.1 software.

2.10. Electron microscopy

Droplets of sample were placed on formvar coated copper grids and were negative contrasted with 2% uranyl acetate in 50% ethanol. Samples were studied in a Jeol 1230 electron microscope at 100 kV (Jeol, Akishima, Tokyo, Japan). Digital electron micrographs were taken with a Gatan multiscan camera model 791 with corresponding software v3.6.4 (Gatan Inc, Pleasanton, Calif, USA).

2.11. Thioflavin Tassay

Kinetic studies of amyloid formation were performed in Sigmacote (Sigma-Aldrich, St. Louis, Mo, USA) treated black 96 well plates (Labsystems) in a sample volume of 100 μL. Synthetic IAPP was diluted from a DMSO stock solution (5 mM) to a final concentration of 50 μM in thioflavin T (ThT) in assay buffer (50 mM glycine, 25 mM sodium phosphate buffer, pH 7.0, and 10 μM ThT). Mature IAPP fibrils (30 nM) were included to decrease the amyloid lag phase. Samples consisting of ThT assay buffer with 1% DMSO and ThT assay buffer with 30 nM IAPP fibrils and 1% DMSO were included in the assay. Fluorescence was measured every thirty minutes at an excitation wavelength of 442 nm and an emission wavelength of 486 nm. Each sample was measured in 12 individual wells, and data presented are mean values ± SEM.

2.12. Statistical analysis

Statistics were performed in GraphPad InStat version 3.06 (GraphPad Software Inc., San Diego, Calif, USA). Unpaired t-test was used when two groups were compared and one-way analysis of variance (ANOVA) with Dunnett multiple comparisons test when several groups were analysed. A P-value less than 0.05 was considered significant.

3. RESULTS

3.1. Evaluation of the method

Autofluorescence from different solutions was analysed at emission wavelengths 535 nm and 480 nm (see Figure 1(a)). The KRHG buffer had the lowest fluorescence of the investigated solutions and was therefore used as assay buffer throughout the study.

To determine if the fluorescent signal from the pFRET2-DEVD transfected B-TC-6 cells was sufficient for detection in the plate reader the signal was compared to the signal from untransfected B-TC-6 cells. B-TC-6 cells expressing pFRET2-DEVD had a 6.5-fold higher fluorescence signal at 535 nm and a 2.3-fold higher signal at 480 nm when compared to the untransfected B-TC-6 cells (see Figure 1(b)). Fluorescence form transfected B-TC-6 cells differed significantly at both wavelengths compared to untransfected B-TC-6 cells in an unpaired t-test ($P < .0005$). The 535 nm/480 nm ratio for living pFRET2-DEVD transfected B-TC-6 cells was 2.2. Three hours incubation with the apoptosis inducer staurosporine (2 μM) decreased the FRET ratio to 1.2. Synthetic human and rat IAPP peptides in monomeric form, at concentrations 25 and 50 μM, were incubated with pFRET2-DEVD B-TC-6 cells. Only negligible reduction in FRET signal was detected after 12 hour incubation, and cell survival was calculated to 96% and 98% after incubation with rat IAPP and human IAPP, respectively. There was no difference between cells incubated with 25 or 50 μM (data not shown). In the confocal microscope, the pFRET2-DEVD B-TC-6 cells revealed a strong cytoplasmic fluorescence at excitation wavelength 488 nm (see Figure 1(c)). This was not present in untransfected cells (see Figure 1(d)).

3.2. Amyloid formation and loss of FRET

FRET reduction as a result of amyloid formation was initially investigated with synthetic IAPP peptides. The amyloid formation from 50 μM monomeric IAPP seeded with 30 nM IAPP fibrils was monitored in the ThT assay and with the FRET assay in parallel (see Figure 2). In the ThT assay, amyloid specific fluorescence of seeded IAPP was detected after a 3-hour lag phase and reached a plateau after 9 hours (see Figure 2(a)). No increase in basal fluorescence was detected for the sample with ThT buffer alone or ThT buffer with low concentration of premade IAPP seeds. To further study the amyloid aggregation process, aliquots from the seeded 50 μM IAPP solution were collected hourly and prepared for electron microscopy. After 2 hours, small ring shaped structures with an outer diameter of approximately 15 nm could be detected at high magnification (see Figure 2(b)). After 4 hours of incubation, very thin thread-like fibrils were detected (see Figure 2(c)) and after 12 hours of incubation fibrils with a more mature fibrillar appearance were visible (see Figure 2(d)).

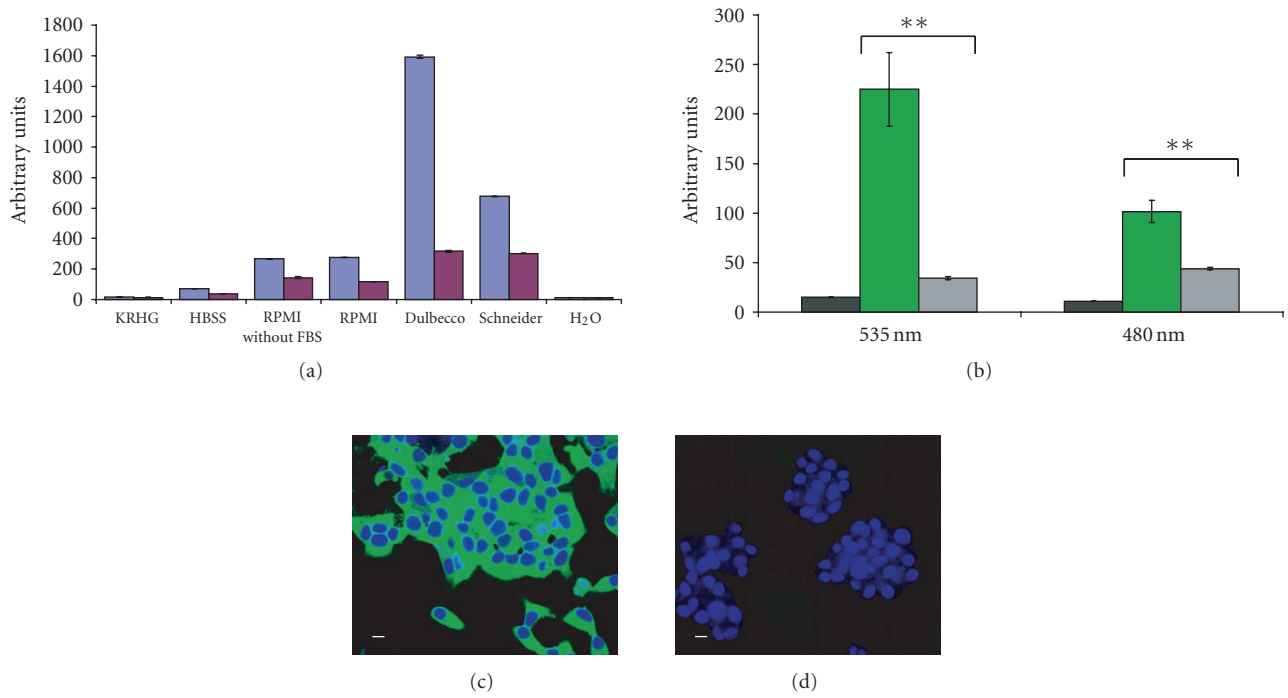

Figure 1: Determination of assay buffer and investigation of pFRET2-DEVD expressing B-TC-6 cells. (a) Solutions (KRHG, HBSS, RPMI without FBS, RPMI, Dulbeccoçs modified medium, Schneiderçs drosophila medium, and H_2O) were analysed for autofluorescence at wavelength 535 nm (blue columns) and 480 nm (red columns). Data presented are mean values ±SEM ($n = 8$). (b) Fluorescence at 535 nm and 480 nm was measured for KRHG buffer (black columns), B-TC-6 cells expressing pFRET2-DEVD (green columns), and untransfected B-TC-6 cells (grey columns). Data presented are mean values ±SEM ($n = 8$). Difference in fluorescence signal between B-TC-6 cells expressing pFRET2-DEVD and untransfected B-TC-6 was considered to be significant ($P < .0005$) in a two-tailed unpaired t-test. (c) Confocal image of pFRET2-DEVD expressing B-TC-6 cells and (d) untransfected B-TC-6 cells. Argon 488 nm and HeNe 633 nm lasers were used at the same energy levels in the two images. Green fluorescence indicates expression of pFRET2-DEVD and blue fluorescence nuclear staining TO-PRO-3. Scale bars represent 10 μm.

In the FRET measurements, pFRET2-DEVD expressing B-TC-6 cells incubated with staurosporine used as positive control showed an instant reduction of the 535 nm/480 nm ratio. After 4 hours, the ratio was reduced to 1.2 (see Figure 2(e)). The FRET ratio for pFRET2-DEVD expressing B-TC-6 cells incubated with KRHG buffer and 30 nM IAPP seeds used as negative control were relative stable at a ratio of 2.0 through out the assay. pFRET2-DEVD expressing B-TC-6 cells incubated in 50 μM IAPP peptide with 30 nM IAPP seeds showed a reduced FRET signal compared to the negative control (see Figure 2(e)). The measurements were done hourly for 12 hours, and the calculation was performed as follows. The FRET ratio 535 nm/480 nm, determined after 12 hours of incubation with the apoptosis-inducer staurosporine, was set as baseline and corresponds to 0% survival cells. All cells were considered viable after incubation with preformed fibrils, and the value for the FRET ratio 535 nm/480 nm was set as 100% after subtraction of the baseline value.

The FRET ratio of the B-TC-6 cells incubated in amyloid forming IAPP peptide corresponds to a population of 65% apoptotic cells (see Figure 2(f)). B-TC-6 cells incubated in amyloid forming IAPP differed significantly from the negative control in a two-tailed unpaired t-test ($P < .006$).

3.3. Characterisation of recombinant peptides

The recombinant peptides *rec*proIAPP, *rec*N+IAPP, *rec*IAPP, and *rec*IAPP+C were expressed as fusion proteins and when the GST-tag was enzymatically removed, all four peptides formed aggregates during the 12 hours time period. The aggregates from the different recombinant peptides stained with Congo red and revealed green birefringence (see Figures 3(a)–3(d)). Negative contrasted aggregates showed typical amyloid-like fibrils with a diameter of 10 nm and of variable length (see Figures 3(e)–3(h)).

The expected amino acid sequences of *rec*proIAPP, *rec*N+IAPP, *rec*IAPP, and *rec*IAPP+C was used to determine the expected molecular masses (see Figure 4(a)).The produced peptides were run on Tricine SDS-PAGE and bands corresponding to the molecular masses of each individual peptide were cut out, trypsinised and analysed by electrospray ionisation tandem mass spectrometry (see Figure 4(b)). The expected tryptic fragments from each peptide were identified in full scan spectrum (data not shown), and the sequence of each fragment was confirmed by collision-induced fragmentation mass spectrometry. All four IAPP peptides had a 10-amino acid residue sequence consisting of residues GSRRASVGSP N-terminally which is a

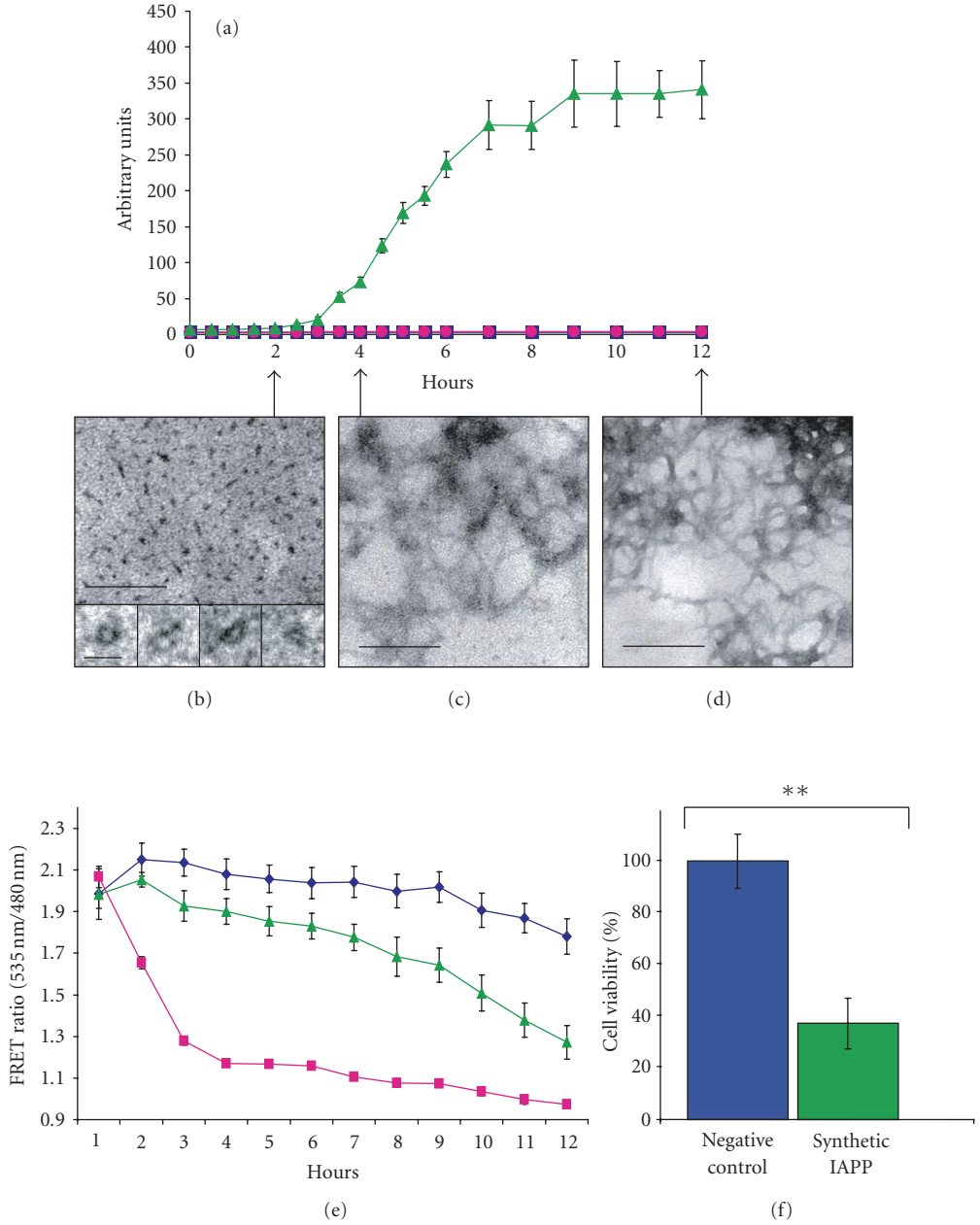

Figure 2: Parallel performed ThT assay, electron microscopy, and FRET assay of synthetic IAPP peptide. (a) ThT assay of synthetic IAPP peptide (50 μM) seeded with preformed IAPP fibrils (30 nM) (▲), ThT assay buffer seeded with preformed IAPP fibrils (30 nm) (●), and ThT assay buffer (■). Data presented are mean values ±SEM ($n = 12$). Synthetic IAPP peptide (50 μM) seeded with preformed IAPP fibrils (30 nM) incubated for (b) 2 hours of 50 μM, (c) for 4 hours, (d) and for 12 hours; all samples were negative contrasted. In (b), the higher magnification shows small prefibrillar ring shaped structures. In (c), thin thread-like protofibrils are visible and in (d) more mature amyloid-like fibrils are apparent. Large-scale bars represent 100 nm, and the smaller-scale bar in (b) represents 20 nm. (e) FRET ratio of 535 nm/480 nm measurements of KRHG buffer with seeds of preformed IAPP fibrils (30 nM) (♦), synthetic IAPP peptide (50 μM) seeded with preformed IAPP fibrils (30 nM) (▲), and staurosporine (2 μM) (■). Measurements were performed during a 12-hour period with individual measurements each hour. Data presented are mean values ±SEM ($n = 9$). (f) FRET ratio after 12 hours of measurements. Staurosporine sample was set as zero and was subtracted from assay measurements, and the negative control was set as 100% viable cells (blue column). The FRET ratio of the B-TC-6 cells incubated in synthetic IAPP peptide (50 μM) seeded with preformed IAPP fibrils (30 nM) was 37% of the negative control corresponding to a population of 65% apoptotic cells (green column). Data presented are mean values ±SEM ($n = 9$). The difference between the negative control and IAPP was considered significant in a two-tailed unpaired t-test ($P < .0006$).

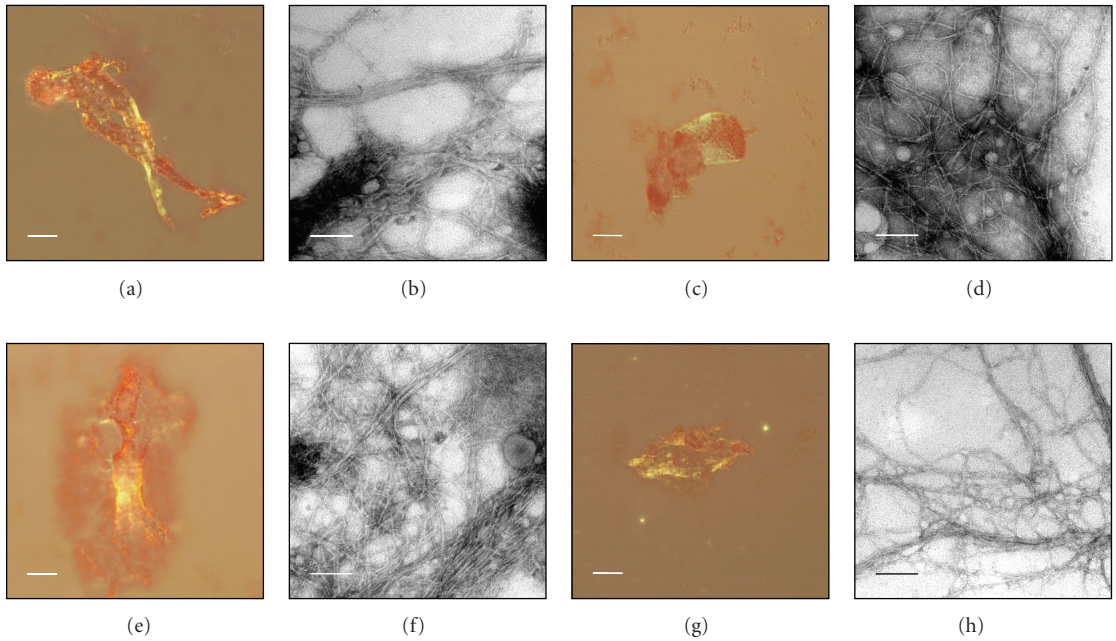

Figure 3: Congo red staining and electron micrographs of amyloid-like fibrils from *rec*proIAPP, *rec*N+IAPP, *rec*IAPP, and *rec*IAPP+C. Congo red staining viewed in polarised light showing amyloid specific green birefringence of (a) *rec*proIAPP, (c) *rec*N+IAPP, (e) *rec*IAPP, and (g) *rec*IAPP+C. Scale bars represent 20 μm. Electron micrographs of negative contrasted amyloid-like fibrils of (b) *rec*proIAPP, (d) *rec*N+IAPP, (f) *rec*IAPP, and (h) *rec*IAPP+C. Scale bars represent 100 nm.

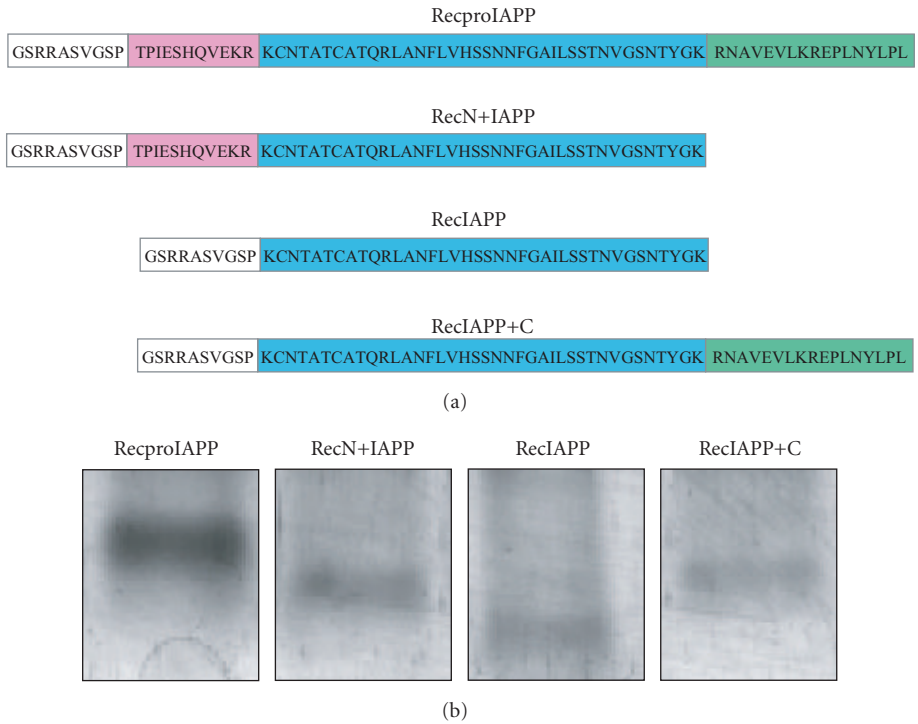

Figure 4: Characterisation of *rec*proIAPP, *rec*N+IAPP, *rec*IAPP, and *rec*IAPP+C. (a) A cartoon showing the amino acid sequences of *rec*proIAPP, *rec*N+IAPP, *rec*IAPP, and *rec*IAPP+C peptides. N-terminally, a fragment consisting of 10 residues originating from the GST-tag is present (white box). (b) Silver stained tricine SDS-PAGE of *rec*proIAPP, *rec*N+IAPP, *rec*IAPP, and *rec*IAPP+C. Bands were removed from the tricine gel, trypsinised and analysed by electrospray ionisation tandem mass spectrometry.

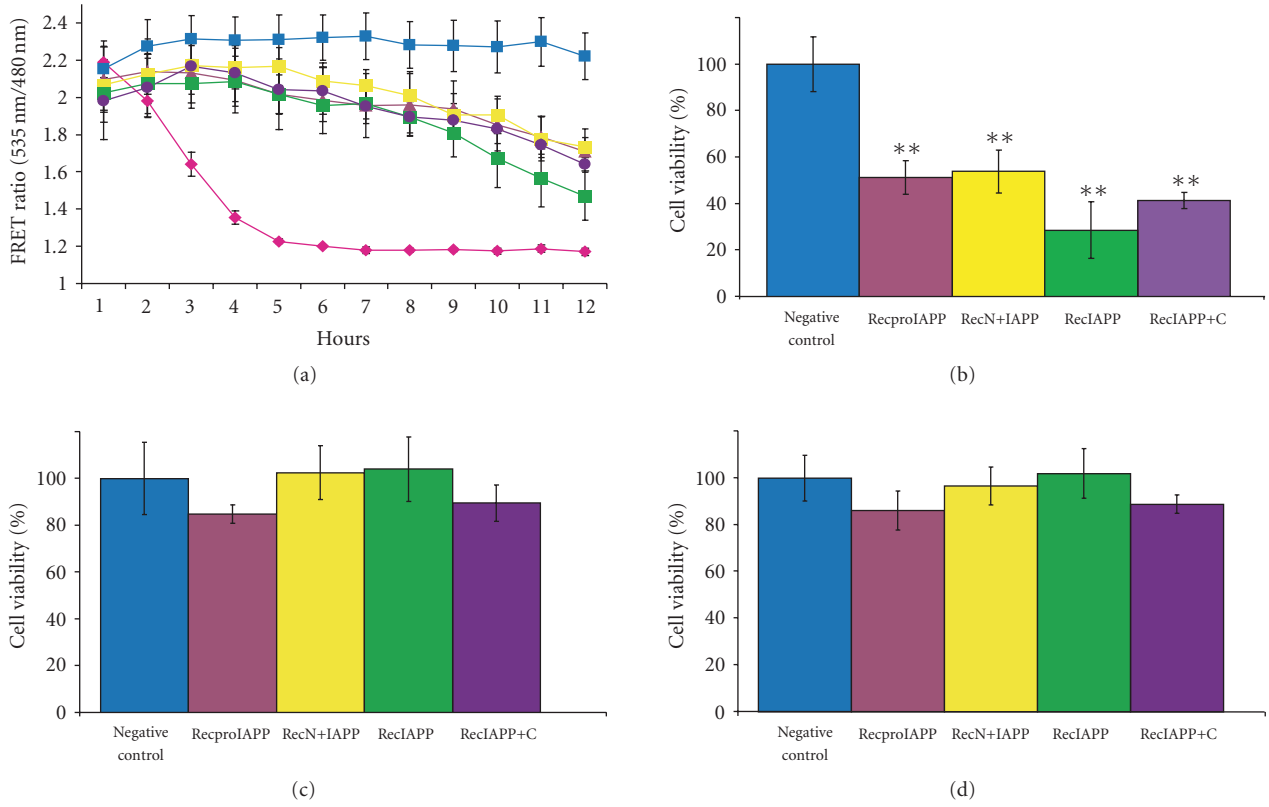

Figure 5: *FRET assays of rec*proIAPP, *rec*N+IAPP, *rec*IAPP, and *rec*IAPP+C. (a) B-TC-6 cells expressing pFRET2-DEVD were incubated with solubilised recombinant peptides *rec*proIAPP (50 μM) (▲), *rec*N+IAPP (50 μM) (■), *rec*IAPP (50 μM) (■), and *rec*IAPP+C (50 μM) (●), all supplemented with preformed IAPP fibrils at a concentration of 30 nM or incubated with preformed IAPP fibrils (30 nM) alone (■), or staurosporine (2 μM) (●). The FRET ratio at 535/480 nm was determined hourly over 12 hours. Data presented are mean value ±SEM ($n = 5$). (b) Cell viability after incubation for 12 hours with solubilised recombinant peptides supplemented with preformed IAPP fibrils (30 nM). Data are presented as mean value ±SEM ($n = 5$). Relative to the control, cell viability was determined to 51% for *rec*proIAPP (▲), 54% for *rec*N+IAPP (■), 28% for *rec*IAPP (■), and 41% for *rec*IAPP+C (●). Compared to the control, a significant difference in the FRET ratio was observed for all four recombinant peptides in an ANOVA test ($P < .0005$). (c) FRET ratio of pFRET2-DEVD expressing B-TC-6 cells after 12 hours of incubation with recombinant amyloid-like fibrils corresponding to 50 μM. *Rec*proIAPP (▲), *rec*N+IAPP (■), *rec*IAPP (■), and *rec*IAPP+C (●) and control incubation with buffer alone (■). Relative to the control, cell viability after incubation with *rec*proIAPP was 85%, with *rec*N+IAPP 102%, with *rec*IAPP 104% and with *rec*IAPP+C 89%. No statistically difference between the negative control and the four recombinant peptides was observed in an ANOVA test ($P < .5$). (d) Incubation of pFRET2-DEVD expressing B-TC-6 cells with recombinant peptides in solubilised form (50 μM). *Rec*proIAPP (▲), *rec*N+IAPP (■), *rec*IAPP (■), and *rec*IAPP+C (●) and control incubation with buffer alone (■). Relative to the control, cell viability after 12 hours incubation with *rec*proIAPP was 86%, *rec*N+IAPP 97%, *rec*IAPP 102%, and *rec*IAPP+C 89%. The four recombinant peptides did not differ significantly from the negative control in an ANOVA test ($P > .06$).

rest from the GST cleavage site. These extra residues did not interfere with the capability of the recombinant peptides to form amyloid-like fibrils as shown in Figure 3.

3.4. Apoptotic effect of recombinant peptides

pFRET2-DEVD expressing B-TC-6 cells were incubated with 50 μM of *rec*proIAPP, *rec*N+IAPP, *rec*IAPP, and *rec*IAPP+C together with 30 nM IAPP seeds in KRHG buffer. A reduction of the FRET ratio was detected during the time laps of the assay (see Figure 5(a)). After 12 hours of incubation, all four recombinant peptides had generated a large reduction of the FRET signal. The FRET ratio of the positive control was set as zero and subtracted from all other measurements and the negative control was set as 100% viable cells. The FRET ratios for *rec*proIAPP, *rec*N+IAPP, *rec*IAPP, and *rec*IAPP+C were 51%, 54%, 28%, and 41%, respectively, when compared to the negative control. This corresponds to a population of 49%, 46%, 72%, and 59% apoptotic cells (see Figure 5(b)). All four groups differed significantly from the negative control in an ANOVA test ($P < .0005$). No significant difference within the four recombinant peptide groups was detected in an ANOVA test ($P > .2$).

pFRET2-DEVD expressing B-TC-6 cells was also incubated with mature amyloid-like fibrils from *rec*proIAPP, *rec*N+IAPP, *rec*IAPP, and *rec*IAPP+C. No difference in FRET ratio was observed over time when compared to the negative control (data not shown). After 12 hours of incubation,

FRET ratios of *rec*proIAPP, *rec*N+IAPP, *rec*IAPP, and *rec*IAPP+C were 85%, 102%, 104%, and 89%, respectively, when the positive control was subtracted and the negative control was set as 100% viable cells (see Figure 5(c)). No significant differences between the negative control and the recombinant fibrils and no difference between the four different peptides ($P > .5$) were detected.

FRET measurements were also performed on pFRET2-DEVD expressing B-TC-6 cells incubated with 50 μM solubilised and filtered recombinant peptides. When compared to the negative control, no loss of FRET was detected during 12 hours of measurements (data not shown). After 12 hours of incubation and subtraction of the positive control, FRET ratios for *rec*proIAPP, *rec*N+IAPP, *rec*IAPP, and *rec*IAPP+C were 86%, 97%, 102%, and 89%, respectively, compared to the negative control (see Figure 5(d)). No significant difference between the negative control and the monomeric peptides and no differences between the four different recombinant peptides ($P > .06$) were detected.

4. DISCUSSION

The pFRET2-DEVD vector has earlier been demonstrated by Köhler et al. to be an excellent reporter for apoptosis induced by caspase-3-like proteases in the insulin producing beta-cell lines RINm5F and MIN6 [29]. By measuring loss of FRET on individual transiently transfected cells, the course of apoptosis was monitored in real-time. Here, we used the pFRET2-DEVD vector to establish a novel assay with stable transfected B-TC-6 cells that allows accurate real-time studies of apoptosis in 96 well plates. The assay was used for studies of beta-cell apoptosis during amyloid formation, and the toxicity of *rec*proIAPP and the processing metabolites *rec*N+IAPP, *rec*IAPP, and *rec*IAPP+C is evaluated.

Initially, it was essential to find an assay buffer with very low autofluorescence for measurement of FRET signal from cells cultured in a black 96 well plate. The KRHG-buffer revealed the lowest background and was selected for the assay, but with the disadvantage of being a rather poor medium. After 12 hours of FRET measurement, the negative control started to show some reduction of FRET and therefore measurements beyond this time point are not presented throughout this work. The fluorescent signal detected from the pFRET2-DEVD transfected B-TC-6 cells was adequate for plate reader measurements and since it is the ratio between 535 and 480 nm, that is, given differences in cell density can be ignored. Synthetic IAPP peptide was initially used for the setup of the method.

One step in the evaluation procedure of the FRET method was to determine the amyloid fibril formation progress under the used peptide concentrations and correlate it to the induction of apoptosis. For this, a ThT assay was run in parallel with identical IAPP concentrations. When monomeric IAPP was seeded with preformed IAPP amyloid-like fibrils, an increase in ThT-fluorescence signal appeared after a three hours lag phase and reached maximum after nine hours of incubation. Fibril formation could only be detected in seeded IAPP samples, and not in samples with seed alone. In samples collected for morphological evaluation, an amorphous material was present after two hours and at higher resolution ring-like structures with an outer diameter of 15 nm could be seen. After four hours of incubation, thin slender fibrils were present. Since no fibrilar material was present at the earlier time points we conclude that these thin fibrils were newly formed and did not represent the low amount of sonicated preformed fibrils added as seed. In samples taken after 12 hours, fibrils with a more distinct fibrilar appearance had emerged. The decrease in FRET ratio after incubation with 2 μM staurosporine starts under the first hour and continues over a five-hour period. Staurosporine is a potent inducer of apoptosis, a transient biological process that persists for 3-4 hours. In this positive control, all cells undergo apoptosis. In transfected cells incubated with monomeric IAPP and preformed fibrils, apoptosis was initiated after approximately seven hours and this is in line with the expected time frame if oligomers are responsible for the induction of apoptosis.

The B-TC-6 cell line is of mouse origin, and it has previously been suggested that mouse IAPP has an anti-amyloidogenic effect on human IAPP at least intracellularly [31]. In vitro studies show that insulin also has an inhibitory property on amyloid formation of human IAPP [32, 33]. Prior to the experimental procedure, the B-TC-6 cells were washed in KRHG buffer which has a low glucose concentration (2 mM). Therefore, exocytosis of mouse IAPP and insulin was considered to be very low during the assay and not to influence the amyloidogenicity of human IAPP.

The predominant hypothesis of amyloid cytotoxicity is that the prefibrillar assemblies are able to incorporate into cellular membranes causing cation influx [10, 34, 35]. Oligomeric species from different peptides would there share a common structure and act cytotoxic by the same mechanisms. A common pathway for apoptosis triggered by amyloid pore formation has not yet been proposed. Apoptosis is the major cause of beta-cell reduction in type 2 diabetic patients and has been shown to occur during formation of islet amyloid in a transgenic mouse model [15, 36]. Two apoptosis studies on beta-cell lines have been performed where activation of the caspase cascade in parallel to IAPP amyloid formation has been observed [19, 20]. Both authors have used RINm5F cells and Zhang el al. have also used the human insulinoma cell line CM. Both groups reported the activation of the common downstream protease caspase 3 with upstream activated JNK pathway (c-jun NH2-terminal kinase/stress-activated protein kinase). Zhang et al. also reported activated caspase 8 and caspase 1 proteases upstream of caspase 3. The exact pathways of IAPP triggered apoptosis are not clear but caspase 3 acts as a common downstream effector. Zhang et al. state that caspase 3 activation was detected after 8 hours of incubation with preseeded synthetic IAPP and reached a maximum after 16 hours [20]. No measurements between these time points were performed. Our observation of the reduced FRET signal goes well with these data, and upstream activation must occur before we detect FRET reduction by caspase 3 activation.

All four recombinant peptides, *rec*proIAPP, *rec*N+IAPP, *rec*IAPP, and *rec*IAPP+C possess amyloidogenic properties

and form fibrillar aggregates. The extra amino acid residues N-terminally of the recombinant peptides do not interfere with the amyloidogenic propensity since all four peptides form amyloid-like fibrils. The apoptotic effects of the recombinant peptides were investigated using the developed FRET assay. The recombinant peptides were studied in solubilised seeded, fibrillar, and in solubilised nonseeded form. A loss of FRET was detected for all four seeded solubilised recombinant peptides. At the end of the assay, an apoptotic rate ranging form 46–72% was observed for the four different seeded recombinant peptides though no statistically significant difference between the groups was distinguished. Important, the degree of apoptosis did not differ between cells incubated with synthetic IAPP (65%) or *rec*IAPP (72%) ($P > .5$) pointing out that the addition of the 10 residues at the N-terminus of the recombinant IAPP did not interfere with the cytotoxicity of the peptide.

B-TC-6 cells expressing pFRET2-DEVD were incubated with mature amyloid fibrils from *rec*proIAPP, *rec*N+IAPP, *rec*IAPP, and *rec*IAPP+C and no apoptosis was detected. Since the amyloid-like fibrils were extensively washed with water, a pure fibril fraction without any oligomeric species would be expected. Solubilised nonseeded recombinant peptides did not elicit a reduction of the FRET signal, most likely due to a long lag phase. From this we conclude that the cytotoxic species of synthetic and recombinant amyloidogenic IAPP peptides are early oligomers or protofibrils. This is in consensus with earlier studies [16, 17, 37].

A new and very interesting finding is that *rec*proIAPP and the processing intermediates *rec*N+IAPP and *rec*IAPP+C trigger beta-cell apoptosis. Earlier we and others have shown that islet amyloid deposition may start intracellularly and that aberrant processing of proIAPP can be an initiating event [26, 27]. Intracellular deposits containing proIAPP have been found both in transgenic mice expressing human IAPP and in human beta-cells transplanted under the renal capsule of mice fed a high fat diet [28]. In the latter study, we also found intra-granular amyloid-like fibrils consisting of proIAPP. It has previously been shown that amyloid formation of IAPP was strongly enhanced by phospholipid bilayers and that amyloid elongation occurred from the surface of the lipid bilayer [38]. Hypothetically, the membrane of the secretory granule or endoplasmatic reticulum may be the location of initial amyloid formation and where oligomeric pore structures can incorporate. By exocytosis, the granule membrane will fuse with the outer cell membrane and a cation influx and activation of apoptotic pathways might occur. Here, we demonstrate that *rec*proIAPP and the processing intermediates *rec*N+IAPP and *rec*IAPP+C can induce caspase 3 activation and trigger beta-cell apoptosis. This is achieved by prefibrillar toxic species since fibrillar and monomeric forms of the recombinant peptides did not trigger caspase 3-like activity. This further strengthens our hypothesis that aberrant processing of proIAPP plays a key role in early islet amyloidogenesis.

Apoptosis is a transient event, and the established assay allows analysis over time of the same cell population. It is a system with high reproducibility, and it is cost effective and easy to handle. Apoptosis assays where Ac-DEVD-AMC is used as fluorogenic substrate is often labour intense and the commonly used MTT assay, where only living cells are measured, is not a true assay for apoptosis. The Vybrant apoptosis detection kit uses three different fluorescent nuclear stains with the propensity to penetrate cell membrane according to an apoptotic or nonapoptotic state. This method is performed on living cells and must be analysed microscopically. It is work intense and dependent on the interpretation of the analyst. Also TUNEL and DNA fragmentation methods are labour intense and similar to all the methods described above, only measurement at one time point is possible. Factors such as equal amounts of cells in each well or assay and rate of cell division are very important to consider when to deal with the described methods. The weakness of our FRET assay is the poor medium in which the assay is performed. Further investigations of possible media to prolong the survival of the cells and thereby allow measurements over a more extended period of time would be valuable. Future prospects for this method are to study apoptosis in presence of antiamyloidogenic or amyloid enhancing factors depending on strategy to reduce toxic species in the amyloid forming process.

ABBREVIATIONS

DMSO:	Dimethyl sulfoxide
ECFP:	Enhanced cyan fluorescent protein
EYFP:	Enhanced yellow fluorescent protein
FBS:	Fetal bovine serum
FRET:	Fluorescence resonance energy transfer
GST:	Glutathione S-transferase
HBSS:	Hank's balanced salt solution
IAPP:	Islet amyloid polypeptide
IPTG:	Isopropyl β-D-1 thiogalactopyranoside
KRHG:	Krebs-Ringer salt solution with hepes and glucose
PC:	Prohormone convertase
*rec*IAPP:	Recombinant islet amyloid polypeptide
*rec*IAPP+C:	Recombinant islet amyloid polypeptide with C-terminal flanking peptide
*rec*N+IAPP:	Recombinant islet amyloid polypeptide with N-terminal flanking peptide
*rec*proIAPP:	Recombinant pro islet amyloid polypeptide
ThT:	Thioflavin T

ACKNOWLEDGMENTS

This work was supported by the Swedish Research Council, Swedish Diabetes Association, Foundation in Memory of Lars Hierta, Lions Research Fund against Disease, European Union FP6 Program, and Östergötland County Council.

REFERENCES

[1] B. Bukau, J. Weissman, and A. Horwich, "Molecular chaperones and protein quality control," *Cell*, vol. 125, no. 3, pp. 443–451, 2006.

[2] E. D. Eanes and G. G. Glenner, "X-ray diffraction studies on amyloid filaments," *Journal of Histochemistry & Cytochemistry*, vol. 16, no. 11, pp. 673–677, 1968.

[3] G. G. Glenner, "Amyloid deposits and amyloidosis. The beta-fibrilloses (first of two parts)," *The New England Journal of Medicine*, vol. 302, no. 23, pp. 1283–1292, 1980.

[4] P. Westermark, M. D Benson, J. N. Buxbaum, et al., "Amyloid: toward terminology clarification. Report from the Nomenclature Committee of the International Society of Amyloidosis," *Amyloid*, vol. 12, no. 1, pp. 1–4, 2005.

[5] H. Puchtler, F. Sweat, and J. G. Kuhns, "On the binding of direct cotton dyes by amyloid," *Journal of Histochemistry & Cytochemistry*, vol. 12, no. 12, pp. 900–907, 1964.

[6] J. T. Jarrett and P. T. Lansbury Jr., "Seeding "one-dimensional crystallization" of amyloid: a pathogenic mechanism in Alzheimer's disease and scrapie?" *Cell*, vol. 73, no. 6, pp. 1055–1058, 1993.

[7] P. Westermark, "Aspects on human amyloid forms and their fibril polypeptides," *FEBS Journal*, vol. 272, no. 23, pp. 5942–5949, 2005.

[8] N. Arispe, E. Rojas, and H. B. Pollard, "Alzheimer disease amyloid β protein forms calcium channels in bilayer membranes: blockade by tromethamine and aluminum," *Proceedings of the National Academy of Sciences of the United States of America*, vol. 90, no. 2, pp. 567–571, 1993.

[9] B. Caughey and P. T. Lansbury, "Protofibrils, pores, fibrils, and neurodegeneration: separating the responsible protein aggregates from the innocent bystanders," *Annual Review of Neuroscience*, vol. 26, pp. 267–298, 2003.

[10] A. Quist, I. Doudevski, H. Lin, et al., "Amyloid ion channels: a common structural link for protein-misfolding disease," *Proceedings of the National Academy of Sciences of the United States of America*, vol. 102, no. 30, pp. 10427–10432, 2005.

[11] P. Westermark, C. Wernstedt, E. Wilander, and K. Sletten, "A novel peptide in the calcitonin gene related peptide family as an amyloid fibril protein in the endocrine pancreas," *Biochemical and Biophysical Research Communications*, vol. 140, no. 3, pp. 827–831, 1986.

[12] P. Westermark, E. Wilander, G. T. Westermark, and K. H. Johnson, "Islet amyloid polypeptide-like immunoreactivity in the islet B cells of type 2 (non-insulin-dependent) diabetic and non-diabetic individuals," *Diabetologia*, vol. 30, no. 11, pp. 887–892, 1987.

[13] P. Westermark and L. Grimelius, "The pancreatic islet cells in insular amyloidosis in human diabetic and non-diabetic adults," *Acta Pathologica et Microbiologica Scandinavica A*, vol. 81, no. 3, pp. 291–300, 1973.

[14] A. Clark, C. A. Wells, I. D. Buley, et al., "Islet amyloid, increased A-cells, reduced B-cells and exocrine fibrosis: quantitative changes in the pancreas in type 2 diabetes," *Diabetes Research*, vol. 9, no. 4, pp. 151–159, 1988.

[15] A. E. Butler, J. Janson, S. Bonner-Weir, R. Ritzel, R. A. Rizza, and P. C. Butler, "β-cell deficit and increased β-cell apoptosis in humans with type 2 diabetes," *Diabetes*, vol. 52, no. 1, pp. 102–110, 2003.

[16] T. A. Mirzabekov, M. C. Lin, and B. L. Kagan, "Pore formation by the cytotoxic islet amyloid peptide amylin," *Journal of Biological Chemistry*, vol. 271, no. 4, pp. 1988–1992, 1996.

[17] J. Janson, R. H. Ashley, D. Harrison, S. McIntyre, and P. C. Butler, "The mechanism of islet amyloid polypeptide toxicity is membrane disruption by intermediate-sized toxic amyloid particles," *Diabetes*, vol. 48, no. 3, pp. 491–498, 1999.

[18] M. Anguiano, R. J. Nowak, and P. T. Lansbury Jr., "Protofibrillar islet amyloid polypeptide permeabilizes synthetic vesicles by a pore-like mechanism that may be relevant to type II diabetes," *Biochemistry*, vol. 41, no. 38, pp. 11338–11343, 2002.

[19] L. Rumora, M. Hadzija, K. Barisic, D. Maysinger, and T. Z. Grubiic, "Amylin-induced cytotoxicity is associated with activation of caspase-3 and MAP kinases," *Journal of Biological Chemistry*, vol. 383, no. 11, pp. 1751–1758, 2002.

[20] S Zhang, J. Liu, M. Dragunow, and G. J. Cooper, "Fibrillogenic amylin evokes islet β-cell apoptosis through linked activation of a caspase cascade and JNK1," *Journal of Biological Chemistry*, vol. 278, no. 52, pp. 52810–52819, 2003.

[21] A. Lorenzo, B. Razzaboni, G. C. Weir, and B. A. Yankner, "Pancreatic islet cell toxicity of amylin associated with type-2 diabetes mellitus," *Nature*, vol. 368, no. 6473, pp. 756–760, 1994.

[22] T. Sanke, G. I. Bell, C. Sample, A. H. Rubenstein, and D. F. Steiner, "An islet amyloid peptide is derived from an 89-amino acid precursor by proteolytic processing," *Journal of Biological Chemistry*, vol. 263, no. 33, pp. 17243–17246, 1988.

[23] M. K. Badman, K. I. Shennan, J. L. Jermany, K. Docherty, and A. Clark, "Processing of pro-islet amyloid polypeptide (proIAPP) by the prohormone convertase PC2," *FEBS Letters*, vol. 378, no. 3, pp. 227–231, 1996.

[24] C. E. Higham, R. L. Hull, L. Lawrie, et al., "Processing of synthetic pro-islet amyloid polypeptide (proIAPP) 'amylin' by recombinant prohormone convertase enzymes, PC2 and PC3, in vitro," *European Journal of Biochemistry*, vol. 267, no. 16, pp. 4998–5004, 2000.

[25] L. Marzban, G. Trigo-Gonzalez, X. Zhu, et al., "Role of β-cell prohormone convertase (PC)1/3 in processing of pro-islet amyloid polypeptide," *Diabetes*, vol. 53, no. 1, pp. 141–148, 2004.

[26] J. F. Paulsson and G. T. Westermark, "Aberrant processing of human proislet amyloid polypeptide results in increased amyloid formation," *Diabetes*, vol. 54, no. 7, pp. 2117–2125, 2005.

[27] L. Marzban, C. J. Rhodes, D. F. Steiner, L. Haataja, P. A. Halban, and C. B. Verchere, "Impaired NH_2-terminal processing of human pro-islet amyloid polypeptide by the prohormone convertase PC2 leads to amyloid formation and cell death," *Diabetes*, vol. 55, no. 8, pp. 2192–2201, 2006.

[28] J. F. Paulsson, A. Andersson, P. Westermark, and G. T. Westermark, "Intracellular amyloid-like deposits contain unprocessed pro-islet amyloid polypeptide (proIAPP) in beta cells of transgenic mice overexpressing the gene for human IAPP and transplanted human," *Diabetologia*, vol. 49, no. 6, pp. 1237–1246, 2006.

[29] M. Köhler, S. V. Zaitsev, I. I. Zaitseva, et al., "On-line monitoring of apoptosis in insulin-secreting cells," *Diabetes*, vol. 52, no. 12, pp. 2943–2950, 2003.

[30] H. Schägger and G. von Jagow, "Tricine-sodium dodecyl sulfate-polyacrylamide gel electrophoresis for the separation of proteins in the range from 1 to 100 kDa," *Analytical Biochemistry*, vol. 166, no. 2, pp. 368–379, 1987.

[31] G. T. Westermark, S. Gebre-Medhin, D. F. Steiner, and P. Westermark, "Islet amyloid development in a mouse strain lacking endogenous islet amyloid polypeptide (IAPP) but expressing human IAPP," *Molecular Medicine*, vol. 6, no. 12, pp. 998–1007, 2000.

[32] P. Westermark, Z. C. Li, G. T. Westermark, A. Leckström, and D. F. Steiner, "Effects of beta cell granule components on human islet amyloid polypeptide fibril formation," *FEBS Letters*, vol. 379, no. 3, pp. 203–206, 1996.

[33] E. T. Jaikaran, M. R. Nilsson, and A. Clark, "Pancreatic β-cell granule peptides form heteromolecular complexes which

inhibit islet amyloid polypeptide fibril formation," *Biochemical Journal*, vol. 377, pp. 709–716, 2004.

[34] R. Kayed, E. Head, J. L. Thompson, et al., "Common structure of soluble amyloid oligomers implies common mechanism of pathogenesis," *Science*, vol. 300, no. 5618, pp. 486–489, 2003.

[35] C. G. Glabe and R. Kayed, "Common structure and toxic function of amyloid oligomers implies a common mechanism of pathogenesis," *Neurology*, vol. 66, supplement 1, no. 2, pp. S74–S78, 2006.

[36] A. E. Butler, J. Janson, W. C. Soeller, and P. C. Butler, "Increased β-cell apoptosis prevents adaptive increase in β-cell mass in mouse model of type 2 diabetes," *Diabetes*, vol. 52, no. 9, pp. 2304–2314, 2003.

[37] J. J. Meier, R. Kayed, C. Y. Lin, et al., "Inhibition of human IAPP fibril formation does not prevent β-cell death: evidence for distinct actions of oligomers and fibrils of human IAPP," *American Journal of Physiology*, vol. 291, no. 6, pp. E1317–E1324, 2006.

[38] J. D. Knight and A. D. Miranker, "Phospholipid catalysis of diabetic amyloid assembly," *Journal of Molecular Biology*, vol. 341, no. 5, pp. 1175–1187, 2004.